UNIVERSITY OF SOUTHAMPTON

FACULTY OF NATURAL AND ENVIROMENTAL SCIENCES

School of Biological Sciences

Spatio-temporal Properties of Neurotrophin Signalling in Tauopathy

by

Prutha Patel

Thesis for the degree of Doctor of Philosophy

June, 2019

UNIVERSITY OF SOUTHAMPTON

ABSTRACT

FACULTY OF NATURAL AND ENVIROMENTAL SCIENCES

School of Biological Sciences

Thesis for the degree of Doctor of Philosophy

SPATIO-TEMPORAL PROPERTIES OF NEUROTROPHIN SIGNALLING IN TAUOPATHY

Prutha Patel

Neuronal cells form a highly organised neuronal network that allows us to function in everyday life. In order to maintain a healthy network, neuronal brain cells synthesise and secrete growth factors. Brain-derived neurotrophic growth factor (BDNF) is one of the growth factors widely expressed in the brain. Its role is to induce cell growth and strengthen connections between neuronal cells.

A significant decrease in the amount of BDNF has been detected in the brains of individuals who have suffered from neurodegenerative diseases such as Alzheimer's disease, compared to healthy brains. Upregulating BDNF could be a potential therapeutic strategy to strengthen the connections of vulnerable neurons before the onset of neuronal death.

My PhD project looks to investigate to which degree BDNF-TrkB signalling is intact, both locally and over long-distances in neuronal brain cells that express a disease relevant mutation and whether these signals can support the vulnerable neuronal brain cells. In order to investigate this, I expressed a tauopathy related mutation (Tau^{P301L}) in embryonic mouse neuronal brain cells. I have observed disruption in BDNF transport and a significant change in the expression of its receptor, TrkB, at distal axons on Tau^{P301L}-expressing neurons. To assess BDNF signal relay, I have set-up a microfluidic platform that allows us to investigate both local and long-distance intracellular signalling of BDNF. I have seen a disruption in BDNF signalling in Tau^{P301L}-expressing neurons. This research gives us insight into whether growth factors are feasible for therapeutic strategies.

Table of Contents

Table of Tables

Table of Figures

Academic Thesis: Declaration of Authorship

I, Prutha Patel declare that this thesis and the work presented in it are my own and has been generated by me as the result of my own original research.

Spatio-temporal Properties of Neurotrophin Signalling in Tauopathy

I confirm that:

1. This work was done wholly or mainly while in candidature for a research degree at this University;
2. Where any part of this thesis has previously been submitted for a degree or any other qualification at this University or any other institution, this has been clearly stated;
3. Where I have consulted the published work of others, this is always clearly attributed;
4. Where I have quoted from the work of others, the source is always given. With the exception of such quotations, this thesis is entirely my own work;
5. I have acknowledged all main sources of help;
6. Where the thesis is based on work done by myself jointly with others, I have made clear exactly what was done by others and what I have contributed myself;
7. None of this work has been published before submission

Signed: .....

Date: .....

:|| સ્વામી શ્રીજી ||:

Dedicated to my parents, and husband

Without whom none of this would possible

Acknowledgements

These past three years in Southampton have been incredible, and all the people I have met along the way have made my PhD journey truly memorable.

Firstly, my heartfelt gratitude to my supervisor Dr Katrin Deinhardt, for her continuous support and guidance. You have taught me to question many aspects of research, and for that I have become a better scientist. Thank you for always taking the time to give advice and feedback on my work. Thank you to my co-supervisor, Dr Jonathan West, for his continuous words of encouragement, advice and motivation.

Thank you to Professor Vincent O'Connor, Dr Mark Coldwell and Dr Mark Willet for helping me with many aspects of my project.

To Dr Jo Bailey and Dr Shmma Quraishe, thank you for being great mentors and friends. You have taught me the numerous techniques which have helped me achieved many of my results. To my fellow lab mates, thank you for the being my mini family in Southampton. My PhD journey would not have been the same with you all.

Dr Grace Hallinan, we started this PhD journey together and no words can ever describe how truly thankful I am of having you as my partner in crime.

I am very blessed to have a wonderful family who have continuously supported me. To my parents: thank you mum and dad for everything you have done for me. To my brother, thank you for your constant support and words of encouragement. To my mother- and father-in-law, thank you for supporting me on this journey.

Lastly, to my darling husband, Hari, your patience and love is more than anything I could ever ask for. I am forever grateful for your understanding and sacrifice living apart these past three and a half years. You have been my rock throughout all of this. Thank you.

Definitions and Abbreviations

AD	Alzheimer's disease
Arc	Activity-Regulated Cytoskeleton-Associated Protein
BDNF	Brain-Derived Neurotrophic Factor
CamKII	Calcium Calmodulin Kinase II
CCV	Clathrin-Coated Vesicles
CNS	Central Nervous System
CPE	Carboxypeptidase E
CRE	Cyclic AMP Response Element
DAG	Diacylglycerol
DAPI	4', 6-diamidino-2-phenylindole
DHC	Dynein Heavy Chain
DIC	Differential Interference Contrast
DIV	Days in Vitro
DRG	Dorsal Root Ganglion
EB3	End Binding Protein 3
EGFP	Enhanced Green Fluorescent Protein
EGR1	Early Growth Response 1
EPSCs	Excitatory Postsynaptic Currents
ER	Endoplasmic Reticulum
Erk1/2	Extracellular Signal-Regulated Kinase 1/2
ESCRT	Endosomal Sorting Complex Required for Transport

FBS	Foetal Bovine Serum
FITC	Fluoescein Isothiocyanate
FL-Trk	Full-Length Trk
FTLD17	Frontotemporal-Lobe Dementia Linked to Chromosome 17
Gab1	Grb2-Associated Binding Protein 1
GFP	Green Fluorescent Protein
Grb2	Growth Factor Receptor Bound Protein 2
IEGs	Immediate Early Genes
IP3	Inositol-Tris-Phosphate
LTP	Long-Term Potentiation
MAP	Microtubule Associated Protein
MAPK	Mitogen-Activated Protein Kinase
mBDNF	Mature BDNF
mEPCs	Miniature Excitatory Postsynaptic Currents
MKP	MAPK Phosphatase
MMP	Matrix Mellaoproteases
MVBs	Multivesicular Bodies
NBM	Neurobasal Medium
NGF	Nerve Growth Factor
NTF	Neurotrophic Factors
NT3	Neurotrophin 3
NT4	Neurotrophin 4
PBS	Phosphate Buffer Saline

PC	Prohormone Convertases
PCR	Polymerase Chain Reaction
PDMS	Polydimethylsiloxane
PI3K	Phosphoinositide 3-Kinase
PKC	Protein Kinase C
PLC	Phospholipase C
PNS	Peripheral Nervous System
RFP	Red Fluorescent Protein
RPM	Rotations per Minute
SEM	Standard Error of the Mean
TBS	Tris Buffer Saline
TGN	Trans-Golgi Network
TRITC	Tetramethylrhodamine Isothiocynate
TRK	Tropomyosin Receptor Kinase
WT	Wild-type

1 Introduction

1.1 Neurotrophic Factors

Growth factors play a critical role in the development and maintenance of the nervous system[1]. Among them are a family of highly conserved secretory proteins known as neurotrophic factors that influence the activity of neuronal cells as well as the vasculature in the central and peripheral nervous system[2,3]. The family of structurally related neurotrophins include nerve-growth factor (NGF), brain-derived neurotrophic factor (BDNF), neurotrophin (NT)3 and NT4[4]. Neurotrophic factors bind to two distinct types of receptors: a high affinity tropomyosin receptor kinase (Trk)[5] and a low affinity nerve growth factor receptor, p75[6]. All neurotrophic factors bind to p75 with similar nanomolar affinities[7]. There are three types of Trk receptors: TrkA, TrkB and TrkC that are all expressed on the plasma membrane. Secreted NGF binds to TrkA, BDNF and NT4 binds to TrkB and NT3 binds to TrkC and with lower affinity to TrkA (Figure 1-1)[8].

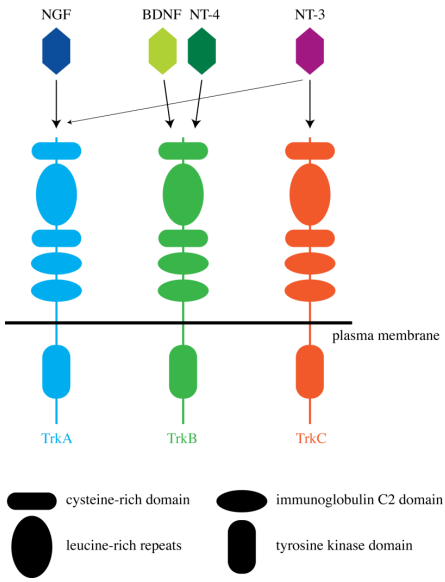

Figure 1-1 Neurotrophins and Trk neurotrophin receptor family of proteins.
Figure highlighting the fate of neurotrophic ligand and receptor interaction. Where secreted NGF binds to TrkA, BDNF and NT4 binds to TrkB and NT3 binds to TrkC and with lower affinity to TrkA. P75 receptor interaction is not shown in this diagram (Figure taken from Deinhardt & Jeanneteau, 2012).

1.1.1 Nerve Growth Factor (NGF)

NGF was the first growth factor to be identified as part of the neurotrophic growth factor family[10]. In the peripheral nervous system (PNS), it is an essential cue for neuronal survival and growth[11]. Produced by target cells, NGF specifically binds to TrkA receptors on the plasma membrane[12]. The NGF-TrkA complex is internalised and undergoes retrograde transport over long distances along the axon to the cell soma[13]. During this time, the NGF-TrkA complex can continuously signal and the autophosphorylation of TrkA is maintained during the complex transport to the cell body, where CREB is phosphorylated[14]. Eventually the NGF-TrkA complex becomes degraded in lysosomes[15]. The retrograde transport of neurotrophic factors was first established for NGF, but now extends to all neurotrophins[15].

1.1.2 Neurotrophin 3 (NT3)

NT3 is required for the survival of neuronal populations where it binds to TrkC to induce a survival response and with lower affinities to TrkA[16]. Studies haves used NT3 knockout mice and found severe disruptions of cholinergic axonal ingrowth[16]. During rodent development at late foetal stages, basal forebrain cholinergic neurons send out axons that reach the deep cortex layers and the hippocampus[16]. Studies have shown axonal grow into the cortical regions that express NT3[17]. Expression of NT3 is widespread in developing cortex compared to the mature cortex and it appears that the cholinergic axons are the first to arrive in the cortex, extending into regions which express NT3[18]. Moreover, Kuruvilla and colleagues (2004) show NT3 and NGF signal via TrkA to influence sympathetic neuron development, with NT3 supporting axon growth and NGF supporting both neuronal growth and survival[19].

1.1.3 Neurotrophin 4 (NT4)

BDNF (described in section 1.2) and NT4 both have similar high affinities with TrkB, influencing cell fate. NT4 plays a role in synaptic plasticity, similar to BDNF[20]. NT4 enhances glutamatergic synaptic transmission in cultured hippocampal neurons[21], where overexpression of NT4 in Xenopus nerve muscle cultures results in increased spontaneous synaptic activity and enhanced synaptic transmission[22]. Studies have also shown that BDNF and NT4 increase neurite outgrowth and elongation rates in mammalian cerebellar mossy fibres[23]. Regardless of the similarities between BDNF and NT4, it has been demonstrated that NT4 cannot compensate for the loss of BDNF function. Jaenisch and colleagues (2000) replaced the coding region of BDNF, with the NT4 sequence in mice[24]. They found mice expressing NT4 in place of BDNF were viable compared to BDNF null mice, which died shortly after birth. However, the mice expressing NT4 in place of BDNF showed reduced body weight, neck skin lesions and other vasculature defects. This shows that replacing the BDNF coding sequence cannot fully restore the health of mice to the same extent of BDNF actions. This demonstrates the unique properties of both BDNF and NT4 signalling via the same TrkB receptor[24].

1.2 Brain Derived Neurotrophic Factor (BDNF)

BDNF is encoded by the *BDNF* gene (Figure 1-2) and is the second member of the neurotrophic family to be discovered after NGF[25]. BDNF transcription is a highly regulated process, where two forms of BDNF mRNA are transcribed. Long 3'UTR BDNF is located in the dendrites, and it is thought that upon neuronal activity, this mRNA is translated and release from the dendrites whereas short 3'UTR mRNA is restricted to the cell soma[26]. Mu-Ming Poo and colleagues (2014) show dendritic release of BDNF at sites where glutamate was applied[27]. Once secreted, neurotrophic factors are able to bind to their receptors (which are expressed across the entire plasma membrane) and undergo retrograde transport[28].

The expression of BDNF in the mammalian brain is widespread and regulated by neuronal activity[29]. In the adult brain, BDNF promotes neurogenesis[30], dendritic spine organisation, axonal branching and synaptic strengthening via the activation of TrkB receptors[31]. The role of BDNF in mammalian central nervous system and its expression during normal aging and disease will be discussed in detail in this review.

1.2.1 Autocrine actions of BDNF

The human BDNF gene has eleven exons of which, exons 1-10 are noncoding exons and exon 11 encodes the BDNF protein[32] (Figure 1-2). In the human BDNF gene, there are nine functional promoters that produce 24 different transcripts that can be translated into an identical mature BDNF protein[32]. Within the *BDNF* gene, exon IV and I transcription is calcium-dependent. The promoter region of BDNF exon IV contains three calcium response (CRE) elements.

BDNF is shown to act in an autocrine manner where BDNF activity-dependent secretion and subsequent binding to TrkB causes an influx of calcium via PLCɣ activity (described in section 1.5.3). Activated PLCɣ leads to further calcium release from ER stores, and induces BDNF transcription. This goes to release BDNF and thus forms a positive feedback loop[33].

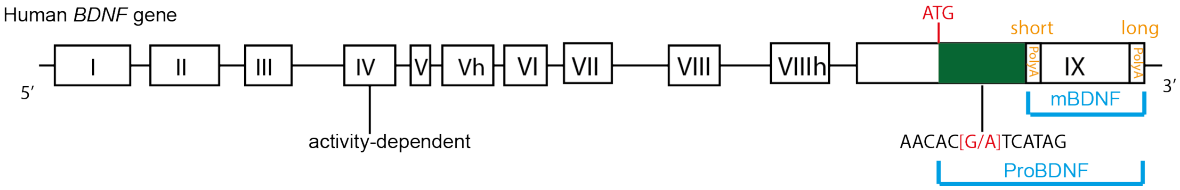

Figure 1-2 Simplified schematic representation of the human *BDNF* gene.
Human *BDNF* gene consists of eleven exons (I-IX, plus Vh and VIIIh). Exon IV is activity dependent. The coding sequence (green box) is in exon IX with an ATG start codon for transcription. Within this sequence lies the G>A single neucleotide polymorphism at codon 66 (valine to methionine, inidcated in red). The 3'-UTS of BDNF is composed of either short or long polyA tail.

1.2.2 proBDNF

All neurotrophic factors are initially synthesised as precursor proteins which undergo various processing to generate pro and mature forms (mature form discussed in section 1.3). To briefly review the processing of BDNF, BDNF is translated as a pre-proprotein (proBDNF) that contains an N-terminal pro-domain and a C-terminal mature-domain (mBDNF)[34]. Cleavage of proBDNF by furin or proconvertases in the trans-Golgi network or in secretory granules, respectively, generates a pro-domain and mBDNF[35]. Alternatively, proBDNF can be released and cleaved extracellularly by plasmin or matrix metalloproteinases to produce the mature form of BDNF[36].

In neonatal rodent brains, the expression of the proBDNF is relatively low, but it increases during adolescence and adulthood, similar to mBDNF[37]. Moreover, parallel to mBDNF, the pro-domain is released from neurons upon depolarisation[38]. Once released, proBDNF

can induce neuronal apoptosis via p75 receptor binding[38]. Bai Lu and colleagues (2004) have shown proBDNF to play a role in hippocampal plasticity. They found proBDNF induced apoptosis in hippocampal slices. In terms of morphological changes, the prodomain is also shown negatively regulate neuronal remodelling and induce acute growth cone retraction[35,39]. This highlights the 'ying and yang' properties of BDNF and proBDNF and demonstrates the importance of the cleavage process during BDNF synthesis.

1.2.3 BDNF polymorphism

Within the human *BDNF* gene (Figure 1-2), at codon 66, there is a single nucleotide polymorphism (SNP) leading to a valine (Val) to methionine (Met) substation within the pro-domain[34]. This has been identified in approximately 25% of the population[35] . The BDNF Val66Met polymorphism is associated with altered memory and implicated in several neurological and psychiatric disorders[35]. Those exhibiting this mutation have altered memory and an increased risk of developing anxiety and depression in humans. It should be noted that this is seen in Caucasian population only[34,40,41].

In terms of the mechanistic implications, the Met66-pro-domain-BDNF variant demonstrates decreased binding to sortilin which results in altered intercellular trafficking and reduced secretion[34,42]. Sortilin is a protein that acts as a chaperone to direct intracellular trafficking of pro-BDNF to the regulated secretory pathway (see section 1.3.1)[35]. This alteration is found to affect neuronal cells in the CNS exclusively[42]. Looking closer at the role of the pro-domain, the Met66-pro-domain results in acute growth cone retraction in hippocampal neurons[35]. This action was not elicited by the Val66 pro-domain. These negative actions on neuronal morphology by the Met66 pro-domain is mediated by the SorCS2 receptor (sortilin-related VPS10 domain containing receptor 2) that serves as a co-receptor with p75[43]. Through this polymorphism, the Met66 pro-domain is identified as a new active ligand that negatively modulates neuronal morphology via p75 and SorCS2 receptors[35,37,43].

1.3 Biosynthesis of BDNF

BDNF, like other neurotrophic factors, is synthesised as a precursor in the endoplasmic reticulum (ER) as a 32 kDa precursor protein (proBDNF). ProBDNF moves through the Golgi to the trans Golgi network (TGN) where it goes into one of two secretory pathways: regulated or constitutive (Figure 1-3).For the regulatory pathway, BDNF binds to lipid-raft-associated sorting receptor carboxypeptidase E (CPE) in the TGN[44]. These vesicles are transported to areas for activity-dependent release. The rise in cytosolic calcium concentrations triggers fusion of the secretory vesicle membranes with the plasma membrane, releasing the BDNF[45]. Calcium concentrations are detected via calcium detectors synaptotagmin-6[46] and synaptotagmin-4[47] which localises with BDNF-containing vesicles. Within the constitutive pathway, proteins are continuously released. Here, BDNF is packaged at the TGN similar to what occurs in the regulated secretory pathway. The BDNF vesicles are then transported to the plasma membrane where they fuse and can release both pro and mature forms of BDNF[48].

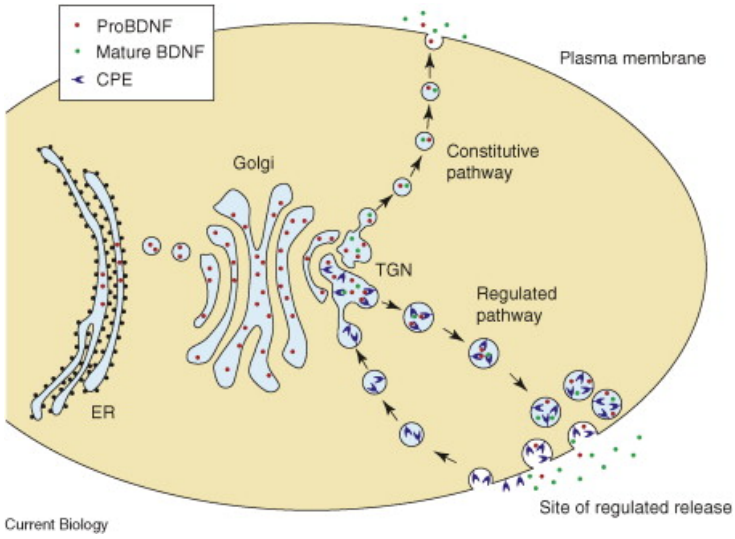

Figure 1-3 BDNF release via the regulatory and constitutive pathways.
BDNF is released from cells via the regulatory or constitutive secretory pathways. BDNF undergoes various processed via the ER, to the Golgi, into the TGN and finally released from the cell. The presence of CPE in secretory vesicles is indicative of the regulatory pathway. (Figure taken from Thomas & Davies, 2005).

1.3.1 BDNF processing

In the TGN, proBDNF can be cleaved intracellularly by prohormone convertases (PCs)[49] and/or furin and secreted as a 14 kDa mature BDNF protein[2] (Figure 1-4). Proteolytic conversion of proBDNF to mature BDNF can occur extracellularly by proteases such as plasmin and matrix metalloproteases (MMPs)[28]. The mature forms of neurotrophic factors elicit their biological processes by binding to their respective Trk receptors [2]. However, pro-neurotrophins elicit functions via p75 receptor binding[50,51]. The activation of p75 leads to apoptotic signalling, an effect in direct contrast to the pro-survival action of mature neurotrophic factors[52]. Thus, the proteolytic cleavage of pro-neurotrophins is an important regulatory process for neurotrophic function[53]. From herein, mature BDNF will be referred to as BDNF unless specified otherwise.

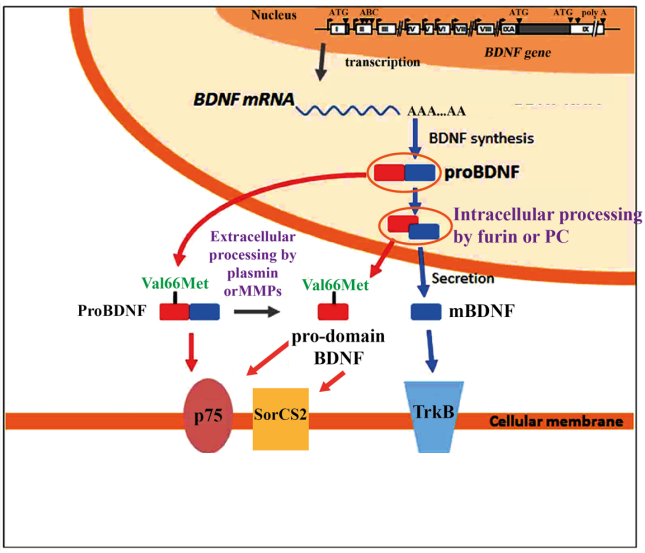

Figure 1-4 Schematic representing the synthesis and processing of BDNF. The BDNF gene is transcribed to BDNF mRNA, which is then targeted for translation to pro-BDNF. This is either released or cleaved before release by furin or proconvertases (PC). The cleaved mature BDNF (mBDNF) binds to TrkB. The released pro-BDNF can bind to p75 or be cleaved extracellularly by plasmin or MMPs to generate mBDNF and the pro-domain BDNF. The pro-domain can bind to P75 and SorCS2 receptors. Within the pro-domain of BDNF lies the Val66Met polymorphism recorded in roughly 25% of the population (Figure adapted from Mizui et al., 2014).

1.4 BDNF internalisation and regulation

BDNF bound to TrkB is internalised and encapsulated within an endosome. Multiple studies have isolated and characterised these endosomes in an attempt to understand the mechanisms that drive retrograde transport of neurotrophic factors. Howe and colleagues (2001) observed clathrin-coated vesicles (CCVs) that carry neurotrophic signals retrogradely to the cell body[55]. Clathrin proteins form a triskelion structure around the endocytosed vesicle. The recruitment of clathrin-mediated endocytosis occurs via adaptor proteins which are a major component of the vesicle that sits in the inner layer of the coat, between the clathrin cage and the membrane. Studies have shown AP2 adaptor protein to mediate BDNF-TrkB endocytosis[56].

Once internalised, BDNF-TrkB endosomes can be destined to one of three pathways: degradation, recycling of TrkB receptors or long-distance signalling. This process is regulated by Rab proteins. The presence of specific Rab proteins to these endosomes are indicative of the pathway destined for BDNF-TrkB complex (i.e. signalling, recycling or degradation).

Deinhardt *et al* (2006) show Rab5-positive endosomes are present in the early stages of the sorting pathway. These Rab5 endosomes are present shortly after BDNF-TrkB internalisation[57]. The signalling endosomes that are transported to the cell body are Rab7-positive. They studied the transport of a fragment of tetanus neurotoxin (TeNT Hc) which shares that same retrograde transport pathway to BDNF[57]. They observed, that moving vesicles occur through Rab7-positive endosomes, whereas Rab5 endosomes remain stationary[57]. This further support the notion that Rab5-positive endosomes occur during the early stages of BDNF-TrkB transport.

The other routes taken by BDNF-TrkB once internalised is the recycling and degradation pathway. The recycling of TrkB back to the plasma membrane occurs through Rab11-positive endosomes[58]. Alternatively the BDNF-TrkB complex can become degraded in the

lysosome[59]. The mechanism by which BDNF-TrkB complex moves into the late endosome from the early endosome is thought to occur via maturing endosomes called multivesicular bodies (MVBs)[60]. In MVBs, the bound BDNF and TrkB complex could separate, and in turn, sequester any signal, resulting in dampened BDNF signalling. However, the precise mechanism by which BDNF unbinds from TrkB in the MVB remains unclear. The sorting of BDNF-TrkB complex into the degradation pathway requires ubiquitin tags[60]. These ubiquitin tags are recognised by ESCRT proteins (endosomal sorting complex required for transport), which bind to the intraluminal vesicles in MVBs[60]. From the MVBs, degradation occurs in the late endosome. The mature lysosomes form from the late endosome by a gradual maturation process. The lysosome is pH is 5.0 and this acidic environment is maintained by the H+ pump[60].

1.5 Signalling pathway

The binding of neurotrophins to the Trk receptors induced autophosphorylation of several conserved tyrosine sites in the cytoplasmic domains of each receptor[61]. Three of these (Y702, Y706 and Y707 in human TrkB) form an activation loop of the kinase domain[62]. Phosphorylation of additional tyrosine residues (Y516 and Y817) create docking sites for adaptor such as SH2 for Y516, and recruitment of phospholipase C (PLC)γ pathway for Y817[63]. These adaptors activate various intracellular signalling pathways, the three most well-characterised pathways include: (1) the phosphoinositide (PI)3-kinase(PI3K)/Akt, (2) PLCɣ and (3) the mitogen-activated protein kinases/extracellular signal-regulated kinases (MAPK/Erk) pathway[53,62,64]. Thus, the phosphorylation of these residues is required to activate the downstream signalling pathways (Figure 1-5).

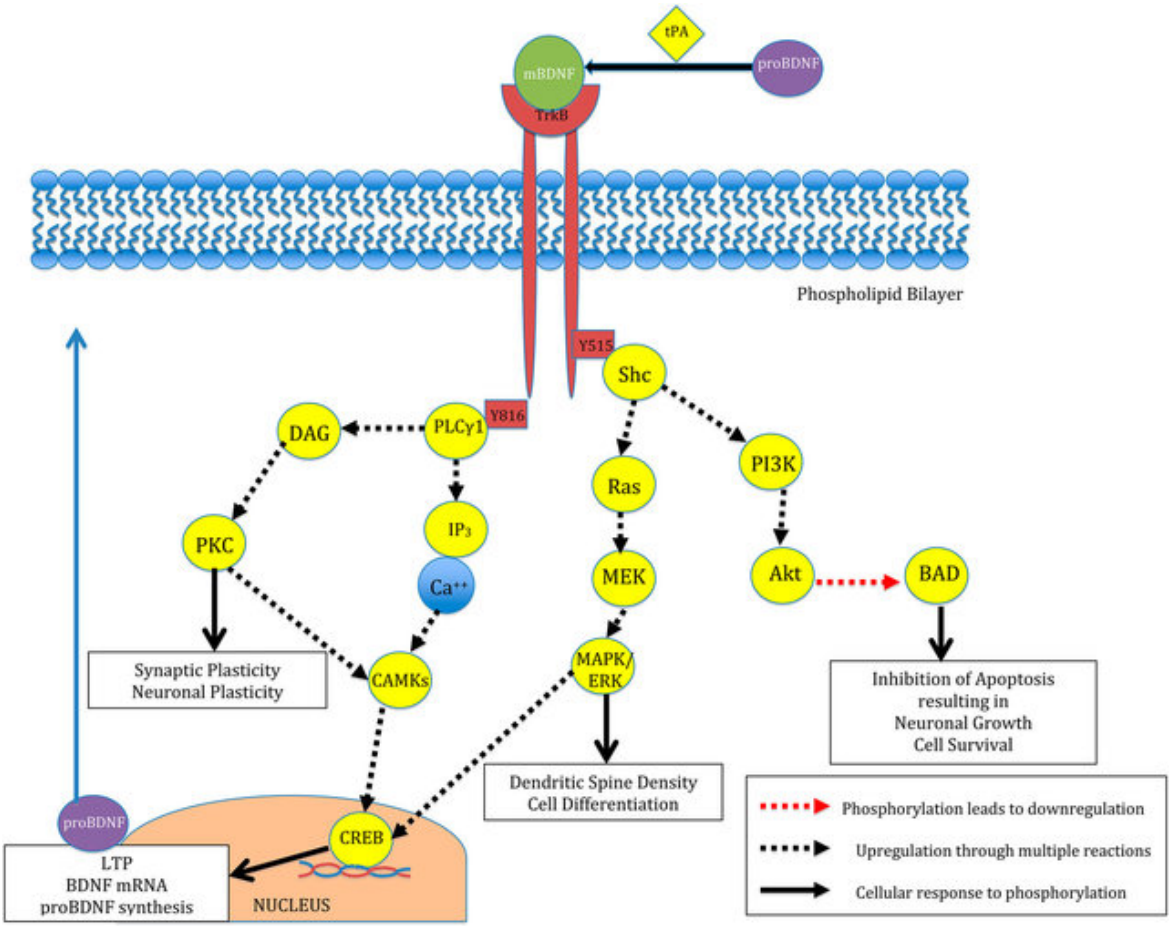

Figure 1-5 Detailed illustration of the BDNF signalling pathways.

BDNF binds to the extracellular domain of TrkB which induces dimerisation and activation of the intracellular tyrosine kinase domain (Y702, Y706, Y707). This results in autophosphorylation of tyrosine residues (Y516 for human and Y515 for rodents, Y817) that serve as sites for the interaction of adaptor proteins and the subsequent activation of intracellular signalling cascades: the MAPK, PI3K/Akt and the PLCγ pathways. Phosphorylation of tyrosine 516 of TrkB recruits the Shc adaptor protein, followed by the recruitment of Grb2 and SOS. This leads to the activation of the Ras–MAPK pathway. Shc–Grb2 can also lead to recruitment of GAB1 and the activation of the PI3K–Akt pathway. Phosphorylation of the TrkB tyrosine residue 817 recruits PLCγ, which leads to the formation of IP3 and the regulation of intracellular Ca^{2+} and DAG, which activates PKC. The activation of these pathways leads to the transcription of IEGs that regulates cellular activity.(Image taken from Slutsky & Etnier, 2016).

1.5.1 P13K/Akt

Phosphorylation of TrkB at Y516 creates a Shc binding site[66]. This activates phosphatidylinositol 3-kinase (PI3K) via growth factor receptor bound protein 2 (Grb2) and GRB2-associated binding protein 1 (Gab1). Subsequently, Akt translocates to the plasma membrane initiating its activation[28].

A critical role of Akt is to promote cell survival downstream of BDNF-TrkB activation[56]. Increased cell survival occurs via this pathway as pro-apoptotic processes are blocked[56]. Akt is responsible for directly phosphorylating and inhibiting activity of BAD, a member of the Bcl2 homology domain-3 (BH3)-only proteins responsible for cell death[67]. It is reported that PI3K-Akt pathways is able to crosstalk with other pathways to induce pro-survival signalling[56]. Under certain conditions, activation of PI3K-Akt inhibits JNK/p38 apoptotic signalling[68]. Thus, Akt is able to act as a versatile mediator of cell survival.

1.5.2 MAPK/ERK

Mitogen-activated protein kinases (MAPKs) are a group of kinases that convert extracellular stimuli into a cellular response. They evolutionarily conserved TxY motif must be phosphorylated on both threonine and tyrosine residues and induce transcription factors[69]. MAPKs includes the extracellular signal-regulated kinase 1/2 (Erk1/2), c-Jun (N)-terminal kinases 1/2/3 (JNK1/2/3), p38 isoforms (α, β, γ, and δ) and Erk5[70].

Each of these MAPKs cascades are composed of a set of three acting kinases: a MAPK (noted above), a MAPK kinase (MAPKK) and a MAPKK kinase (MAPKKK). The MAPKKKs are protein Ser/Thr kinases and are activated in response to extracellular stimuli. The MAPKKK activation leads to the phosphorylation and activation of MAPKK, which then subsequently stimulates MAPK activity. This leads to the phosphorylation of

several substrates known as MAPK-activated protein kinases (MAPKAPKs)[70] (Figure 1-6).

The highly conserved Erk1/2 pathway is activated at the conserved Thr-Glu-Tyr (TEY) motif, upon BDNF-TrkB binding leading the autophosphorylation of residue Y516 located at the intracellular segment of TrkB[69]. This initiates the recruitment of Shc that interacts with Grb2, in-turn activating guanine nucleotide exchange factor SOS[71]. SOS stimulates the removal of GDP from Ras, in exchange for GTP and activates Ras. Once active, Ras initiates downstream kinases Raf-B (MAPKKK), MEK1/2 (MAPKK) and Erk1/2 (MAPK)[53,61]. The phosphorylation of Raf-B activates MEK, which subsequently activates Erk1/2. The phosphorylated Erk1/2 translocates to the nucleus from the cytosol where it influences transcriptional changes[72].

1.5.2.1 Role of MAPKs in the CNS

There is substantial evidence that MAPK has an important role in spatial learning[73]. To support this view mice carrying a mutation in the downstream activator of the Erk1/2 pathway, Ras, show defects in spatial learning memory[74]. Reports have also suggested that induction of long-term potentiation (LTP, a process whereby persistence stimulation during membrane depolarisation results in long-lasting strengthening of synapses) in the hippocampus activates MAPK[75,76]. Together, this highlights the importance of MAPK/Erk signalling in establishing LTP and supporting its involvement memory consolidation.

Erk5 is another MAPK, however it is much larger in comparison to Erk1/2 (88 kDa vs. 42-44 kDa, respectively). The N-terminal sequence of Erk5 is homologous to Erk1/2[77]. It contains a large C-terminus of 400 amino acids which is not found in the other MAPKs. Erk5 is phosphorylated by MEK5, which is specific to Erk5, as it does not phosphorylate any other MAPKs[70,77]. In terms of its role, the expression of Erk5 is found in the brain during early embryonic development, after which it declines as the brain matures. Studies have highlighted the importance of the Erk5 during this developmental period, as Erk5 knockout is lethal in mice[78].

Upon BDNF binding to TrkB on the plasma membrane, the receptor-mediated endocytosis activates Erk5 in both the PNS and CNS. MEKK2/3 and MEK5 have been identified as upstream components in Erk5 signalling[79]. Studies have looked at the role of Erk1/2 and Erk5 within rodent primary cultures to see if there are any overlapping similarities within these two kinases. Inhibition of both Erk1/2 and Erk5, shows an increase in BDNF mRNA, whereas MEK1/2 specific inhibition did not affect BDNF mRNA levels. Furthermore, this study transfected a dominant active construct of Erk5 into C6 cells (rat glial tumour cells), which resulted in the suppression of BDNF expression[77]. However, in cultured DRG neurons, BDNF stimulation in distal axons resulted in retrograde signalling and induction of Erk5 in the cell soma and subsequent neuronal survival[80]. Therefore, Erk1/2 and Erk5 may have distinct roles on BDNF expression.

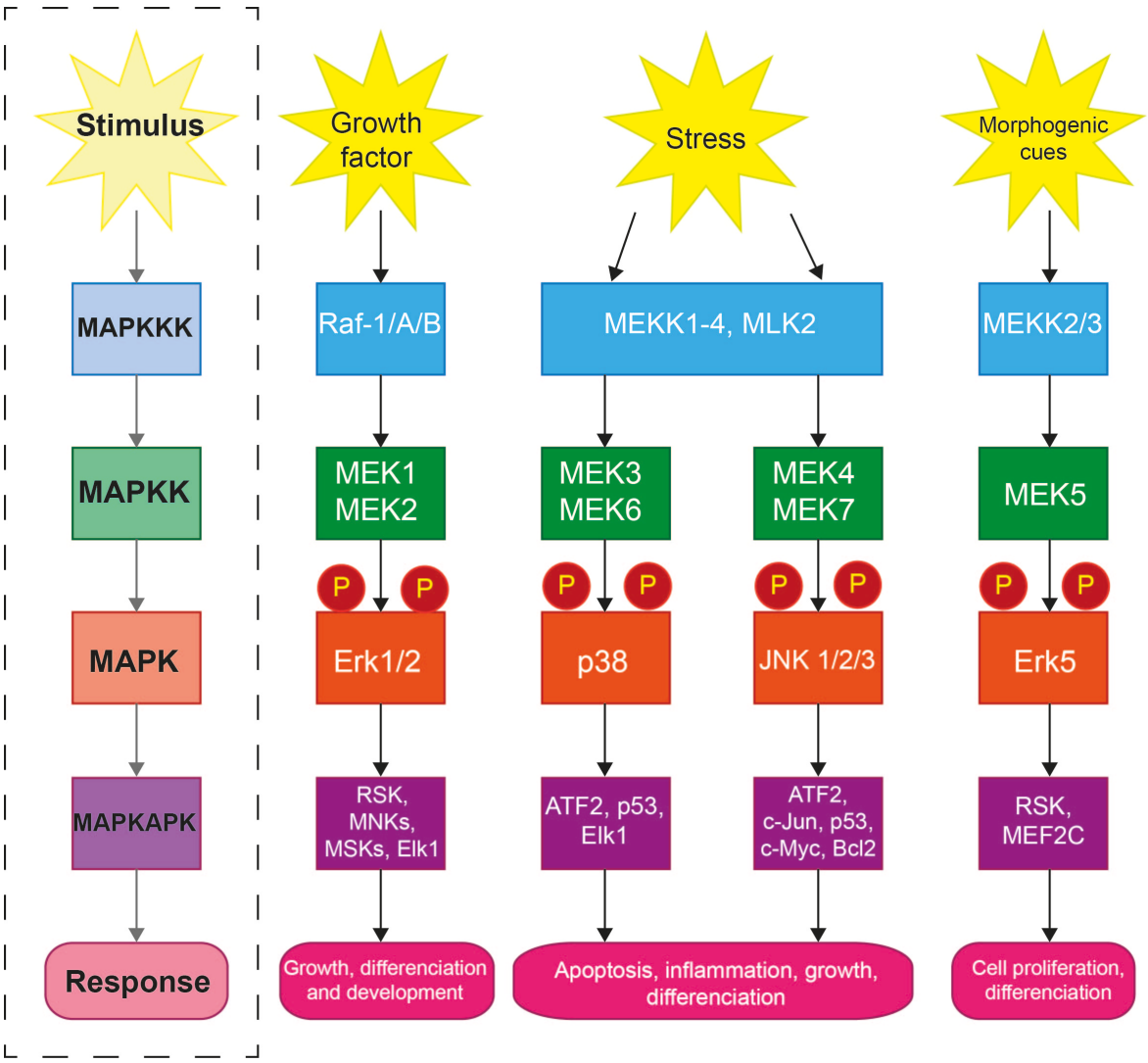

Figure 1-6 Simplified overview of mammalian MAPK family pathways.
There are four distinct MAPK cascades: ERK1/2, ERK5, p38 (α, β, γ, δ) and JNK 1/2/3. Mitogens such as growth factors or environmental stresses act via specific receptors to stimulate the MAPK activation. In the case of neurotrophic factors, activation of Trk receptors or p75 receptors activates MAPKs. The response phosphorylates MAPKKK, which sequentially phosphorylates and activates the downstream MAPKK. The MAPKK in turn dual phosphorylates (shown by circled P) specific threonine (T) and tyrosine (Y) residues of the conserved T–x–Y motif present within the kinase domain. This leads to a variety of downstream substrate activation such as transcription factors that become phosphorylated and elicit transcriptional changes resulting in a specific cellular response such as cellular proliferation/differentiation, sustained cellular survival or the initiation of cell death by apoptosis.

1.5.3 PLCɣ

The phosphorylation of TrkB at Y817, recruits and activates PLCɣ, which hydrolyses phosphatidylinositol(4,5)biphosphate ($PI(4,5)P_2$) into diacylglycerol (DAG) and inositol tris-phosphate (IP_3)[28]. The production of DAG activates protein kinase C (PKC), which induces ERK signalling[6]. In contrast, IP_3 activation results in increased intracellular Ca^{2+} levels, activating calcium-calmodulin dependent kinase (CamKII) and the phosphatase calcineurin[66]. These elevated calcium levels are particularly important in BDNF signalling in the postsynaptic cell[81].

PLCɣ plays a role in cell proliferation, survival and differentiation; and in regulating synaptic plasticity[82]. Several studies have also found PLCɣ to be involved in the modulation of synaptic activity[5]. Numakawa *et al* (2002) found increased PLCɣ expression in immature cortical neurons in neonatal rats at days *in vitro* (*DIV*) 5, alongside spontaneous calcium oscillations[83]. It has been established that spontaneous calcium oscillations coincide with the formation of synapses and this oscillation plays a role in the expression of neurotransmitters and neurite extension[84]. Therefore, the ability of PLCɣ to generate calcium signals is essential in regulating calcium oscillation, and in turn, mediates changes in synaptic plasticity.

1.5.4 Immediate early gene activation

Immediate early genes (IEGs) are rapidly activated by multiple signalling cascades and play an essential role in LTP[72], strengthening of synapses and enhanced cell morphology here, Arc, Fos, and egr1 will be discussed.

1.5.4.1 Activity-Regulated Cytoskeleton-Associated Protein (Arc)

The activity-regulated cytoskeletal-associated protein, Arc, is regulated by BDNF activity[85]. Arc is thought to be involved in the stabilisation of synaptic changes and synaptic plasticity, influence LTP and regulate the consolidation of long-term memory[86].

As discussed previously, MAPK/Erk, PLCɣ and PI3K/Akt are the three major pathways activated by BDNF-TrkB initiation[29]. Studies have previously shown that Arc expression is dependent on the MAPK/Erk pathway. Inhibition of MEK with U0126, a pharmacological inhibitor, significantly suppresses Arc expression upon BDNF stimulation[29,86]. However, the inhibition of the PLCɣ pathway with U73122 inhibitor, had no effect on Arc up-regulation[29].

During synaptic activity, levels of Arc mRNA are increased[87]. Moreover, the distribution of Arc mRNA in dendrites localises to areas of synaptic activity[88]. To determine the effects of BDNF stimulation on dendritic translation of Arc, Yin *et al* (2001) quantified BDNF-induced changes in synaptic Arc levels. They suggest a selective up-regulation of Arc expression upon BDNF stimulation[89]. Arc mRNA is promptly synthesised in response to LTP stimulation[90] and transported to active regions of dendrites, its role in synaptic plasticity has been well established[91].

1.5.4.2 Fos

The IEG *Fos* is thought to play an active role in neuronal survival[92,93]. *Fos* forms a heterodimeric transcriptional factor with Jun family of proteins forming activator protein-1 (AP-1)[94]. To determine which signalling pathways, govern *Fos* activity, studies have incubated cells with pharmacological inhibitors of the three activation pathways. They found, that upon MAPK/Erk inhibition, *Fos* activity is diminished[95]. Studies have also

found increased *Fos* activity during learning processes. Anokhin *et al* (1991) found elevated levels of *Fos* mRNA in cerebral cortex of young chicks upon experience dependent stimulation[96]. Conversely, animals with Fos deficiency show spatial and associated learning difficulties correlating with decrease in synaptic plasticity. These studies confirm a direct relationship between Fos activity and learning[96].

1.5.4.3 Early Growth Response 1 (EGR1)

EGR1 (also known as zif268), was discovered as an IEG by its response to NGF treatment in neuronal differentiation[97]. It is widely studied for its role in reconsolidation of memory and its ability to establish long-term spatial localisation memories[98]. In the rat brain, constitutive expression of egr1 mRNA and protein is expressed in several areas of the neocortex, cerebellar cortex, the striatum and in the hippocampus and immunoreactivity of egr1 is found in the nucleus[99].

As the MAPK/ERK pathway is implicated in Arc and Fos activity, the role of MAPK/Erk seems promising in the activation of EGR1[100]. Similar to Arc and Fos, independent studies have either (1) blocked MAPK/ERK activation, (2) inhibited CREB function or (3) inactivated egr1, all of which resulted in deficits in LTP and long-term memory recognition[101]. To further support this view, two independent groups show an increased activation of egr1 in the dentate gyrus after LTP induction. Studies have used mutant mice to highlight the link between egr1 and LTP. Jones *et al* (2001) examined the performance of mutant egr1 mice in a complex task and found egr1 mutant mice were severely impaired in recognising novel objects 24 hours after its initial exposure[100]. They concluded that LTP, which was normal in the first hour was not sustained over 24 hours in awake animals. Together with evidence above, egr1 activity via MAPK/ERK signalling pathway is induced upon BDNF stimulation and is sufficient to modify molecular changes essential for the formation of long-term memories via synaptic plasticity.

1.6 Trk receptor activity

All neurotrophins dimerise and bind to their respective Trk receptors with high affinity. TrkA was the first identified tropomyosin-related kinase; later TrkB and TrkC were identified due to their high homology to TrkA[61]. Thus, all Trk receptors share a common structural organisation of their extracellular domains. All Trk receptors have three leucine-rich 24-residue motifs flanked by two cysteine clusters[53]. There are two C2-type immunoglobulin-like domains adjacent to these structures, followed by a single transmembrane domain and a cytoplasmic domain that contains a tyrosine kinase domain as well as several tyrosine-containing motifs[5,102,103]. Neurotrophins binding to the Trk receptors resulting in autophosphorylation of the cytoplasmic tyrosine that regulates the tyrosine kinase activity[12,63,10412,63,104]. This in turn allows the recruitment of adaptor molecules that mediate the initiation of the intracellular signalling cascade (discussed in section 1.5)[1515]. The expression of TrkB receptors along neuronal cells is widespread. Trk receptors are expressed along the entire length of surface of the plasma membrane[105]. TrkB receptors are also found to be expressed within the cells in endosomes, with an increased expression in the soma (where TrkB receptor are synthesised)[105]. This is in contrast to truncated TrkB receptors which are expressed mainly in somato-dendritic compartments and proximal processes[105].

Depending on the homeostatic status of the cell, Trk receptors can undergo degradation, where the receptors are internalised, even if bound to BDNF. The degradation pathway is one of three which can occur during endocytic trafficking. A study has found TrkB receptors are predominantly sorted to the degradation pathway, whereas TrkA is predominantly sorted to the recycling pathway[106]. This is occurs due to the specific juxtamembrane region within TrkA receptors, that when transplanted in TrkB, also changes TrkB receptor sorting to the recycling pathway[106]. This difference is evolutionary as TrkA receptors emit survival signals and therefore recycling TrkA will increase the number of receptors on the surface, allowing increased NGF binding[1,14]. However, for TrkB, increased recycling would result in over stimulation and toxicity of the cells[37,107].

1.6.1 Isoforms of Trk receptors

Differential splicing of exons results in various forms of Trk isoforms[108]. RNA splicing of TrkB generates three well characterised TrkB isoforms that bind to BDNF and NT4 (Figure 1-7). The first is a full length TrkB (FL-TrkB) isoform that has an extracellular ligand-binding domain and an intracellular kinase domain[108]. The other two isoforms, T1-TrkB and T2-TrkB have the same extracellular domain as the FL-TrkB, but lack the intracellular kinase domain and are known as 'truncated TrkB'[28,61]. The function of T1-TrkB and T2-TrkB receptors are thought to have dominant negative effects and sequester neurotrophic signalling[109]. For instance, when BDNF binds to the T1 isoform, autophosphorylation fails to occur (due to the absence of the tyrosine kinase domains). These truncated forms are also able to dimerise with the FL-Trk receptors, directly inhibiting the activation of downstream neurotrophic-mediated pathways[109]. A study by Tessarollo and colleagues investigated the role of truncated TrkB receptors in motor neurons. They found the deletion of T1-TrkB in mice expressing the human SOD1 mutation (a mutation commonly found in patients with this disease), slowed the onset of disease and delayed the development of muscle weakness, a common feature in motor neuron disease[110]. Overall, their study demonstrates the role of truncated receptors in disease pathology and strengthens their role as dominant-negative receptors. Thus, the variations in the Trk receptors can have distinct effects on the cell, regulating the activation of the signalling cascade.

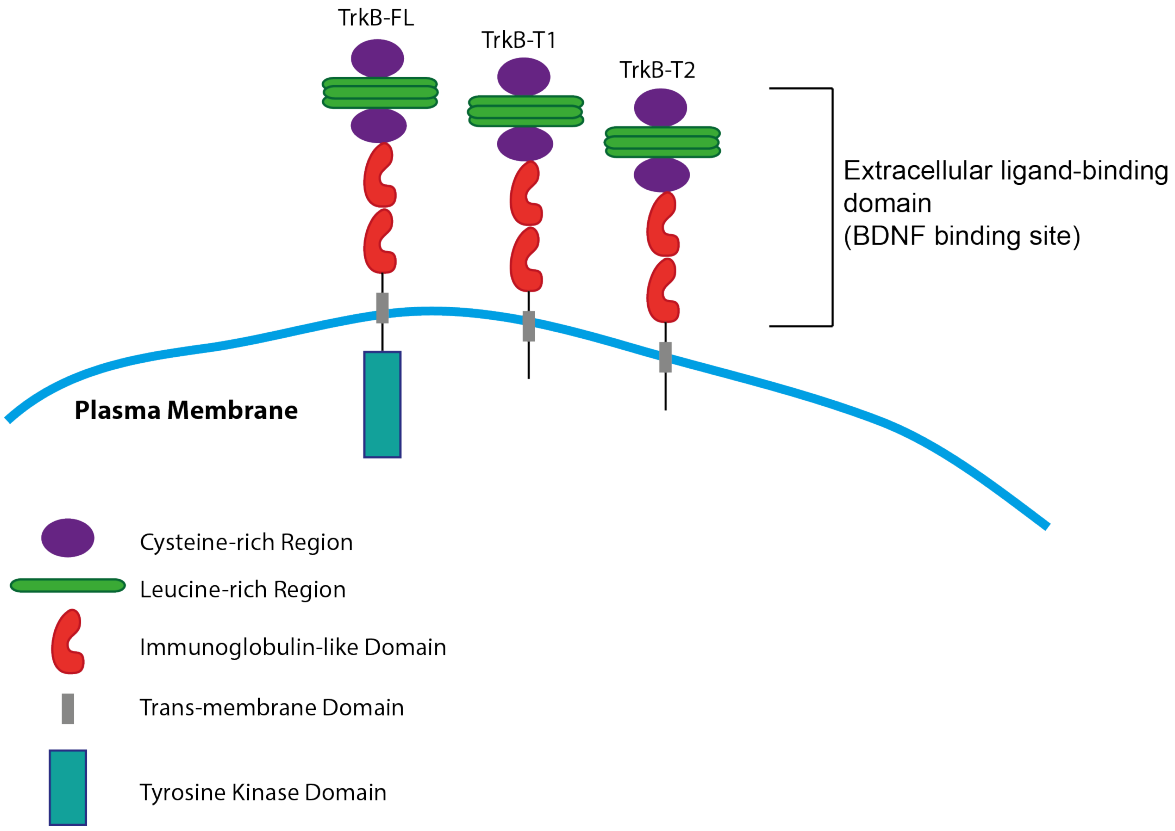

Figure 1-7 Schematic illustration of the TrkB receptor isoforms.

All isoforms of contain two cysteine rich regions, leucine rich region and two immunoglobulin-like domains in the extracellular region and the transmembrane domain. These extracellular domains form the ligand-binding sites. Only the full-length TrkB (TrkB-FL) contains the tyrosine kinase domain. The truncated TrkB receptors (TrkB-T1 and TrkB-T2) lack this full cytoplasmic region, abolishing any signalling process.

1.7 Axonal transport

A large aspect of this project is focusing on the transport of neurotrophic factors, and the propagation of signals from far-stretching axonal ends to the cell soma. The transport of neurotrophic factors and themselves is bidirectional, undergoing both retrograde and anterograde transport[111]. The mechanisms that drive bidirectional transport is dependent on axonal integrity, and more importantly based on microtubule motor proteins[112].

Within a typical neuron, the longest protrusion is the axon, composed of unidirectional microtubule 'tracks'[113]. Along the microtubules are a diverse range of motor proteins, kinesins and dynein, which transport a wide range of neuronal cargo, one of which are neurotrophic factors[114]. The failure of these proteins to transport the ligand-receptor complex to the correct sites results in deregulated neurotrophic support, a common occurrence in many neurodegenerative diseases[111,115,116].

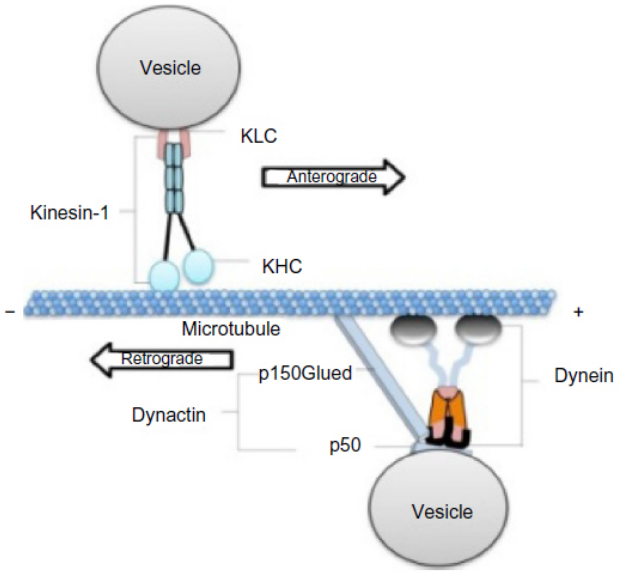

Figure 1-8 Kinesin-1 and cytoplasmic dynein motor complex on a microtubule for axonal transport.

Kinesin-1 through the KHC head motor domains binds to microtubules. Vesicles associate with kinesin-1 via the KLC (kinesin light chain). Cargo attached to kinesin-1 are transported anterogradely (towards the plus end of microtubules). Cytoplasmic dynein associates with dynactin for retrograde transport. Dynactin consists of multiple proteins, but only p150Glued and p50 are shown here. Dynein interacts with dynactin via p150Glued and DIC (dynein intermediate chain) subunits. Dynein binds to microtubules via the DHC (dynein heavy chain). Dynactin also associates with microtubules via the N-terminal globular domain of p150Glued. Dynein–dynactin motor complex transports cargoes retrogradely (toward the minus end of the microtubules). (Figure taken from Gunawardena, Anderson, & White, 2014).

1.7.1 Axon cytoskeleton

During this project, cell signalling from distal axons will be investigated. The term 'distal' in this case is defined as an axonal segment which is at minimum at least 50 μm away from the cell body. Within the CNS, axons are far stretching, and signals are relayed from great distances from nerve terminal ends[118]. Within the laboratory setting, an experimental platform will be established to investigate how signals from neuronal ends travel to the cell body and induce IEG induction. A microfluidic platform will be used to investigate long distance signalling (section 1.9).

Within the axonal stretch, the cytoskeleton is well-organised and contains specialised structures, including the axon initial segment (AIS) and presynaptic boutons. AIS is important for the initiation of action potentials and maintaining neuronal polarisation. The AIS is proximal to the axon with a dense cytoskeleton and scaffolding proteins[119]. The length of the AIS is approximately 40 μm in lengths[120]. In terms of the internal structure, the microtubules within the axon are composed of fast-growing plus-ends and stable minus-end[119]. The microtubules are orientated in a uniform manner, where plus ends are towards the distal end of the axon[121].

The distal axon areas measured during this project were beyond the AIS, and thus over 40 μm. In some experiments, distal regions were measured beyond 200 μm. The reason behind measuring such distances were two-fold, the first is because when using microfluidic devices to measure long distance signalling, the distal axonal ends will stretch over 500 μm in length from the microchannels into the axonal chamber; the second is because under physiological conditions, in the CNS, axons large distances.

1.7.2 Retrograde transport

Neurotrophic signals can relay retrogradely along the axon to the cell body, activating specific pathways to elicit growth and survival[122]. The motor molecules that drive retrograde transport are crucial for maintaining neurotrophic support during axonal insult and injury[123].

There are distinct phases of retrograde signalling. First, the ligand, such as BDNF, bind to its receptor, TrkB which is expressed on the plasma membrane[3], stimulating receptor-ligand internalisation, also known as a signalling endosome[86] . This receptor-ligand complex remains active and is targeted by specific retrograde microtubule-based motor proteins[124].

Having identified the characteristic of the endosomes, studies have examined how signals are rapidly propagated to the soma from the distal axon. Delcroix and colleagues (2003) provided evidence to suggest that in the DRG neurons, NGF signalling is transmitted retrogradely through an endosome that contains NGF, TrkA and activated signalling proteins (Erk and p38)[125]. Since then, multiple studies have identified active signalling proteins, pErk1/2 and pAkt within these endosomes, which mediate the rapid gene expression response[57,126,127]. These endosomes termed as 'signalling endosomes' due to the presence of active signalling proteins.

1.7.2.1 Dynein family (minus-end movement)

Dynein is the motor protein responsible for retrograde transport of BDNF-TrkB endosomes from synapses to the cell body, moving towards the minus end of the microtubules[114]. Dynein uses energy from ATP hydrolysis to function and fall into only two major classes based on function and structure: axonemal and cytoplasmic dyneins[128]. Axonemal dynein's

are responsible for ciliary and flagellar beating, whereas cytoplasmic dyneins are involved in intracellular transport, mitosis, cell polarisation and directed cell movement[129,130]. The movement of BDNF-TrkB endosomes is governed by cytoplasmic dyenins[131].

In brief, an axoneme is a highly specialised array of microtubules[130]. Motile axonemes in flagella and cilia consist of 20 microtubules, two of which are centrally located and nine are fused pairs, known as outer doublets that form a surrounding cylinder[130]. Dynein's connect the outer doubles and force them to slide against each other[128].

There are two forms of cytoplasmic dynein, cytoplasmic dynein 1 and cytoplasmic dynein 2[132]. Cytoplasmic dynein 1 is highly abundant in all microtubule-containing cells and is responsible for retrograde transport[133]. However, cytoplasmic dynein 2 is found exclusively within and around the base of flagella and cilia, where it is involved in retrograde intraflagellar transport and required for axonemal maintenance[130].

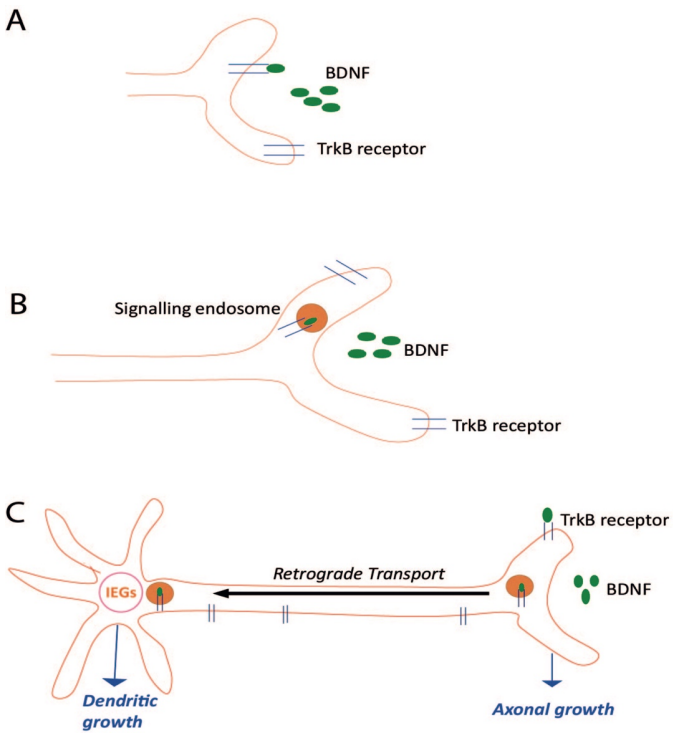

Figure 1-9 Schematic representing BDNF retrograde transport.
(A) BDNF binds to its receptor TrkB on the plasma membrane. Upon binding, B) BDNF-TrkB complex becomes internalised and C) the signalling endosome can be transported via retrograde transport to the cell body to activate IEGs.

1.7.3 Anterograde transport

BDNF can also undergo anterograde transport, where BDNF is synthesised and transported to nerve terminals or during dendritic release of BDNF[114]. The kinesin superfamily of proteins are responsible for fast axonal anterograde transport[134]. Studies have shown various forms of kinesin to regulate BDNF anterograde transport, mediating its movement from the cell body to the synapses[114]. Compared to dynein, kinesins appear to be smaller and simple in organisation[135,136]. Most are 500 kDa or smaller in size containing between one and four copies of a principle polypeptide that contains the motor domain[114]. This motor domain is responsible for ATP-dependent force generated along the microtubules[114].

1.7.4 Mechanisms of bidirectional transport

The transport of BDNF and other neurotrophic factors occurs bi-directionally and here I will review common theories behind motor protein transport. It is important to understand that kinesins and dynein motor proteins do not act distinctly separate from each other, but rather work in tandem in transporting cargo. There are one of three scenarios that can occur (Figure 1-11): (1) there is only one motor bound to the cargo, and therefore transport is unidirectional (2) both motors are simultaneously bound to the cargo and microtubules, and engage in a 'tug-of-war', with the stronger motor determining the direction of movement (3) both motors are attached to the cargo but their activities are coordinated so only one motor is engaging with the microtubules. The first scenario can be ruled out immediately. A study replaced the intermediate chain of cytoplasmic dynein with a GFP-fusion construct. They saw that the fluorescent dot moved in both directions along the microtubule and frequently undergoes the reverse direction[132]. As the fluorescent signal represents dynein, it can be said that dynein remains attached to the cargo during plus-end movement. Numerous other studies have also determined that both motor proteins remain bound to the cargo[132,137,138]. Therefore, I will summarise the remaining two theories and its supporting experimental evidence.

1.7.4.1 The ‘tug-of-war’ concept

The tug-of-war model, also known as mechanical competition model, describes the mechanistic competition between kinesin and dynein motors bound to the same cargo[139]. This model emerged from the observation of stationary cargo which was thought to be caught in the middle between opposite-polarity motors pulling in equal forces. Moreover, the observation of ‘saltatory motion’ defined as cargo moving bidirectionally, reversing direction every few seconds also led to this ‘tug-of-war’ theory[140].

In order for this theory to be correct, a greater force would need to be exerted to drive transport towards a specific direction, and during saltatory motion, the force exerted would decrease. Studies have shown constant velocity irrespective of the direction of movement suggesting that motor proteins are not competing in a tug-of-war play[141]. This particular study found step sizes to be consistent suggesting no tug-of-war between motor proteins and that movement is regulated, being tuned on or off[141]. To further negate this theory, studies have looked closely at the recruitment of motor proteins driving the tug-of-war movement. The hypothesis for anterograde movement would suggest that an increase in kinesin motors recruitment results in a greater pull towards the plus-end polarity. An early study by Martin and colleagues (1999) show that inhibition of dynein results in both retrograde and anterograde cargo accumulation along neuronal processes. This suggests that the two motor proteins are interdependent during axonal transport. Therefore, the co-ordinated movement between kinesin and dynein is a realistic theory.

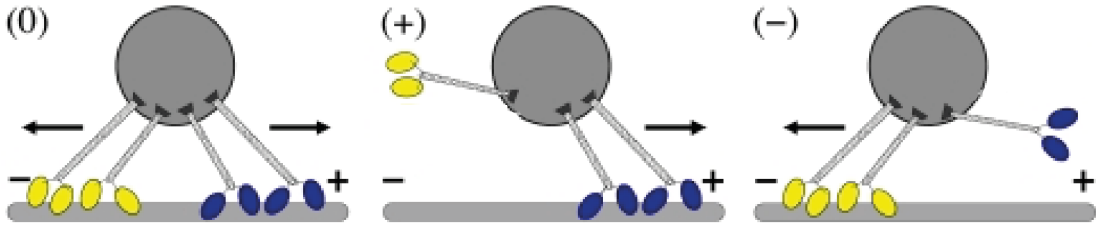

Figure 1-10 Schematic representation of cargo transport in the tug-of-war theory. Cargo is transport by two kinesin motor proteins (blue) and two dynein motor proteins (yellow). Within the tug-of-war theory, one of three possible transport profiles can occur. The first is (0) movement where motors block each other so that the cargo does not move. The second is (+) anterograde transport whereby kinesin drives the strongest force pulling cargo towards the plus end. The third profile is for retrograde movement, (-) where increased dynein recruitment drives transport towards the minus end (Figure adapted from Müller et al., 2008).

1.7.4.2 The co-ordination and co-dependence concept

Having discussed two out of the three theories behind cargo transport, substantial evidence suggests that co-ordination between the two motor proteins is the likely mechanism that delivers cargo delivery back and forth within the cell. The number of motors bound to the individual vesicles range from one up to five[142]. This suggests that motor proteins are present and stably interacting on the same organelle. Moreover, as detailed already, demolishing one specific motor protein alters both anterograde and retrograde transport. Similar results were seen in a study that used fluorescently labelled prion protein (PrP^c) vesicles in mouse hippocampal neurons. Knocking out kinesin light chain 1 or shRNA knockdown of kinesin light chain 2, both of which link kinesin 1 to PrP^c vesicles diminished vesicle run lengths and increased pause timing but also reduced the frequency of retrograde transport[143]. The researchers carried out further tests to ensure these results were not due to altered microtubule dynamics. Studies on cargo transport have suggested that a complex may be involved in governing the co-ordination of dynein and kinesin, however, further investigation is needed to fully validate this hypothesis[139,141,142,144,145]. Lee and colleagues (2004) identified a direct interaction between cytoplasmic dynein and kinesin, mediated by kinesin light chains. Furthermore, co-localisation of both motor

proteins to vesicles was also observed[133133]. This interaction between two opposite polarity motors provides a mechanistic explanation for their interdependency. Nonetheless, ways to exclusively monitor co-ordinated movement have been experimentally challenging. Therefore, further experiments need to be carried out to look at how kinesin and dynein undergo co-ordinated movement. So far, this theory stands because the previously two mentioned theories are negated by multiple experimental evidence (Figure 1-11).

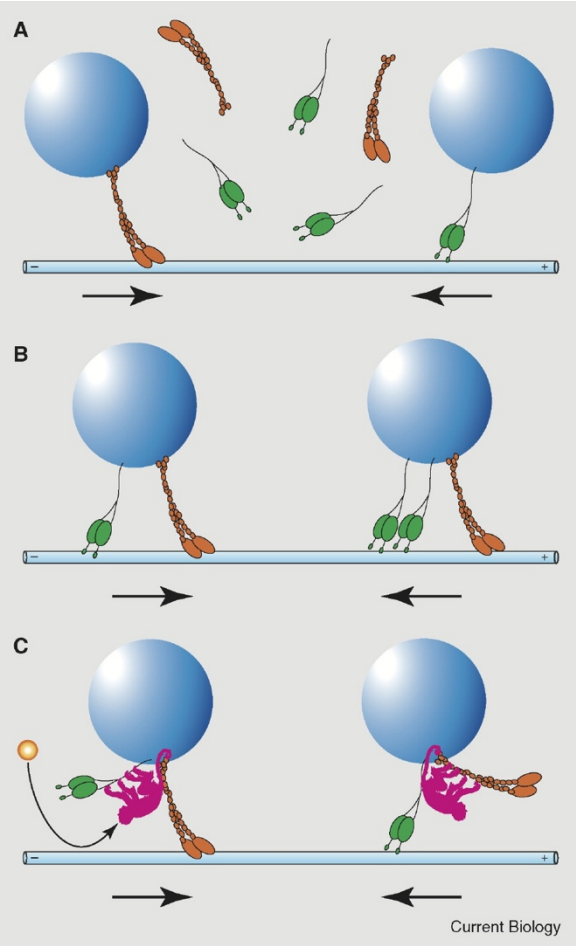

Figure 1-11 Three theories mechanisms of bi-directional transport.
Kinesin motors shown in orange and dynein motors is shown in green, bound to cargo and attached to microtubules. (A) At any given time, only one motor protein is bound to the cargo. Reversible movement occurs when the motor is replaced by one of opposite polarity. (B) Both kinesin and dynein attached to the cargo and microtubules, and direction of movement is determined by the motor that exerts the most force. There the kinesin motor is stronger than the dynein motor and therefore plus-end movement occurs (left), but with two dynein motors, transport is now towards the minus-end (right). (C) Both motor proteins are attached to the cargo, but a complex coordination machinery (pink) modulates which motor remains bound to the microtubules (Figure taken from Welte, 2004).

1.8 BDNF & neurodegeneration

The neurotrophic signalling pathway mediates growth-promoting processes such as strengthening of synapses that governs memory formation[146]. In many neurodegenerative diseases, synaptic dysfunction and process retraction precedes neuronal loss[147]. The level of BDNF expression if found to be severely decreased in the hippocampus, temporal and frontal cortex in patients suffering from Alzheimer's disease (AD)[148]. Due to the growth promoting effects of BDNF, many consider it to be a potential therapeutic strategy. However, is still unclear whether in degenerating cells, neurotrophic signals are still able to propagate over long distances and mediate the growth promoting effects observed under normal healthy conditions. Therefore, there is a clear need to understand which signalling processes are targeted and compromised in neurodegenerative disease models. This will allow for the identification of potential therapeutic targets to strengthen synapses and the neuronal networks. This is the premise for this project.

1.8.1 Neurodegenerative models

Frontotemporal lobe dementia with parkinsonism linked to chromosome 17 (FTLD17), a disease which results in severe neuronal atrophy leading to behavioural disturbances, language impairment, and motor disturbances has been commonly modelled in rodents[149]. FTLD17 is classed as 'tauopathy' that is pathological characterised by aggregated forms of the microtubule protein, tau[150]. Within patients who suffer from FTLD17, tau aggregate deposits are identified via post-mortem assessments[151].

In the human brain, there are six tau isoforms generated by alternative splicing[113]. They are differentiated by the presence or absence of one or two amino-terminal inserts and either three or four microtubule-binding repeats[152] (Figure 1-12). Under normal conditions, tau binds and stabilises microtubules[150]. Tau has a high number of serine and threonine residues that are phosphorylated under physiological condition[147]. In tauopathies, tau becomes hyperphosphorylated at a number of these sites[147]. In general, the phosphorylation

of tau disrupts the binding of tau to microtubules and as a consequence, causes microtubule destabilisation[153]. This results in axonal degeneration and in turn, fatally disrupts axonal transport, a highly regulated and vital mechanism for multiple neuronal functions, including BDNF transport[114]. Pathological forms of tau assemble into neurofibrillary tangles (NFT) that deposit along the somatodendritic compartment to the nerve terminal[153].

Numerous studies have induced various mutations within the tau protein to mimic the pathological conditions observed in Alzheimer's disease and other dementias, including FTLD17[147,150,152,153]. Such models can be used to investigate the molecular mechanisms that are compromised in neurodegeneration. FTLD17 is a common form of dementia that occurs due to a mutation within exon 10 of the tau gene. Here, at position 301, proline is substituted to leucine ((P301L), Figure 1.8-1)[154]. In transgenic mice, this mutation causes hippocampal-dependent memory defects and motor disturbances, similar to that observed in human patients[154,155].

1.8.2 Studying neurodegeneration in culture

In order to study tauopathies in cell cultures, researchers have designed tau mutant plasmids. Hoover and colleagues (2010) have generated plasmids tagged with enhanced green-fluorescent protein (EGFP) with either wild-type human tau ($hTau^{wt}$) or the P301L ($EGFP\text{-}Tau^{P301L}$) mutation[147]. In rTg4510 transgenic mouse models that exhibit regulated expression of P301L hTau, NFTs were first found in the neocortex and progressed into the hippocampus and limbic structures with increasing age. Insoluble hyperphosphorylated tau species (65 kDa) accumulated in an age-dependent manner, consistent with the formation of NFTs. Behavioural studies from these transgenic mice revealed significant cognitive impairments from 4 months of age compared to age-matched healthy control littermates. Furthermore, the memory defects occurred alongside gross forebrain atrophy and neuronal loss in hippocampal CA1 region[156]. Studies have used $EGFP\text{-}Tau^{P301L}$ constructs in primary cells to visualise its cellular distribution and functional consequences. Hoover *et al* (2010) found significant mislocalisation of hyperphosphorylated tau in spines compared to healthy control cells[147]. Furthermore, they showed altered amplitude and frequency of mEPSCs[147]. In line with these observations from transfected primary cells, studies have

measured field EPSCs and whole cell recordings from rTg4510 mice which also show distinct impairments compared to healthy controls[157]. Using such models can provide insight into how pathogenic proteins effect multiple processes leading to neuronal death. Studies such as these also highlight the use of such constructs as a model of neurodegeneration to understand which neurotrophic signals are compromised as a result of the degenerating axonal transport mechanism, a process vital to propagate long-range signalling mediated by BDNF.

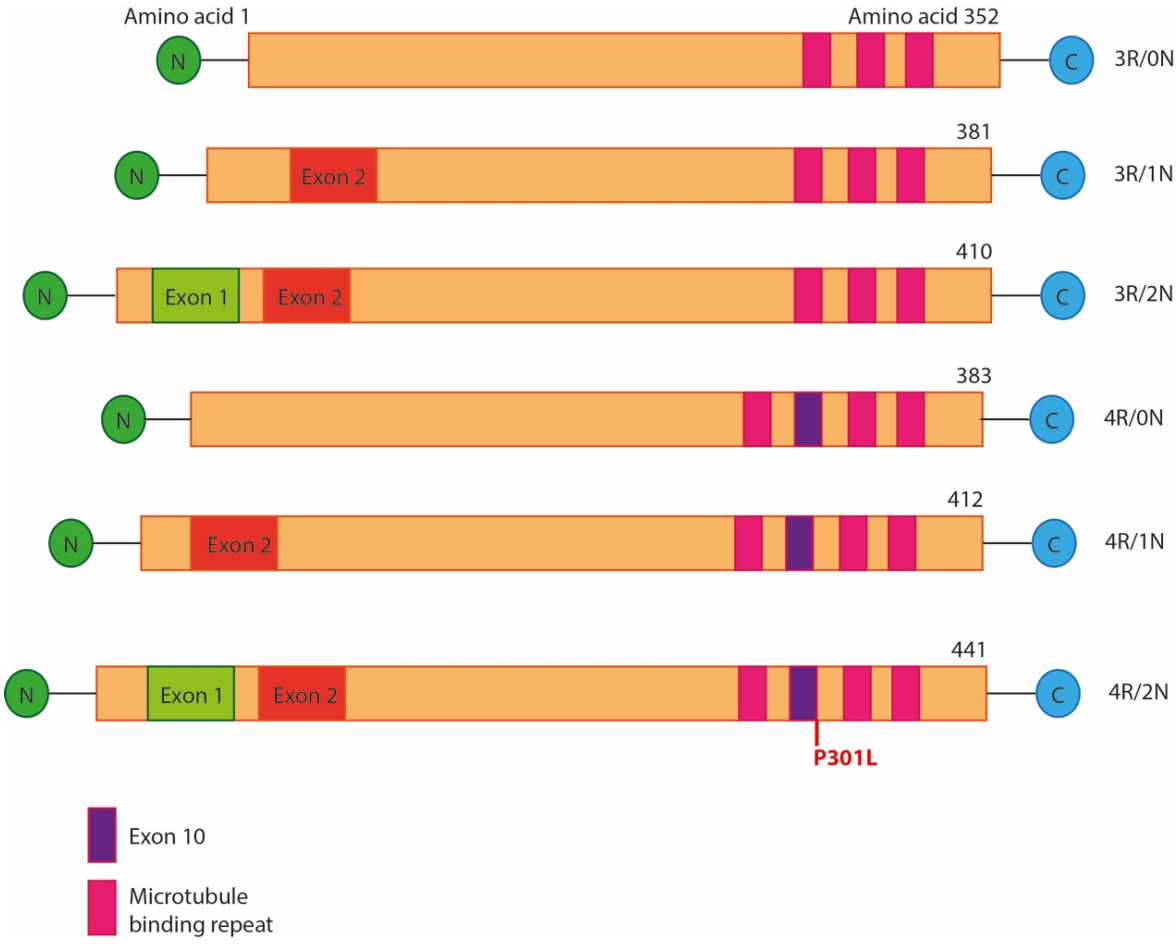

Figure 1-12 Schematic representation of the six tau isoforms that are expressed in adult human brains.

The isoforms can have different number of microtubule-binding domains (three or four repeats located in the C-terminal half of the protein, shown in pink), which are known as 3R or 4R tau isoforms, respectively. They can also differ in the presence zero, one or two N-terminal inserts (shown in green and red). Mutation P301L is located in R2 at position 301 where proline is substituted to leucine.

All of the studies mentioned here use either primary neurons expressing a tauopathy or use transgenic rodent whole brain homogenates or slices. Although these methods have and will provide great insight into disease pathology, they are still too complex to investigate signal propagation. For instance, in primary mass culture, adding BDNF exogenously would indeed induce immediate early genes at the cell soma, however, it would be extremely difficult to decipher whether this activation was due to signal propagation from BDNF binding to TrkB at axonal ends, or from BDNF binding to receptors located locally to the cell soma. Therefore, a simplified platform is required, whereby single axonal projections can be isolated making it easier to identify the cells' soma. Compartmentalised culture platforms have been used by cell biologist for a number of years for this reason[158–162]. As well as other research areas, many researchers have used them to look at neurotrophic signaling as well as axonal transport with great success[143,163–166].

1.9 Culture platforms to investigate BDNF signalling

During this project, a number of elements will be investigated, such as the rate of axonal transport within the Tau^{P301L} expressing cells, level of pathology, the state of microtubule polymerisation, the level of TrkB expression and BDNF signalling. These measurements will be carried out on distal axons of Tau^{P301L} and GFP expressing cells. All experiments bar BDNF cell signalling were carried out in mass culture. To investigate long-distance BDNF signalling, a microfluidic platform was utilised. The below sections highlight the use and rationale for using mass culture and microfluidic platforms for cell culture.

1.9.1 Mass cell culture

The majority of experiments carried out in this project utilise mass culture technique. Primary mouse hippocampal cells are cultured in plates in NBM. Cells are then transfected with GFP-Tau^{P301L} or GFP alone. Appropriate antibodies are then used to identify proteins of interest, such as TrkB receptor expression.

Mass culture allows the user to investigate cellular mechanisms and protein expression in all compartments of the cell. Neuronal cells are grown in appropriate growth medium, allowing the cells to form an interconnected neuronal network (as observed in this project). Any treatments applied to the cells grown in mass culture effect the entire neuronal network. In this respect, mass culture does not allow the user to treat individual cells, or isolated cellular compartments, such as the axonal compartment alone. If this is required, then another cell culture technique must be sought out, such as a microfluidic chamber detailed in section 1.9.2.

The following chapters within this project utilise the mass culture technique:

- Chapter 3: Establishing an in vitro model of axonal degeneration

- Chapter 4: Assessing TrkB receptor expression
- Chapter 6: Neurotrophin modifiers

1.9.2 Microfluidic cell culture platform

In order to investigate long-distance signalling of BDNF, whereby BDNF signals propagate over large distances, from nerve terminals to cell soma, a platform by which isolated axonal ends can be treated with BDNF is required. Compartmentalised culture systems can fluidically isolate different cellular regions, such as, the somato-dendritic compartment (cell body and dendrites) from the nerve terminals. This type of system allows us to selectively treat cellular regions and analyse changes at distal (axonal ends) and proximal (somato-dendritic) areas of the cell. Thus, probing for changes in long-distance signalling in healthy (GFP-expressing) and Tau^{P301L}-expressing cultures can be achieved.

Robert Campenot was the first to develop a method whereby two connected cultures were fluidically independently[159]. Any effect on the cell body was solely attributed to the treatment conditions applied. He developed a tissue culture system where neurites growing from a small cluster of soma are able to extend their protrusions through a fluidically impermeable barrier (Figure 1-13)[159]. This ensured control of the fluidic environment of the distal protrusions independently of the local fluidic environment of the soma and proximal dendrites. To achieve this, he created two fluidically-isolated chambers on a petri dish using a Teflon divider and a collagen-coated coverslips with 'grooves' to guide axonal outgrowth[159]. The Teflon divider, which is partitioned into three chambers, was sealed with silicone grease. This system was initially created to observe neurite outgrowth in response to NGF using peripheral neurons[158]. NGF treatment to the central and third chamber enabled axons to cross and reach the NGF treated chambers[158]. In direct contrast, none of the axons extended into the chambers that lacked the growth factor treatment. The development of such system has led us to understand the activation pathways mediated by neurotrophic factors in greater detail and its influence on cell morphology and survival.

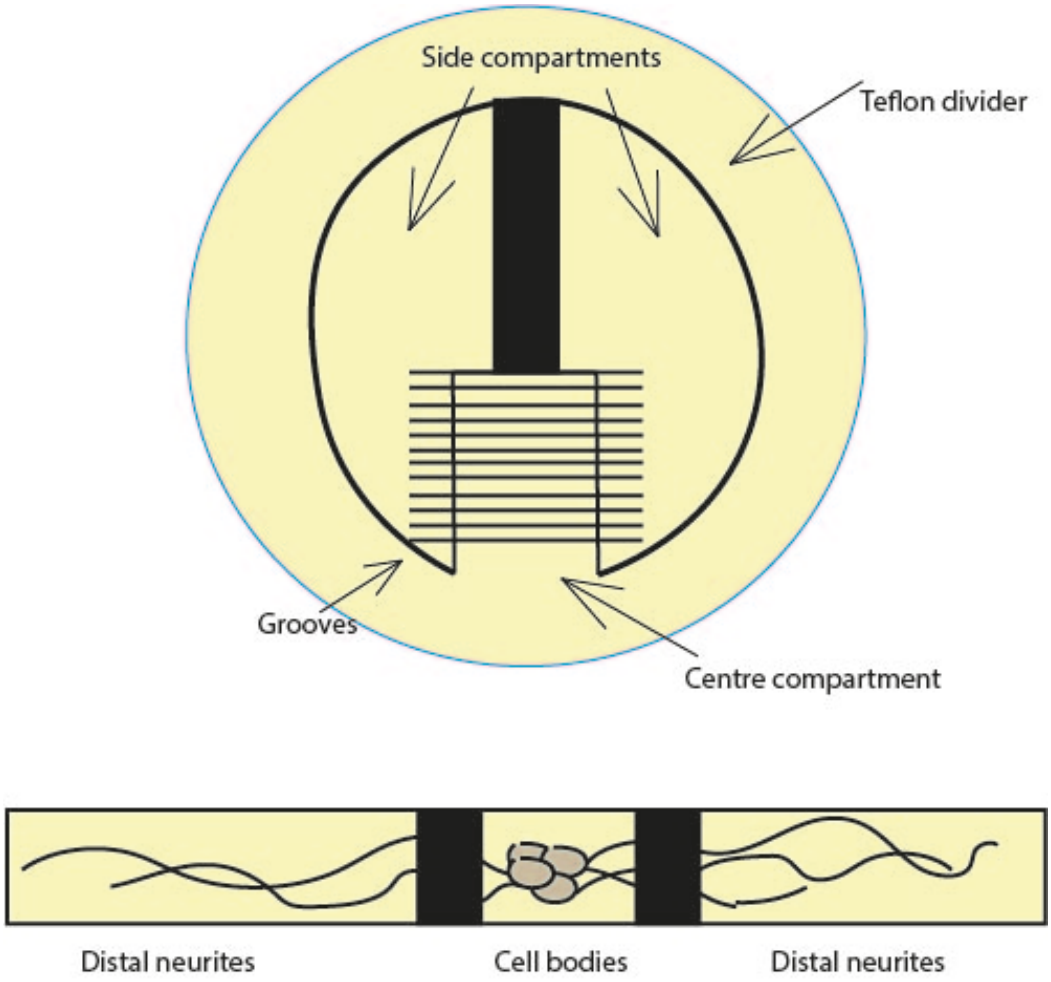

Figure 1-13 Campenot device first designed by Robert Campenot.
The culture dish is coated with collagen, and grooves are imbedded to guide axonal growth. A Teflon gasket with silicon grease on its bottom edges is placed in the chamber over the grooves. Dissociated neurons are plated in the central chamber and allowed to grow (Figure adapted from Filler et al., 2010).

Early studies by Ginty and colleagues who used the Teflon compartmentalised systems to assess the subcellular distribution of activated PI3K and its downstream activator Akt[14]. Proximal cell bodies were exposed to medium containing a neutralising antibody against NGF while the distal axons; approximately 1 mm away, were exposed to medium containing NGF[14]. Here they demonstrated that the binding of NGF to TrkA on distal axons regulates P13K and Akt activity in the both the distal axons and the cell bodies.

The developments made by Campenot have been heightened by Taylor and colleagues[160]. They have adapted the idea of a compartmentalised culture system and fabricated a microfluidic device with similar components (Figure 1-14). In addition they have enhanced fluidic control via the fabrication process[160,161], allowing researchers the flexibility to design a device suited for specific research needs. Figure 1-14 depicts the modern compartmentalised culture system that uses a transparent polymer, poly(dimethylsiloxane) (PDMS), with imbedded outgrowth channels[160,161]. The PDMS device is placed on a poly-d-lysine covered glass coverslip required for cell adhesion. The device created by the Taylor lab has been widely used and adapted to study a wide range of cellular mechanisms. Moreover, similar to the Campenot system, they have also increased our understanding of neurotrophic signalling.

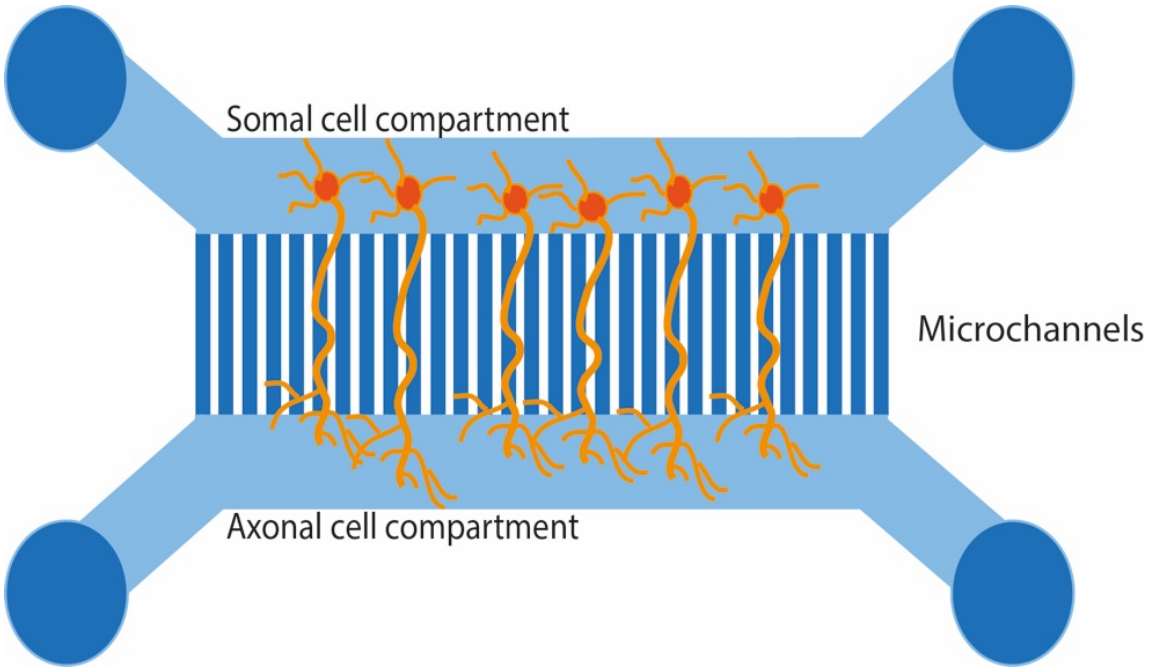

Figure 1-14 Schematic overview microfluidic device designed by 1 and colleagues (2006). Dissociated cells are plated on the somal side of the cell culture chamber, where axons growth through isolated microchannels into the axonal side. Both the somal and axonal cell compartments can be fluidically independent.

Studies have implemented these devices to understand BDNF signalling in healthy neuronal cultures. Using the Taylor microfluidic devices, it was demonstrated that upon BDNF stimulation at the somatodendritic compartment, Arc and Fos expression was induced, highlighting local signal activation[163].This is in contrast to the long-distance signalling that propagates the BDNF-TrkB signal from the distal axonal end to the cell body. Studies have shown MAPK/Erk1/2 activation at the cell body when BDNF is applied distally, to axon nerve terminals[168]. This type of experiment will be replicated in this project, to understand is signal propagation can occur in Tau^{P301L}-expressing cells.

Within the Deinhardt lab, Dr Joanne Bailey, a post-doctoral researcher, has successfully used microfluidic devices to highlight long-distance BDNF signalling in healthy, non-transfected cells. Using devices as depicted in figure 1-14, Dr Bailey has grown health mouse hippocampal cells in microfluidic devices and treated distal axons (which are 900 um away from the cell body) with 15 ng/ml BDNF for a select number of hours. Dr Bailey observed activation of phosphorylated Erk and induction of Arc at the somato-dendritic compartment (Figure 1-15). These experiments by Dr Bailey highlight how long-distance signalling can be measured in microfluidic devices and thus, pave way for the investigation of BDNF long-distance signalling in compromised culture systems.

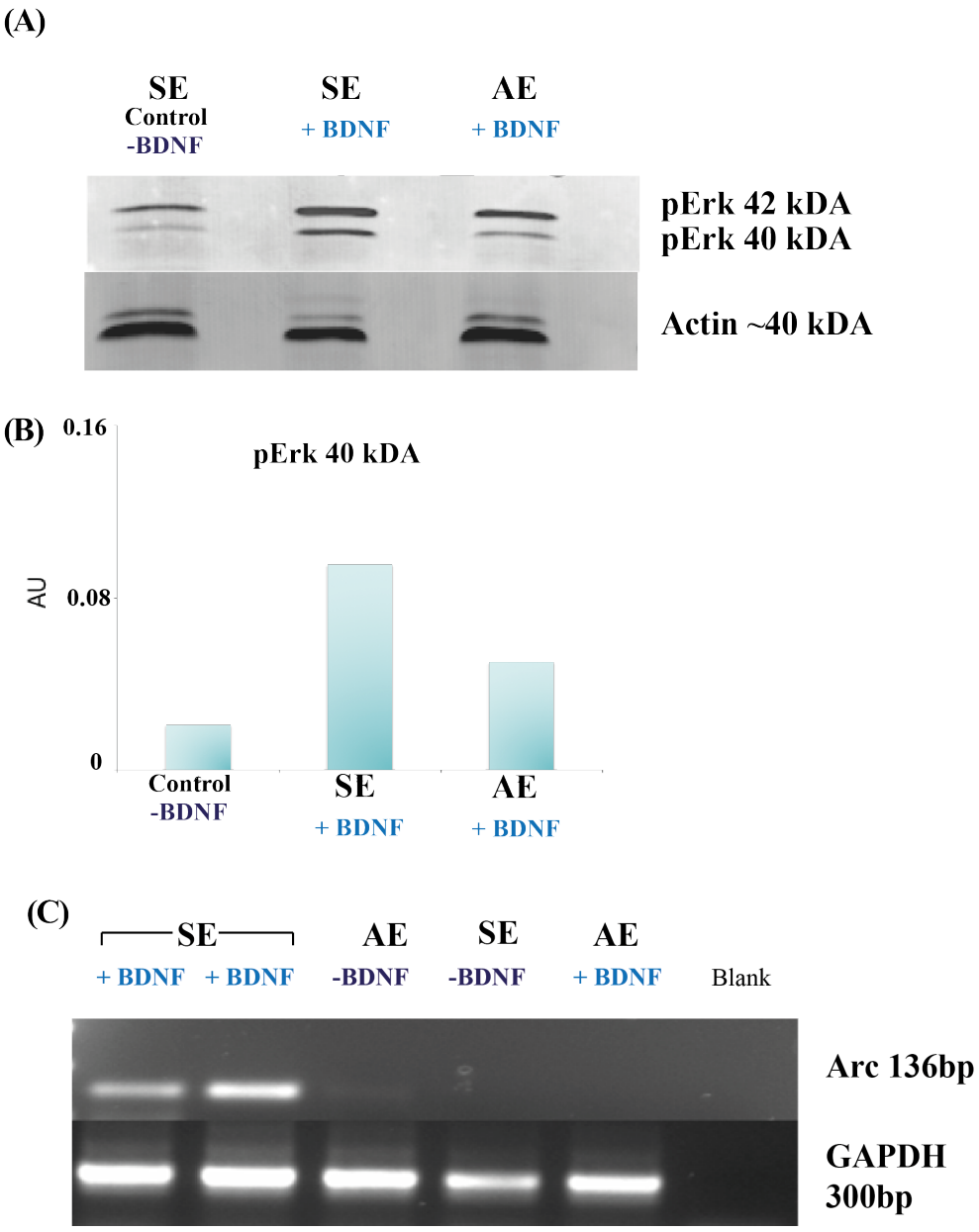

Figure 1-15 Long-distance BDNF signalling is intact in healthy cells.
(A) Western blot analysis and (B) quantification of healthy hippocampal cells treated with BDNF 15 ng/ml distally at axonal ends for 4 hours. Phosphorylation of Erk1/2 was probed at both axonal ends (AE) and at cell soma (SE). The housekeeping protein probed was Actin. (C) PCR amplification of Arc using cDNA extracted from somatic (SE) and axonal (AE) compartments after 6 hours of distal BDNF 15 ng/ml treatment. The housekeeping gene probed was GAPDH. SE: Somal extraction; AE: axonal extraction. For Western blot analysis, n=1; for PCR, n=3. Unpublished data generated by Dr Joanna Bailey.

As microfluidic devices can be designed and created at the University of Southampton, we can incorporate new designs in our device to enhance the orientation and connectivity of cells. For example, the dynamic arraying method developed by Dr Jonathan West and colleagues, is a technique that ensures cells grow in close proximity of each other, and the axons extending out of the microchannels connect with the cell arrayed directly below[169]. This serves as a platform to investigate the propagation of material across two or more population of cells[169]. Additions such as these can be used in combinations as a powerful tool to investigate the long-range soma-to-axon (and vice versa) signalling in cells. This together with Dr Bailey's experiments show how a microfluidic system represents an ideal tool to investigate BDNF signalling.

2. General Methods and Materials

2.1 Materials

All tissue culture materials were obtained from Invitrogen (unless specified otherwise). For other experiments, materials were obtained from Sigma (unless specified otherwise).

2.1.1 Animals

All experiments were conducted in accordance with the Home Office Animal Procedures Act 1986. Adult C57BL/6 pregnant mice were time-mated for embryonic day 15 (E15) and euthanised with CO_2 and cervical dislocation before the embryos were removed.

2.1.2 Oligonucleotides

Primers for amplification of mRFP insert were designed by Dr Grace Hallinan and produced by Eurofins Genomics. The forward primer was designed to include a Cla1 site (blue text below) and a start codon (green text) before the RFP primer (red text).

Forward: 5'-CATGATCGATATGGCCTCCTCCGAGGAC -3';

The reverse primer was designed to contain a BamH1 site (blue text below) before the reverse primer for RFP (red text).

Reverse: 5'-CATGGGATCCGGCGCCGGTGGAGTGGC-3'

2.1.3 DNA Constructs

DNA	Backbone	Resistance	Encodes	Source
GFP	pEGFP-C3	Kanamycin	Green fluorescent protein	ClonTech
GFP-Tau^{P301L}	pRK5	Ampicillin	Tau 0N4R, with proline substituted to leucine at position 301	Ashe Lab, Minneapolis (Addgene #46908)
TrkB-mRFP	pDSRed	Kanamycin	TrkB receptor	Chao lab, NYU
RFP-Tau^{P301L}	pRK5	Ampicillin	Tau 0N4R, with proline substituted to leucine at position 301	Deinhardt Lab, UK
BDNF-RFP		Kanamycin	Brain-derived neurotrophic factor	Lee Lab, Weill Cornell Medical College
mCherry-EB3		Kanamycin	End-binding protein 3	Akhmanova Lab, Utrecht

Table 2-1 List of DNA plasmids used in this project.

2.1.4 Antibodies

Antibody	Source	Species	Dilution for immunocytochemistry	Dilution for Western blot
Tau	Dako	Rabbit	1:2000	
MAP2	Abcam	Chicken	1:50,00	
Arc	Synaptic Systems	Rabbit	1:1500	
TrkB (extracellular)	Millipore	Rabbit	1:1000	
Tyrosinated Tubulin	Sigma	Rabbit	1:1000	
Acetylated Tubulin	Sigma	Rabbit	1:1000	
Transferrin Receptor	Zymed 13-6800	Mouse		1:1000
Tubulin	Sigma T5168	Mouse		1:1000
pErk1/2	Cell Signalling	Mouse		1:1000
pAkt	Cell Signalling	Rabbit		1:2000

Table 2-2 List of antibodies used in this project.

2.2 Molecular cloning for the generation of RFP tagged Tau^{P301L} construct

2.2.1 Amplification of RFP insert

mRFP insert was amplified from an existing TrkB-mRFP construct (from the Chao Lab, USA). Primers outlined in section 2.1.2 (designed by Dr Grace Hallinan) were resuspended in sterile water to generate a concentration of 100 μm.

The PCR experiments was set up as follows:

Reagent	Amount	Final concentration
DNA	10 ng	0.2 ng/ μl
10 mM dNTPs (NEB)	1 μl	200 μm
10 μm Forward primer	1 μl	0.2 μm
10 μm Reverse primer	1 μl	0.2 μm
Q5 Polymerase	1 μl	0.02 units/ μl
5X Q5 buffer	0.5 μl	1X
5X Q5 high GC	10 μl	1X
Sterile water	Up to 50 μl	

Table 2-3 PCR mastermix recipe

This mixture was centrifuged as 13,000 rpm for 30 seconds and then loaded into a thermocycler which was setup with the following settings:

Step	Temperature	Time
Initial denaturing	98 °C	30 seconds
35 cycles of:		
• Denature	98 °C	10 seconds
• Primer annealing	65.9 °C	30 seconds
• Extension	72 °C	30 seconds
Final extension	72 °C	120 seconds
Hold	10 °C	∞

Table 2-4 PCR setup

The PCR products were run on a 1% agarose gel (pH 8.5, see Appendix A for recipe). 5 µl of 10,000X Gel Red (Biotium) was added into the 1% agarose mix and mixed by swirling. The agarose gel was poured into an electrophoresis tank containing a comb and allowed to set. The comb was removed and 1X TAE buffer was poured into the tank, covering the gel. 5 µl of DNA ladder (exACT gene 1 kb ladder, Thermofisher) was pipetted into the first lane and the PCR samples were pipetted into the consecutive lanes. The gel was run at 80 volts for 45 minutes. The gel was removed from the tank and scanned on the UV transilluminator using GeneSnap software. The RFP digested band was cut out of the gel and put into sterile Eppendorf using a UV light box. The PCR clean-up kit (Macherey Nagle) was used according to the manufacturer's protocol to isolate the RFP DNA from the gel. The resulting PCR product was then digested with restriction enzymes following the concentrations in Table 2-3.

2.2.2 Digestion of the pRK5-GFP-Tau^{P301L} backbone

The pRK5-EGFP-Tau^{P301L} vector was digested using Cla1 and BamH1 enzymes (Promega) to cleave the GFP fragment. The digestion was setup as follows:

Reagent	Amount	Final concentration
DNA (GFP-Tau^{P301L})	1 µg	0.05 µg/µl
10X BSA	2 µl	0.2 µg/µl
BamH1	0.5 µl	10 units/µl
Cla1	0.5 µl	10 units/µl
10X Buffer E	2 µl	1X
Sterile H_2O	Up to 20 µl	

Table 2-5 Restriction enzyme digestion mix

The restriction digestion mix was incubated in a water bath at 37°C for one hour. The enzymes were heat inactivated for 15 minutes at 65°C. To prevent re-annealing of the backbone, 1 unit/µl of Thermosensitive Alkaline Phosphate (TSAP, Promega) was added to the digestion mix for 15 minutes at 37°C, and this was then heat inactivated at 74°C for 15 minutes. The pRK5-Tau^{P301L} product was run on a 1% agarose gel, cut and purified as described in section 2.2.1. (see Figure 2-1).

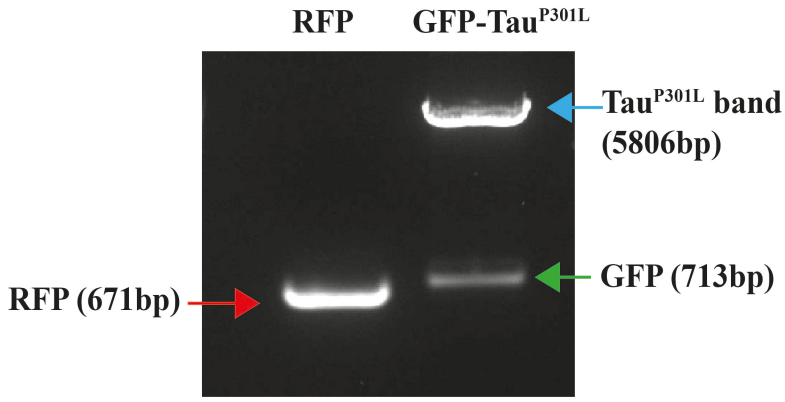

Figure 2-1 Restriction digest of the cleaved RFP product and pRK5-GFP-Tau^{P301L} with Cla1 and BamH1.

Lane 1: The amplified RFP product; lane 2: pRK5-GFP-Tau^{P301L} digested with Cla1 and BamH1. Lane 1 shows the RFP band at 671bp (red arrow). Lane 2 shows a double digestion where Cla1 and BamH1, both of which only cut the vector once, cleaves the GFP insert (green arrow), leaving the linearised pRK5-Tau^{P301L} (blue arrow). This was excised from the gel as described in section 2.2.2 to be ligated with the mRFP (red arrow).

2.2.3 Ligation of the mRFP insert into the pRK5-Tau^{P301L} backbone

The mRFP insert was digested and purified using the PCR clean-up kit as described above. The mRFP insert was ligated into the backbone using a Quick Ligation kit (NEB) for 5 minutes at room temperature detailed in Table 2-6. The ligation reaction mix was incubated at room temperature for 1 minute only. After 5 minutes, the solution was stored at -20°C until transformation.

Reagent	Amount	Final concentration
Vector backbone	50 ng	2.5 ng/µl
mRFP insert	17.2 ng	3-fold molar excess to backbone
Ligase	1 µl	1 unit/µl
2X buffer	10 µl	1x
Sterile H_2O	Up to 20 µl	

Table 2-6 Ligation reaction mix

2.2.4 Agar plate preparation

All bacterial preparation was conducted under sterile conditions near Bunsen flame. LB agar and broth was supplied by the media kitchen at the University of Southampton, UK.

300 ml of melted LB agar (see Appendix A for recipe) was mixed 100 µg/ml ampicillin. The agar mix was poured into 10cm Petri dishes and allowed to set at room temperature. Plates were wrapped in parafilm and stored in the fridge (for maximum of 2 weeks) until use.

2.2.5 Bacterial transformation

Plasmids were mixed with competent DH5α *E.coli* cells were thawed on ice for 30 minutes. 50 µl of thawed cells were mixed gently with 50 ng of the ligation mix from section 0. This mix was placed on ice for 30 minutes. The cells were shocked at 42°C for 30 seconds only and then placed on ice for further 2 minutes. 150 µl SOC medium preheated at 37°C was added to the tube and incubated 37°C for an hour to allow for

recovery. The transformed bacteria were spread over the agar plates containing the ampicillin and incubated at 37°C overnight.

2.2.6 Plasmid mini preparation

Individual colonies from the bacterial transformation (section 2.2.5) were picked using pipette tips and placed in sterelin tubes containing fresh 3 ml LB broth (see Appendix A for recipe) with 100 µg/ml ampicillin. The sterilin tube was shaken at 220 rpm for 4-6 hours at 37°C, after which the broth appeared cloudy. The solution was centrifuged at 6000g for 15 minutes at 4°C to pellet the bacterial cells. The supernatant was discarded and the pellet was purified using the QIAGEN maxi prep kit. The DNA plasmid was resuspended with 500 µl milliQ H_2O and DNA was quantified using a NanoDrop. All plasmids were stored at -20°C.

2.2.7 Test digest of pRK5-RFPTau^{P301L}

To test if the ligation of mRFP insert into pRK5Tau^{P301L} backbone was successful, a test digest was performed with the same restriction enzymes used to insert mRFP (Cla1 and BamH1). The reaction was performed on all samples generated from the mini preparation (section 2.2.6). The resulting purified RFP-Tau^{P301L} DNA was run on 1% agarose gel as before and imaged using the UV transilluminator box. Expected sizes are 671bp for the mRFP and 5806bp for the remaining pRK5-Tau^{P301L} (Figure 2-2).

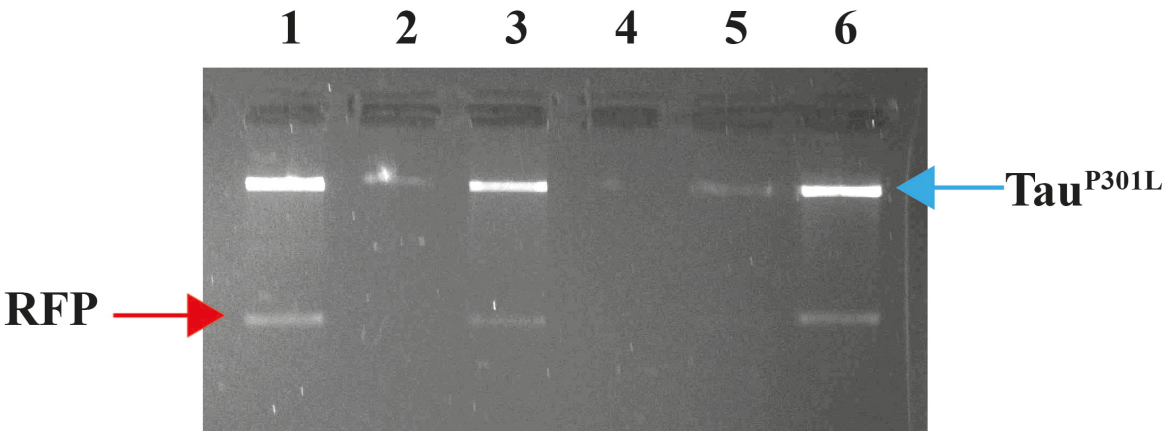

Figure 2-2 Test digest of pRK5-Tau^{P301L} with Cla1 and BamH1 restriction enzymes. Bacterial colonies numbers 1-6 across top. Colonies 2, 4 and 5 contained no plasmid. The other 3 colonies appeared successful in ligation. Samples 1 and 6 were chosen for the maxi prep. RFP= 671 bp; Tau^{P301L}=5806 bp.

To ensure the insertion of the RFP fragment, as opposed to the reinsertion of the GFP fragment, the tested DNA (1 and 6) obtained from the mini preparation (section 2.2.6) was screened in a dividing cell line by transfection (see section 2.4). The samples expressing the red fluorescent expression of microtubule localised protein, with no GFP expression, were used to grow up in the bacterial maxi preparation.

2.2.8 Plasmid maxi preparation

As mentioned in section 2.2.6, the samples grown during the mini bacterial preparation were selected for a maxi bacterial preparation. 2 µl of the mini bacterial preparation DNA solution were separately added into sterelin tubes containing 3 ml LB broth and 100 µg/ml ampicillin. These tubes were shaken at 220 rpm for 6 hours until cloudy. 500 µl of this shaken solution was added to 500 ml fresh LB broth containing 100 µg/ml ampicillin in a large conical flask. This flask was shaken overnight at 220 rpm at 37°C. When the solution appeared cloudy and it was centrifuged at 6000g for 15 minutes at 4°C to pellet the bacterial cells. The remaining pellet was resuspended, lysed, washed and eluted with QIAGEN maxi preparation kit as per manufacturer's instructions. The resulting DNA

plasmid concentration was determined by measuring absorbance on a Nanodrop. Ratios at 260/280 nm and 260/230 nm absorbance were taken to determine nucleic acid purity. For ratio of absorbance at 260/280nm, 1.8 is generally accepted as "pure" for DNA. For ratio of absorbance at 260/230, a range of 2.0-2.2 is considered "pure" nucleic acid.

The resulting DNA plasmid were sent to Eurofin Genomics for sequencing and the obtained sequence matched the expected sequence, confirming the successful cloning of the RFP fragment into the pRK5-Tau^{P301L} backbone.

2.3 Cell Culture Methods

Once the cultures were plated, primary cell cultures and immortal PC12 cell lines were placed in incubators maintained at 37°C and 5% CO_2. When cell cultures are removed from the incubator, changes in CO_2 effects the cultures' pH levels. HEPES-NaOH was used as a buffer to maintain physiological pH between pH 7.2 – pH 7.6 when cultures were removed from the incubator for a significant amount of time, such as for live cell imaging. In the absence of buffers, the pH levels can rise to pH 8-8.5. The final concentration of HEPES-NaOH in solution was 25 mM.

2.3.1 Glass preparation

Before plating cells, glass coverslips were cleaned and pre-treated with poly-*D*-lysine (PDL, Sigma), a positive charged polymer that aids cell adhesion. Glass coverslips for cell culture, coverslips were placed 1M NaOH on a rocker for one hour. The glass was then washed three times in sterile water. The glass was then placed in 1N HCl for one hour and washed three times in sterile water. The glass was left overnight in 70% ethanol, which was replaced with fresh 70% ethanol the following morning. Glass coverslips were then stored in this ethanol for tissue culture use.

For PDL treatment, washed glass coverslips were removed from ethanol and air-dried. The glass coverslips were covered with 0.1 mg/ml PDL in sterile water solution and left to incubate at 37°C overnight. The following morning, the PDL was removed and the glass coverslips were washed with sterile water 3 times and left to air dry.

2.3.2 Primary cell culture

Primary hippocampal and neuronal cultures were derived from E15+ embryos. The hippocampi and cortices were dissected from brains of the foetuses in using fine forceps. Dissected tissue was transferred into a tube of 1 ml PBS and treated with 0.25% w/v trypsin for 6-8 minutes at 37°C. Trypsin activity was deactivated with an equal amount of FBS in DMEM solution and left to rest for 1 minute, after which all the solution was removed as carefully as possible, and 1 ml of neurobasal medium (NBM, supplemented with 2% B27 and 0.5 mM GlutaMAX (Gibco)) was added to the tube. With a pipette, the cell pellet was dissociated and filtered through a cell strainer with a 40μm pore size (FisherScientific). Cell number was counted on a haemocytometer, and cells were diluted to a density of 150,000 – 300,00 cells/ml for mass culture.

2.4 Cell transfection

2.4.1 Day *in vitro* (*DIV*) 5 transfection

All transfections were carried out using a cationic lipid-mediated transfection reagent (Lipofectamine2000) at 1:1 ratio of Lipofectamine:DNA at *DIV5*. 1 µl Lipofectamine and 1 µg of DNA were separately diluted in 150 µl Optimem medium. Lipofectamine and DNA solutions were combined and gently aerated and left for 15 minutes at room temperature. For mass culture in 12-well plates and glass bottom dishes, 300 µl of medium was removed from each well and replaced with 300 µl of Lipofectamine-DNA mix and incubated at 37°C for 40 minutes. After this time, the entire medium was removed and replaced with fresh NBM.

Co-transfections were carried out to introduce two DNA constructs into the same cell, in a similar method as described above. Two DNA constructs, both at 1 µg, were diluted in 150 µl of Optimem. This solution was mixed with 150 µl of Optimem solution containing 1 µl of Lipofectamine and left to rest at room temperature for 15 minutes, after which it was added to either glass bottom dishes, or in microfluidic devices in the same manner as described above.

2.5 Immunocytochemistry (ICC)

Cells were fixed at different *DIV* depending on the experiment. For immunocytochemistry, existing media was removed and washed once with 500 µl PBS for 5 minutes. The PBS was removed and the cells were fixed with 500 µl 4% paraformaldehyde in 20% sucrose in 1X PBS solution at room temperature for 5-10 minutes at room temperature. After fixation, the cultures were treated with 500 µl ammonium chloride in 1X TBS for 2-5 minutes to quench autofluorescence and unreacted aldehydes. At this stage, cells were either mounted with Mowiol (see Appendix A for recipe) for imaging of fluorescent transfected cells or stained with antibodies.

For intracellular antibody detection, cells were permeabilised with 500 µl 0.1% Triton-X-100 in TBS for 5 minutes at room temperature. For cell surface detection, the cells were not permeabilised. Cells were blocked in 10% normal goat serum (NGS) in TBS at room temperature for 1 hour. For primary antibody incubation, cells were incubated with primary antibodies diluted in 10% NGS solution for 1 hour (see Table 2-2 for the list of antibodies used in this project). For Arc and egr1 detection, cells were incubated with these antibodies overnight at 4°C. After this, cells were washed in 1X TBS three times to remove residual antibody solution. Cells were then incubated in secondary antibodies (AlexaFluor 488/555/647 diluted 1:1000 in 10% NGS in TBS solution) for 1 hour at room temperature. The cells were then washed with 1X TBS three times. The second TBS was contained Hoechst 33342 stain (1:3000, FisherScientific) to stain the nuclei. After the final wash, coverslips were dipped in sterile water to remove salt crystals and mounted on microscope slides (76mm x 26mm) containing Mowiol. Mowiol was allowed to dry overnight before imaging. Fixed coverslips were stored in the dark at -20°C.

2.6 Microscopy

Fluorescent images of distal axonal stretches were imaged from coverslips or microfluidic devices on a DeltaVision Elite system (GE Life Sciences) with an SSI 7-baned LED for illumination, using SoftWoRks software (version 6), images were obtained with a monochrome sCMOS camera. 60x/1.42NA Oil Plan APO objective was used. Images of projecting axons within the microfluidic devices were obtained in the same manner detailed above, but also incorporating differential interference contrast (DIC). Images were taken using FITC/TRITC/DAPI/CY5 filters. Data from multiple z-stacks were compressed into a single image by generating the maximum projection of the stack and combining it into one image.

2.7 Image analysis

2.7.1 Staining analysis

To analyse the mean fluorescence of the various proteins and genes expressing in GFP and GFP-Tau^{P301L} expressing cell, ImageJ was used to create masks for area of interest and overlaid on top of the staining image, the mean fluorescence was measured and plotted on GraphPad Prism.

The following steps were carried out in ImageJ to quantify staining:

1. Depending on the area of interest, images were thresholded as outlined below. Stacked images taken in different channels were separated and the image area of interest was used to create a threshold to select the entire area:
    a. For nuclear staining, the nucleus was used as the area of interest in the DAPI channel.
    b. For TrkB, Acetylation and Tyrosination staining, the distal axon of GFP or GFP-Tau^{P301L} expressing cells was used as the area of interest in the FITC channel.
2. The threshold image was used to create a mask. The outlined shape from the mask is selected and added the task manager
3. The outlined mask is overlaid on top of the staining image.
4. Mean fluorescence is measured and plotted on GraphPad Prism.

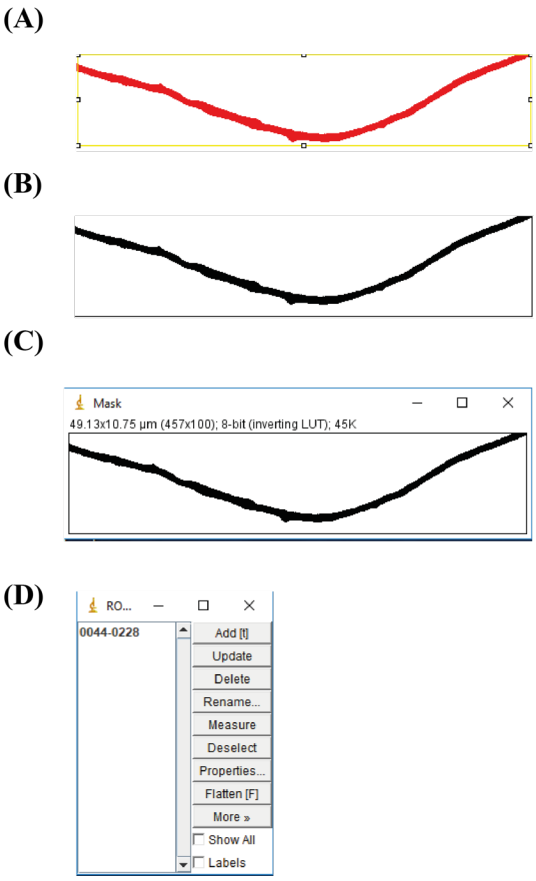

Figure 2-3 Staining quantification method.

To measure mean fluorescence intensity of area of interest, the following thresholding method is used. (A) The chosen area for analysis is selected and thresholded to the point where the entire area is coloured red. (B) From the now threshold area, (C) a mask is created. (D) The area of the mask then added to a 'task manager' which can then be overlaid onto the area which needs to be analysed. For instance, if quantifying TrkB receptors expression along distal axons of GFP-expressing cells: the distal GFP expressing axonal stretch is thresholded to create a mask. The mask is then overlaid on the TrkB receptor image and fluorescence intensity is measured. This ensures only the receptors along the axonal stretch (which has been overlaid) is captured in the measurement, rather than receptors located elsewhere on the cell or image.

2.7.2 TrkB receptor analysis

To measure TrkB expression, GFP or GFP-Tau^{P301L} expressing cells were stained for TrkB receptors and distal axons were processed as highlighted in section 2.7.1. Data was plotted on GraphPad.

2.8 Statistical analysis

Statistical analysis was carried out on GraphPad Prism software. One-way ANOVA (analysis of variance) test was chosen to test a hypothesis in which only one single factor was considered to compare the mean of 3 or more samples. For instance, the number of stationary vesicles (dependent variable) in GPF and Tau^{P301L}-expressing cells (independent variable). A two-way ANOVA test was chosen to test a hypothesis multiple sample means where two factors needed to be considered, such as the relative frequency (dependent variable 1) of various lengths of microtubule lattice production (dependent variable 2) in GPF and Tau^{P301L}-expressing cells (independent variable). A t-test, similar to a one-way ANOVA was used to determine whether there is a significant difference between the means of two groups.

3 Establishing an *In Vitro* model of axonal dysfunction

3.1 Introduction

Neurons are highly polarised cells that form an intricate organised network within the human brain. Neurons contain four distinct regions that are clearly compartmentalised into pre- and post-synaptic areas: the axon terminal, the axon, the cell soma and the dendrites. Within each of these specialised compartments, distinct cellular process simultaneously take place and thus the need for signals to be efficiently relayed between and within neuronal compartments is crucial. In this project, I am focusing on signals that need to be decoded at the cell soma having travelled over large distances along the axonal process from the nerve terminals, a common site of signal initiation.

The length of the axon can typically range from millimetres to centimetres. In the context of neurodegenerative diseases, the structure of the axon itself can become severely compromised. Therefore, it is important to fully understand the implications axonal vulnerability plays in disease. To crudely illustrate this process (Figure 3.1), in early stages of disease, multiple mechanistic failures lead to the dendritic and axonal processes becoming disconnected from the neuronal network. This contributes to major synaptic loss, that tightly correlates with cognitive decline[170–172]. BDNF and TrkB receptors are both expressed by pre- and post-synapses. BDNF is stored in vesicles and can be released upon depolarisation, where it binds to TrkB receptors activating signalling pathways (section 1.4). These signals regulate intricate processes such as neuronal growth, whereby it can influence cytoskeleton remodelling[126] and strengthen synaptic connections, regulating AMPA receptor scaling[173]. Therefore, it can be said that synaptic loss occurring through axonal and dendritic vulnerability is the main factor leading to the altered BDNF signalling in disease.

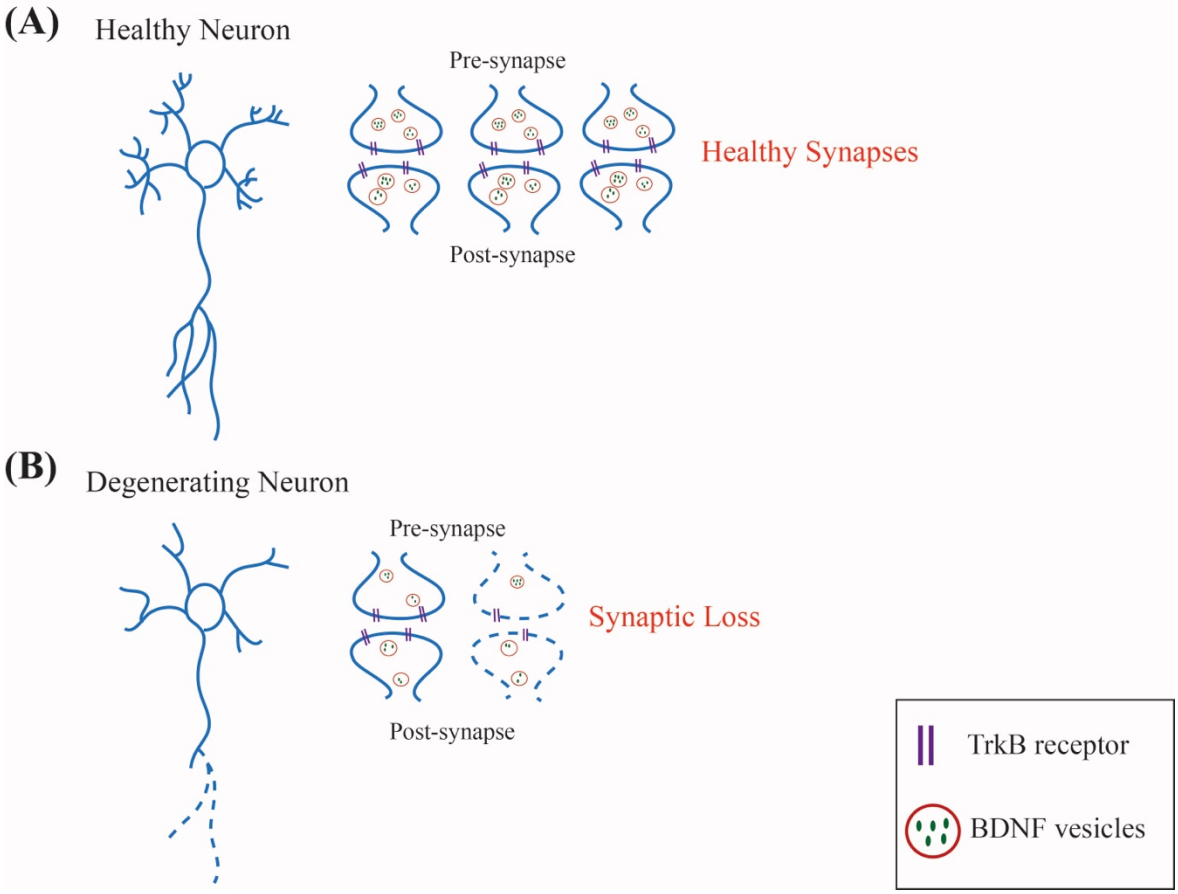

Figure 3.1 Schematic of compromised axonal and dendritic processes leading to synaptic loss in degenerating cells and its relation to BDNF and TrkB expression.
Simplified illustration of neuronal processes and synaptic connections within (A) healthy and (B) degenerating neurons. (A) The health of dendritic and axonal processes is vital for neurons to remain within a connected network. BDNF-containing vesicles and TrkB receptor expression is found in both pre- and post-synaptic regions. BDNF signalling is required for regulated synaptic scaling as well as axonal and dendritic growth. (B) In neurodegenerative diseases, pathogenic mutations disrupt axonal integrity (dashed lines) to the degree where BDNF and TrkB transport becomes severely compromised. In which case, a decrease in the expression is observed. This leads to synaptic loss (dashed lines), whereby neuronal processes ultimately become disconnected from what was a highly organised and regulated neuronal network. This in turn results in neuronal loss, an irreversible process.

In light of this, it is important to establish a cellular model where axonal integrity is compromised in order to look at the changes in BDNF signalling within a disease state. Thus, the first aim on this project was to identify a suitable cellular model where axonal integrity can be manipulated to mimic disease-like changes, to truly represent BDNF signalling in neurodegeneration. From this, the signal transduction can be looked at further and thereafter, signal manipulation can be considered for therapeutic purposes.

In regard to mechanistic functions dependent on axon integrity, the organised transport of various cargo throughout the neuron is required to support its growth and function. For instance, the active anterograde transport of newly synthesised BDNF and TrkB receptor from the cell soma compartment to axon ends is needed for the release of BDNF into the synaptic cleft and the insertion of the TrkB receptor into the plasma membrane[105,174]. Conversely, for signal transduction, the retrograde transport of activated signals transmitted from internalised BDNF-bound TrkB receptor complex from the axon terminals to the cell soma is crucial for the induction of immediate early genes[175,176]. In multiple neurological diseases, varying from numerous types of tauopathies to ALS and HD, defects in axonal transport have been reported to contribute towards neurodegeneration[112,177,178]. In each of these diseases, the accumulation of pathological deposits or mutations in proteins within the axon has been reported to disrupt the efficient transport mechanism. These factors also need to be implemented in the projects *in vivo* model, with a particular emphasis given as to how physiologically relevant the system is in mirroring BDNF deficits seen in neurodegenerative diseases. Therefore, the following facets have been included in this project's *in vitro* model:

in vitro models to understand BDNF signal transduction in neurodegeneration		My Tau^{P301L} *in vitro* model
4	Human disease relevant model	FTLD-17
5	Pathological mutation/protein deposits	Tau aggregates
6	Vulnerable axonal integrity	BDNF transport deficit
7	Synaptic loss	FTLD17 previously reported synaptic deficits[147]

Table 3-1 Features to be considered for a physiologically relevant *in vitro* model replicating disease-like axonal vulnerability.

A way to incorporate these features into an *in vitro* model is to introduce a human disease mutation into primary cells derived from embryonic mice that causes synaptic loss and compromises axonal integrity. I decided to introduce a mutation commonly recognised in FTLD-17, Tau^{P301L}. This is a missense mutation within the human tau gene, where proline is substituted to leucine, at position 301. The pathogenic alterations implicated is the abnormal activity of the tau protein, which under healthy conditions binds to microtubules to stabilise them. In the diseased-state, tau becomes hyperphosphorylated and unbinds from microtubules, the unbound tau then forms filaments of tau deposits within the cell[179]. This disease is considered a 'Tauopathy' due to the accumulation of hyperphosphorylated tau aggregates. The clinical symptoms of this mutation include behavioural and personality disturbances, cognitive decline and motor dysfunction (signs of parkinsonism-linked syndrome)[173]. Moreover, from the Tau^{P301L} transgenic mouse model, we already know that axonal degeneration[180] and impaired axonal transport[179] are both features in this model. Synaptic loss is also well characterised in rTg4510 mice, where a decrease in the number of spines and the expression of synaptic proteins is observed[181]. Moreover, the expression of this mutation *in vitro* has also confirmed synaptic deficits, such as tau mislocalisation to spines and decreased expression of glutamate receptors[147]. Therefore, the expression of Tau^{P301L} in primary neurons meets the outlined requirements (Table 3-1) for a suitable model to investigate BDNF signalling alterations in a disease relevant context.

Despite the number of findings justifying this reasoning behind this model, it was important to address the following questions before investigating BDNF signal propagation in disease. The first was to determine what effect this mutation has on axonal integrity. This was a two-fold assay, where microtubule stability was assessed, followed by a functionality test looking at the impact the mutation has on transport carriers. Finally, the mutation itself was characterised in terms of tau aggregation, quantifying the amount of aggregation occurring in the cell itself. By carrying out these assessments, I was able to link BDNF signal alterations in relation to the pathogenic state of the cell.

3.2 Methods

The culture method used in the following experiments utilised mass culture, where hippocampal cells are grown in plates or live cell imaging dishes, with supplemented NBM. The hippocampal cells are then transfected with the desired construct.

3.2.1 Plot profile analysis of Tau expression

Images of GFP and Tau^{P301L} transacted cells were analysed using ImageJ software (NIH). Axonal lengths were identified as the longest axonal branch extending from the longest neurite. Distal axons were defined as being at least 50 μm away from the cell body. Plot profiles were generated using ImageJ by analysing the pixel intensity of the distal axon. These values were collected in Excel spreadsheet, each file representing an independent culture preparation. This data was analysed using a MATLAB script (see Appendix B). Briefly, the script compares the pixel values of GFP and GFP-Tau^{P301L} (experimental condition) expressing cell against the pixel values from matched time-points of RFP-Tau^{WT} (control condition). It generates a baseline of each individual axonal stretch by subtracting the 10^{th} percentile value from all the values, establishing any points that lie outside 5 times the mean of the standard deviation of all the control axons from the experiment as aggregate containing. The script calculates how many of the experimental axon plot profile values are outside this range and then determines how many of these axons have >10% of their values as aggregated points. The percentages of aggregated points are plotted on GraphPad Prism 7 (version 7.00m Graph Pad Software Inc.). Statistical analysis was performed in GraphPad Prism.

3.2.2 BDNF analysis

Analysis of BDNF (bound to a fluorophore) transport was carried out in GFP and EGFP-Tau^{P301L}-expressing hippocampal cells using live a cell imaging technique as described below. As to whether these BDNF vesicles are derived from endocytosed BDNF, bound to TrkB, or new synthesised BDNF, shuttling from the Golgi was not examined in this assay.

Hence, the bi-directional movement of BDNF recoded in the following experiments could be from either pathways (endocytosed BDNF vs. newly synthesised BDNF).

Experiments carried out to assess the level of disruption caused to the transport mechanism by Tau^{P301L} expression focused on the distal axonal region. The focus on recording transport of BDNF from the distal axon is to understand whether BDNF can propagate its signal over large distances, the very end of the axon (distal region) to the cell soma. Therefore, it is important to determine the status of distal axonal region in Tau^{P301L}-expressing cells.

3.2.2.1 BDNF transport time-lapse imaging

Time-lapse microscopy was used to image BDNF-RFP-containing endosomes in EGFP-Tau^{P301L} and GFP transfected hippocampal cells. For live cell imaging, glass bottom dishes (MatTek) were plated with primary hippocampal neurons (150,000 cells per dish) and co-transfected at *DIV*5 with GFP-Tau^{P301L} and BDNF-RFP or GFP and BDNF-RFP at *DIV*5 for BDNF transport imaging (as described in section 2.4.1). On *DIV*6-7 and *DIV*11-12, 25mM HEPES-NaOH was added to each dish and transfected distal axons were selected for imaging on the DeltaVision Elite system. Images were taken once every 5 seconds for 10 minutes in the TRITC channel. A reference image was taken in FITC of GFP or GFP-Tau^{P301L} expressing axon. Images were taken with a 60x/1.42NA Oil Plan APO objective using SoftWoRks software (version 6), using 0.08 second exposure at 10% light.

3.2.2.2 BDNF stationary vesicle analysis

All BDNF transport data analysis was generated from the BDNF live cell imaging videos mentioned in section 3.2.2.1.

The number of stationary vesicles within each distal axon of GFP or GFP-Tau^{P301L} expressing cell was determined by using ImageJ. Distal axons were traced and using the

MultipleKymograph plugin (J. Rietdorf and A. Seitz), a kymograph was generated, which stacked the still view of each frame below the previous one, plotting time down the y-axis and distance along the x-axis. This gives a 2-D representation of BDNF transport within the distal axon. The length of axon within the field of view ranges from 50-60 μm long. Stationary vesicles were classed as those which did not move the number of stationary vesicles was defined as those that did not reach a cumulative distance of 50 μm. This was then normalised to the length and time. This value was plotted against the total number of vesicles within the axonal stretch as a percentage for each condition on GraphPad. During this analysis, the total number of vesicles in each condition were also plotted.

3.2.2.3 BDNF transport velocity analysis

BDNF vesicle speed was calculated by manually tracking the speed of moving vesicles from distal axons of GFP and GFP-Tau^{P301L} expressing cells. BDNF transport movies were loaded on to ImageJ software and using the particle analysis – manual tracking (F. Cordelieres and J. Schindelin) plugin, individual moving vesicles were tracked through the entire length of the axon within the field of view. The speed of each BDNF vesicle moving from one frame to the next was plotted into an Excel file that binned the individual speeds from all the tracked vesicles in 0.2 μm/s increment bins. The file then generated the number of total vesicles tracked, as well as the total number of vesicle movements that moved within 0.2 μm/s up to 3.6 μm/s between two frames. This value was then divided by the total number of vesicles tracked and plotted as frequency of BDNF vesicle movement along the Y-axis and speed (μm/s) along the X-axis.

3.2.2.4 Cumulative profile analysis

To visualise how often BDNF vesicles pause in each conditions along distal axonal regions, the cumulative distance travelled of all the vesicles was plotted from the velocity measured of each moving BDNF vesicle as described in 3.2.2.3.

3.2.3 EB3 microtubule analysis

To measure EB3 dynamics, a similar co-transfection method was carried out at *DIV*5 in glass bottom dishes (150,000 cells per dish), with mCherry-EB3 DNA instead of BDNF-RFP (as described in section 2.4.1). On *DIV6-7* and *DIV11-12*, 25mM HEPES-NaOH was added to each dish and GFP or GFP-Tau^{P301L} expressing axon were selected for imaging. Images were taken every 2 seconds for 5 minutes in the mCherry channel on the DeltaVision Elite system. A reference image was taken in FITC of the distal axon. Images were taken with a 60x/1.42NA Oil Plan APO objective using SoftWoRks software (version 6), using 0.08 second exposure at 10% light.

To look at microtubule dynamics, a cotransfection was carried out using EB3-mCherry with GFP or GFP-Tau^{P301L} (as described in section 2.4.1) and live cell imaging of EB3 dynamics was conducted as described in section 3.2.2. Kymographs were generated from each live cell imagine video in a similar manner as detailed in section 3.2.2.2. Microtubule lattice lengths were measured from each kymograph and data was plotted on GraphPad Prism.

3.3 Determining axonal integrity of Tau^{P301L}-expressing neurons

Hippocampal cells from embryonic mice were plated and transfected at *DIV5* with EGFP-Tau^{P301L} construct. Cells expressing this mutation will be referred to as Tau^{P301L}-expressing cells from this point onwards, unless specified otherwise. As a control against the pathogenic tau, a GFP-only construct was transfected in hippocampal cells at *DIV5*, which will now be referred to as GFP-expressing cells. The reason why GFP is the most suitable control rather than a non-pathogenic version of tau is because the over-expression of hTau^{wt} in mice has been reported to also compromise axonal integrity and the structure of organelles such as the Golgi[182–184]. Moreover, many researchers use the over-expression of hTau^{wt} as a simplified model of 'early' disease stage[182,184]. Therefore, GFP expression alone was used as a control to compare the effects of Tau^{P301L}-expression on axonal integrity. The reason why both of these constructs were introduced at *DIV5*, is because I wanted to avoid any disruption in neuronal cell polarity development potentially caused by the introduction of pathogenic tau. Therefore, the 5-day transfection time-point was chosen because by this stage, functional polarisation of axons and dendrites has been established[185,186].

Considering the complexity of a neuronal network, maintaining the structure along the entire length of the axon is most vital. Axonal integrity is largely dependent on regulated microtubules architecture as without this, the neuron would not be able to maintain its shape or structure. Microtubules function not only as part of the cells cytoskeleton, but it also act as 'train tracks' along axons, dendrites and growth cones, whereby the transport of cargo is tightly controlled by motor proteins[187]. Therefore, to assess the integrity of the axon within Tau^{P301L}-expressing cells, microtubule polarity and its dynamic growth was examined. The transport of BDNF vesicles along microtubules within pathogenic tau expressing cells was also investigated as a readout of a microtubule-dependent mechanism.

3.3.1 Assessing Microtubule Polymerisation

Microtubules are formed through the polymerisation of α-tubulin and β-tubulin heterodimers which associate laterally to from a tubule. The structure is known to be highly dynamic due to the rapid assembly and disassembly. The slow-growing (minus) end and fast growing (plus) end are regulated by microtubule plus-end-tracking proteins (+TIPs) and are organised in a precise manner, where all microtubules have their plus end facing the axonal ends within axons whereas in the dendrites, the polarity of microtubules is mixed[121]. To assess the degree of disruption to microtubule polarity and its growth, many researchers commonly utilise end-binding (EB) proteins in their assay to track and visualise the growing ends of microtubules[187]. EB protein is a core +TIPs that is located at the plus-end, which in comparison to the minus-end is far more dynamic and explorative [121]. The reason why this is a commonly used fluorescence probe is because around 270 EB dimers can bind to the growing-end of microtubules, forming a comet-like appearance[187]. These comets represent the rapid turnover of several cycles of binding and unbinding before the growing end matures into a microtubule lattice (Figure 3-1)[121]. Therefore, I used EB3 protein fused to a fluorescent probe to track the growing end of microtubules in Tau^{P310L} and GFP-expressing hippocampal cells and determined the mature lattice lengths in both conditions.

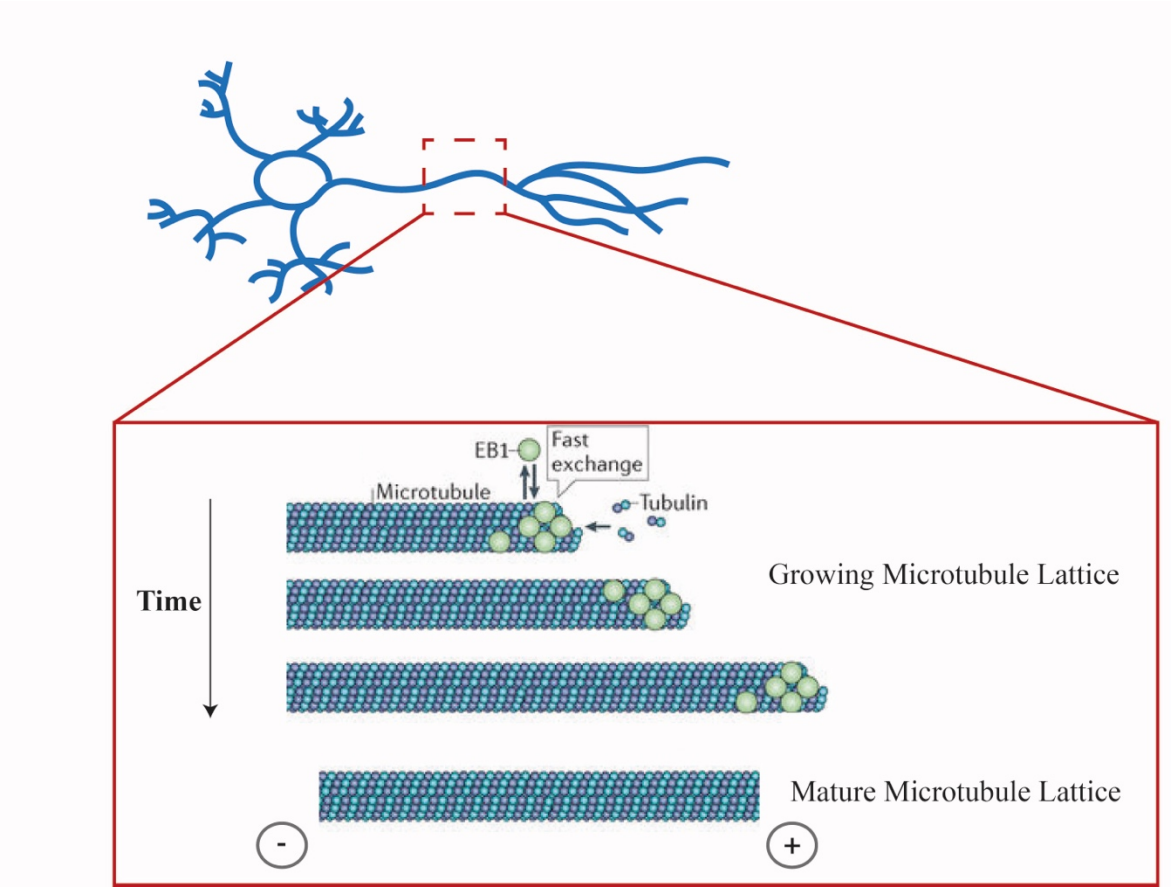

Figure 3-1 Schematic of microtubule growth and EB protein interaction.
Illustration of microtubule growth within an axonal stretch. Mammalian cells express up to three different EB proteins: EB1, EB2 and EB3. Multiple EB proteins bind to the growing end of microtubules, recruiting tubulin dimers and thus elongated microtubule lattices over time. When EB proteins are no longer bound to the growing end, a mature microtubule lattice is generated. Adapted from Akhmanova and Steinmetz (2015).

3.3.1.1 Tau^{P301L}-expression results in shorter mature microtubule production but does not affect microtubule polarity

I co-transfected hippocampal cells at *DIV5* with EB3-mCherry and GFP or Tau^{P301L} and carried out live cell imaging of EB3 events in distal axonal regions which were in focus within the field of view at *DIV6-7* and *DIV11-12*. The videos were analysed using ImageJ and kymographs were generated from each live cell imaging video (Figure 3-2). Kymographs are a 2-D representation of what is seen within each live-cell imaging video, where each frame is stacked below the previous one. This generates a 2-dimentioal view of all the events taken place, where the x-axis represents the distance and the y-axis represents time, from start to finish (Figure 3-3A). Using these kymographs, EB3 bound and unbound state can be visualised and this in turn relates to growing microtubule events in GFP-expressing axons (Figure 3-3B-C) or Tau^{P301L}-expressing axons (Figure 3-3D-E). This length can be measured from the kymographs. Moreover, the polarity of microtubules can be visualised within these kymographs, as EB3 is only bound to the plus-end of microtubules. Therefore, I was able to assess whether pathogenic tau altered the organisation of microtubules within axonal regions.

Significant changes in microtubule polymerisation is observed from *DIV6-7* in Tau^{P301L}-expressing cells (Figure 3-4A). Within these tau pathogenic cells, due to a change in microtubule polymerisation, shorter microtubule lattices are produced compared to what is seen in GFP control cells. What is surprising is that the disruption in microtubule polymerisation occurs earlier in pathogenic tau expressing cells. Moreover, the change is sustained rather when comparing the expression of Tau^{P301L} from *DIV6-7* to *DIV11-12* (Figure 3-4B-C). The mature microtubule polymerisation within the control cells is varying, as short as 1 μm to 10+ μm microtubule lengths are consistent between the two time-points (Figure 3-4D). I also checked the polarity of all the trajectories in each kymograph and the orientation of microtubules did not change. In Tau^{P301L}-expressing cells, microtubule polymerisation is altered (compared to GFP-expressing cells), whereby there is an increase in microtubules that are between 1-3 μm in length. This change is seen from *DIV6-7.* The orientation of microtubules in these cultures is unaffected.

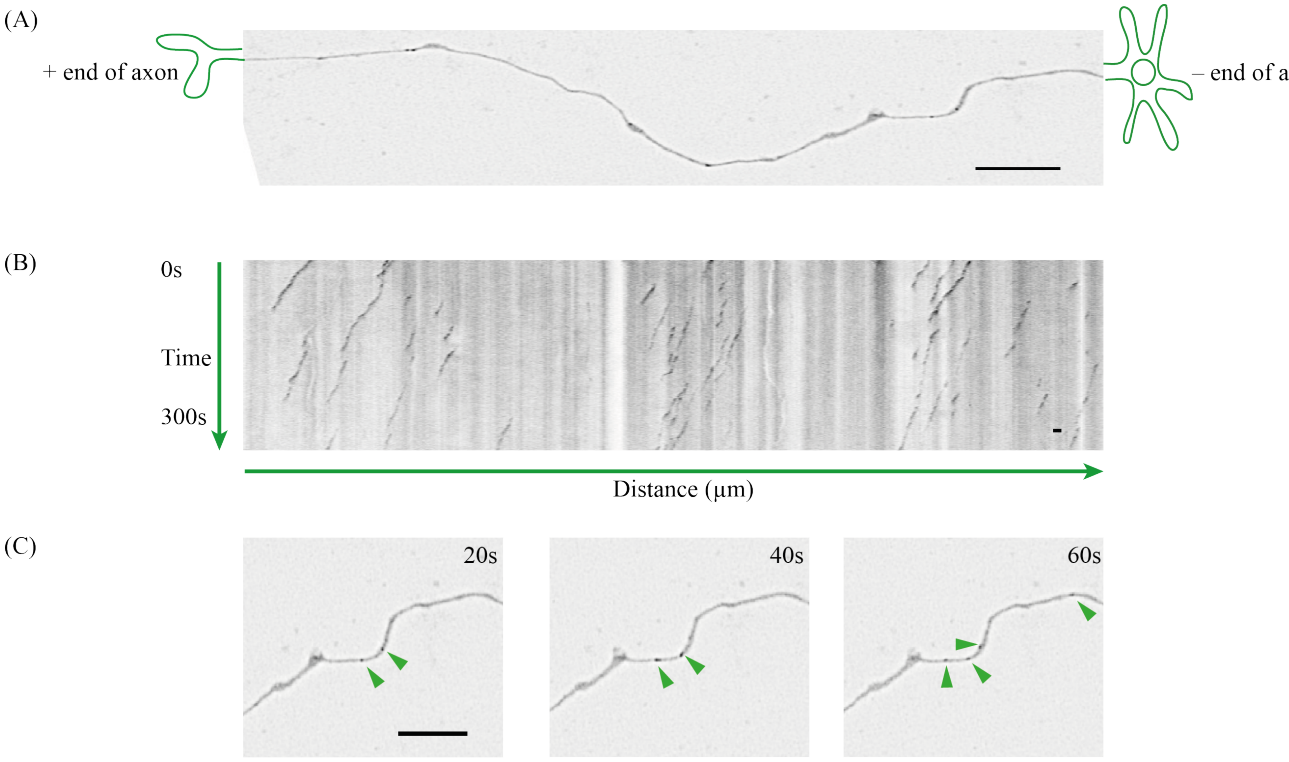

Figure 3-2 Representative EB3 comets from Tau^{P301L}-expressing distal axonal region.

(A) Tau^{P301L}-expressing distal axonal region (*DIV7*) showing EB3 comet projection (dense pixels along the distal axon). (B) Kymograph representing a 2D visual image taken from distal axonal region shown in (A) highlighting the EB3 projections with time down the y-axis and distance along the x-axis. The kymograph shows the comet like projections, where EB3 is bound to the plus end of the microtubules during polymerisation. (C) Still images taken at 20s intervals. Through the 20s interval frames, movement of EB3 can be visualised, moving towards the growing end of the microtubule (green arrow heads). Scale bar: 10 μm.

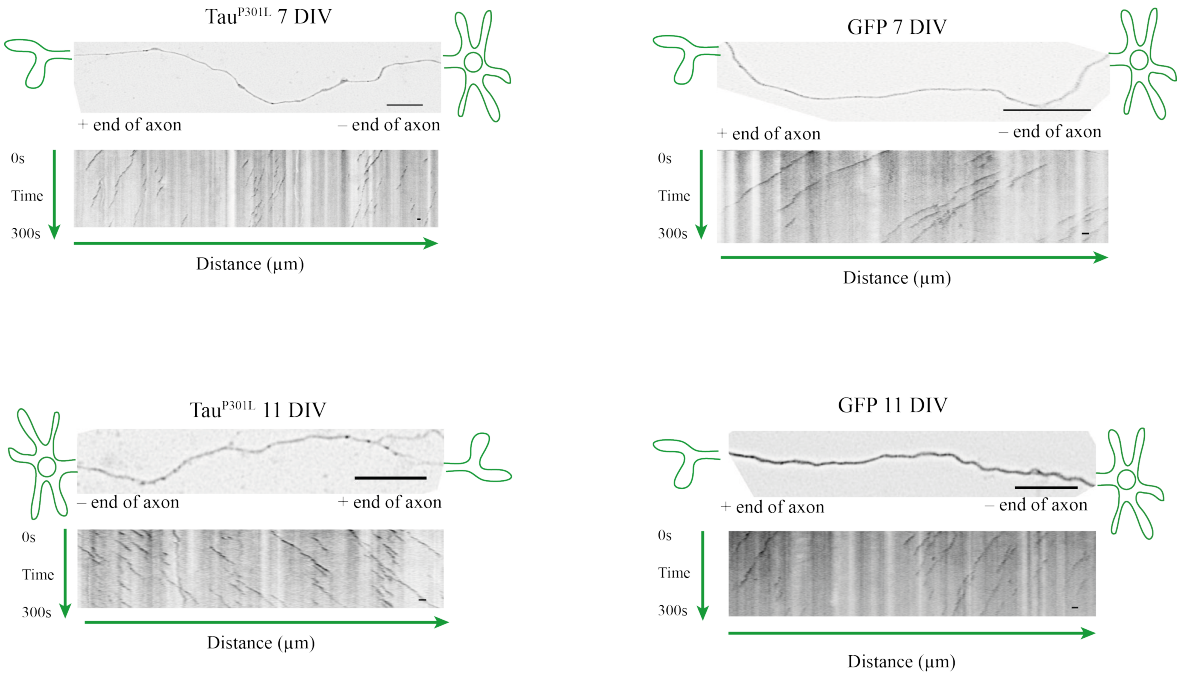

Figure 3-3 EB3 kymographs from GFP and Tau^{P301L}-expressing axons. Representative kymographs taken from GFP-expressing and Tau^{P301L}-expressing at *DIV7* and *DIV11*. The kymographs show 2D representation of EB3 comets moving unidirectionally within the axonal stretch, with distance along the x-axis and time down the y-axis. The dense pixel projections represent EB3 comets at plus-end of microtubules, projecting in a unidirectional manner. Each axonal stretch was roughly 50 µm long. Scale bar: 10 µm.

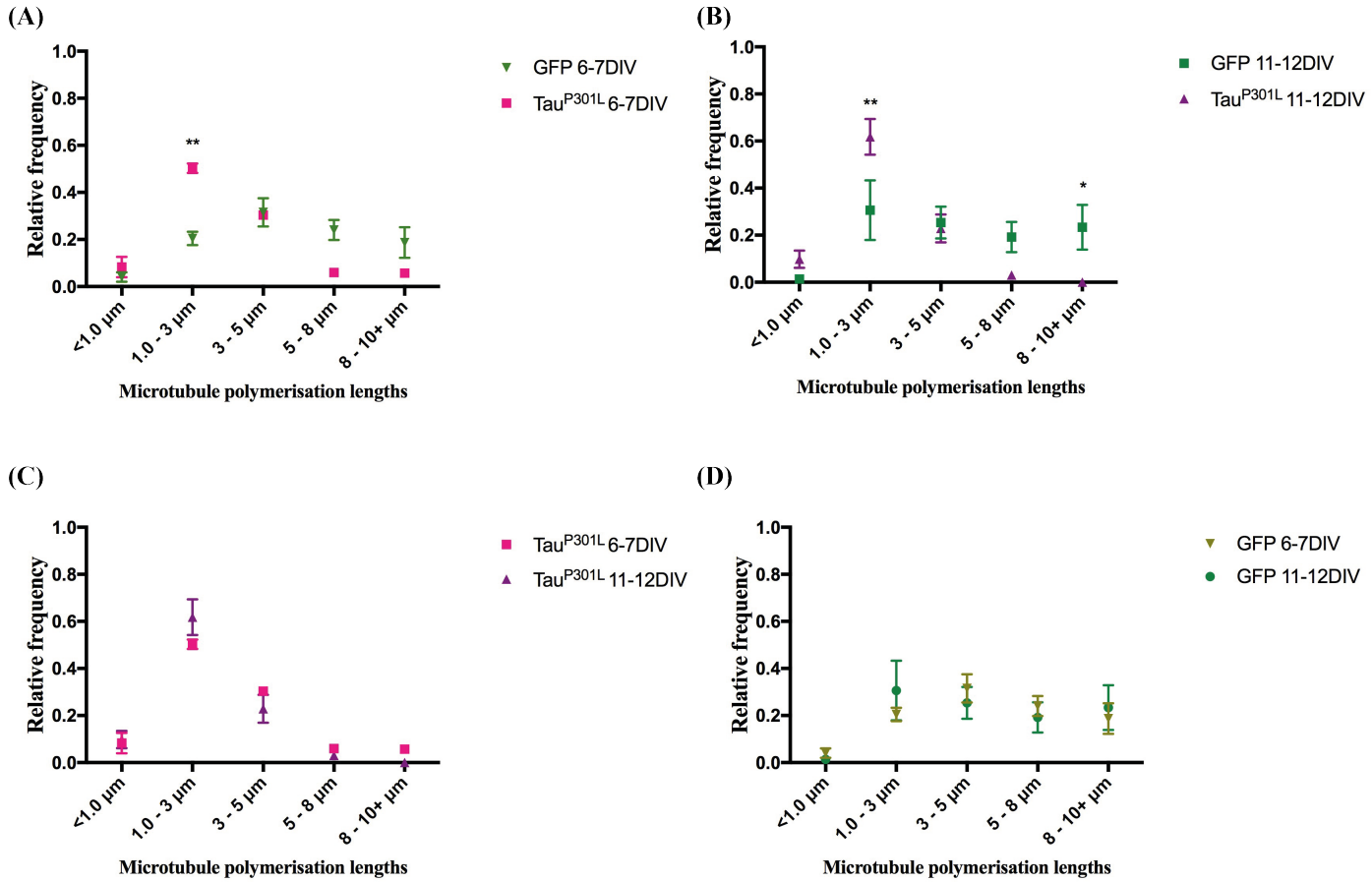

Figure 3-4 Tau^{P301L} expression results in shorter mature microtubules. Quantification of microtubule growth in GFP and Tau^{P301L}-expressing axons. Graphs displaying relative frequency of microtubule polymerisation in each condition. (A) Showing the comparison in microtubule polymerisation in GFP and Tau^{P301L}-expressing axons at *DIV* 6-*7* and (B) *DIV11-12*. Comparing the two different time points (C) shows microtubule polymerisation in Tau^{P301L}-expressing axons both at *DIV*6-7 and *DIV11-12* and (D) showing microtubule polymerisation in GFP-expressing axons at both time points. Two-way ANOVA, $p<0.0001$, n= 3+ axons analysed from 3 independent culture preparations.

3.3.2 Assessing kinesin and dynein-driven transport

Having seen a disruption in microtubule polymerisation, leading to shorter mature microtubule lattice production, I next wanted to see what impact, if any, this had on the transport of cargo within the Tau^{P301L}-expressing cells. In addition to this, as a measure of axonal integrity, a functional test can be carried out. A major component of the axon is to function as 'train tracks' for the efficient transport of cargo back and forth within the cell. Therefore, assessing the transport of BDNF will enable me to understand the degree of disruption to the integrity of the axon.

Researchers have already dissected the differences between kinesin and dynein-driven motors in disease (see section 1.7). As tau is a key neuronal MAP involved in stabilising microtubules, efforts have been made to understand the involvement of tau and motor proteins and thereafter the changes in these motors in various tauopathies. We now know that there are differences in the susceptibility between kinesin and dynein movement in response to varying tau concentrations and that tau is involved in modulating motility of motor proteins[183,188]. From this research, we know that tau controls the balance of microtubule-dependent transport by modulating motor function[188]. Lower concentrations of tau allow kinesin to efficiently bind to microtubules and initiate anterograde transport, whereas high concentrations of tau, results in kinesin unbind to microtubules and facilitates cargo release[183]. Therefore, it can be hypothesised that in areas where high levels of tau accumulate, kinesin transport is disrupted.

In order to assess the level of change in kinesin and dynein-driven BDNF transport, hippocampal cells were co-transfected at *DIV5* with BDNF-RFP and Tau^{P301L} or GFP. Axonal regions which were in focus within the field of view were imaged at *DIV6-7* and *DIV11-12* via time-lapse imaging. These axonal stretches were at least 50 μm away from the cell body. A number of assays were carried out to assess the transport of cargo within healthy and disease-inflicted cells.

3.3.2.1 Tau^{P301L} expression increases the percentage of stationary BDNF vesicles

The first type of analysis carried out was looking at the percentage of stationary vesicles. This was quantified using kymographs generated from each live-cell imaging video (Figure 3-5). Parameters were set to determine moving and stationary vesicles. The requirement for stationary BDNF vesicle is that in total, the vesicle does not move more than 50 μm along an axonal stretch. These values were calculated for each condition and plotted as a percentage. Figure 3-5 shows representative kymographs from each condition at two time-points. The kymographs represent BDNF vesicle movement, where distance is along the x axis and time, from start to finish is down the y-axis. The dark vertical lines represent stationary BDNF vesicles. These are more prominent in Tau^{P301L}-expressing cells suggesting an increase in the number of stationary vesicles. The moving vesicles show the different trajectories of BDNF vesicle movement. From this, the number of stationary vesicles is recorded. The quantification shows an increase the number of stationary vesicles in Tau^{P301L}-expressing cells from *DIV6-7* can be (Figure 3-8). The mean percentage of stationary vesicles is sustained through to the later time-point of *DIV11-12*. This suggests that the onset of disruption is early and that the expression of the mutation over time does not significantly affect the number of stationary vesicles.

3.3.2.2 The number of vesicles in Tau^{P301L}-expressing distal axons is the same as control conditions

From the analysis carried out on stationary vesicles, the same cells were used to calculate the number of total vesicles in GFP and Tau^{P301L}-expressing distal axons (Figure 3-9). These results show no significant difference in the total number of vesicles in the distal axonal regions (relative in 50 μm axonal stretch). This suggests that although there is an increase in the number of stationary vesicles (Figure 3-8), there is the same number of vesicles along the distal axonal regions at both time points in both conditions. The vesicles tracked in this experiment are a product of overexpression (BDNF-RFP) rather than endogenously expressing BDNF, and therefore, the cell is producing a lot more BDNF

than it normal would under physiological conditions. This as a result, can account for why there is an increase in BDNF vesicles along distal axonal regions. In addition, there is a lot of variability in each cell which cannot be controlled, such as expression rate and overall health of the cultures. In this analysis, only carried out 3+ independent culture preparations, therefore an increase in cell numbers is required to fully understand the extent of disruption to the axonal transport system.

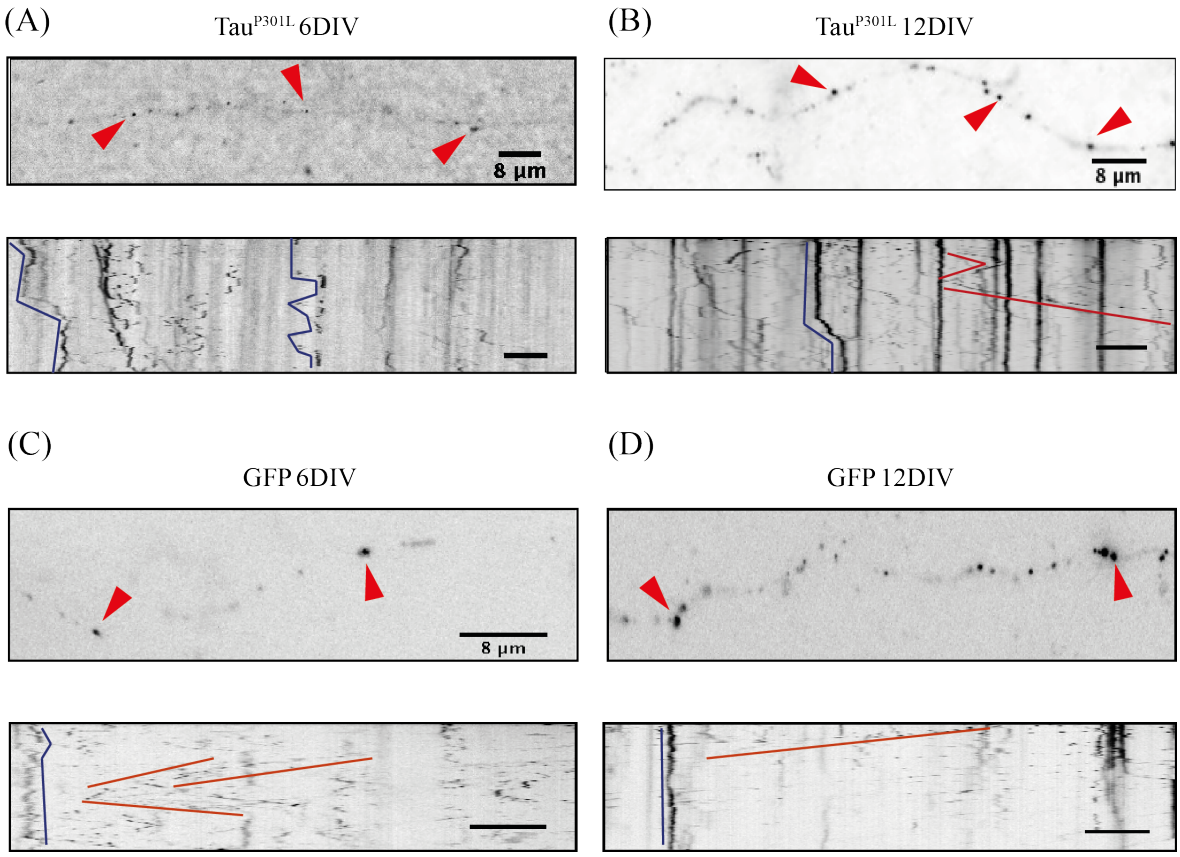

Figure 3-5 Kymographs generated from distal axons of GFP and Tau^{P301L}-expressing cells. Live-cell imaging videos of distal axons from GFP and Tau^{P301L}-expressing cells were used to generate kymographs which show a 2D visual representation of all BDNF vesicles (a few highlighted by the red arrow heads). (A-B) Representative examples taken from Tau^{P301L}-expressing axons at (A) *DIV6* and (B) *DIV12*, with corresponding kymographs directly underneath and (C-D) representative examples taken from GFP-expressing axons at (C) *DIV6* and (D) *DIV12* with corresponding kymographs directly underneath. Vertical trajectories which indicate stationary vesicles are highlighted in by blue lines, and moving vesicles are indicated by red line.

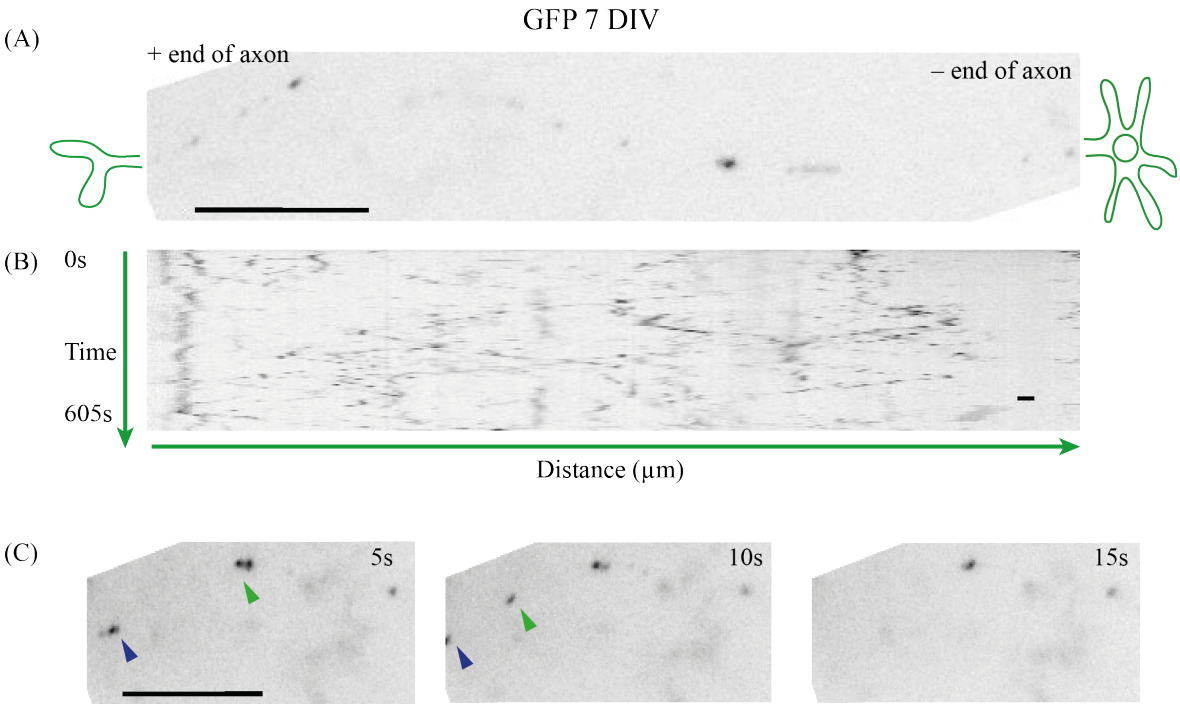

Figure 3-6 Kymograph and live-cell imaging frames representing BDNF vesicle movements in GFP-expressing axon at *DIV7*.

(A) Distal axon expressing GFP at *DIV7* shows BDNF-RFP vesicles (dense pixelated spots). (B) A representative kymograph generated from (A) the GFP-expressing distal axon, shows the trajectories of BDNF movement over time. Vertical trajectories indicate stationary BDNF vesicles. (C) Still images taken from (A), showing BDNF movement at 5s intervals. The green arrow shows the movement of a single BDNF containing endosome, from 5s to 10s. The blue arrow indicates movement from one frame to the next of a separate BDNF containing endosome. Scale bar: 10 µm

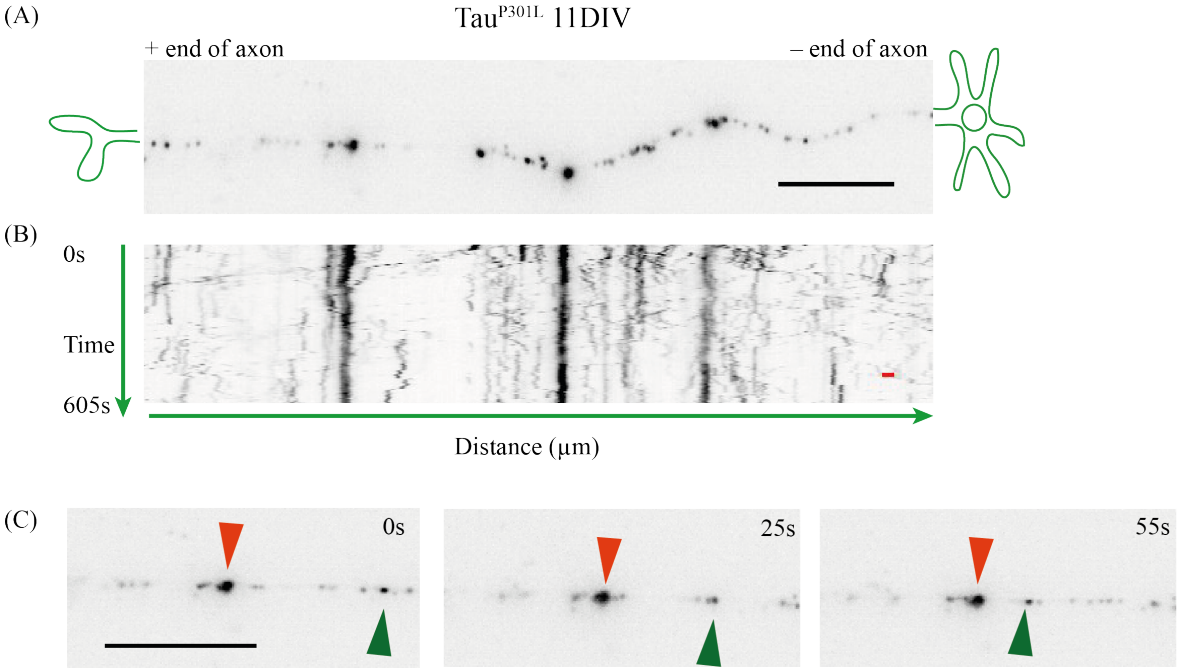

Figure 3-7 Kymograph and live-cell imaging frames representing BDNF vesicle movements in Tau^{P301L}-expressing axon at *DIV11*.

(A) Distal axon expressing Tau^{P301L} at *DIV*11 shows BDNF-RFP vesicles (dense pixelated spots). (B) A representative kymograph generated from (A) the Tau^{P301L} -expressing distal axon, shows the trajectories of BDNF movement over time. Vertical trajectories indicate stationary BDNF vesicles, which have increased in Tau^{P301L}-expressing cells at *DIV11*. (C) Still images taken from (A), showing BDNF movement at varying intervals. The green arrow shows the movement of a single BDNF containing endosome. The red arrow indicates stationary vesicles which has not moved over time. Scale bar: 10 µm.

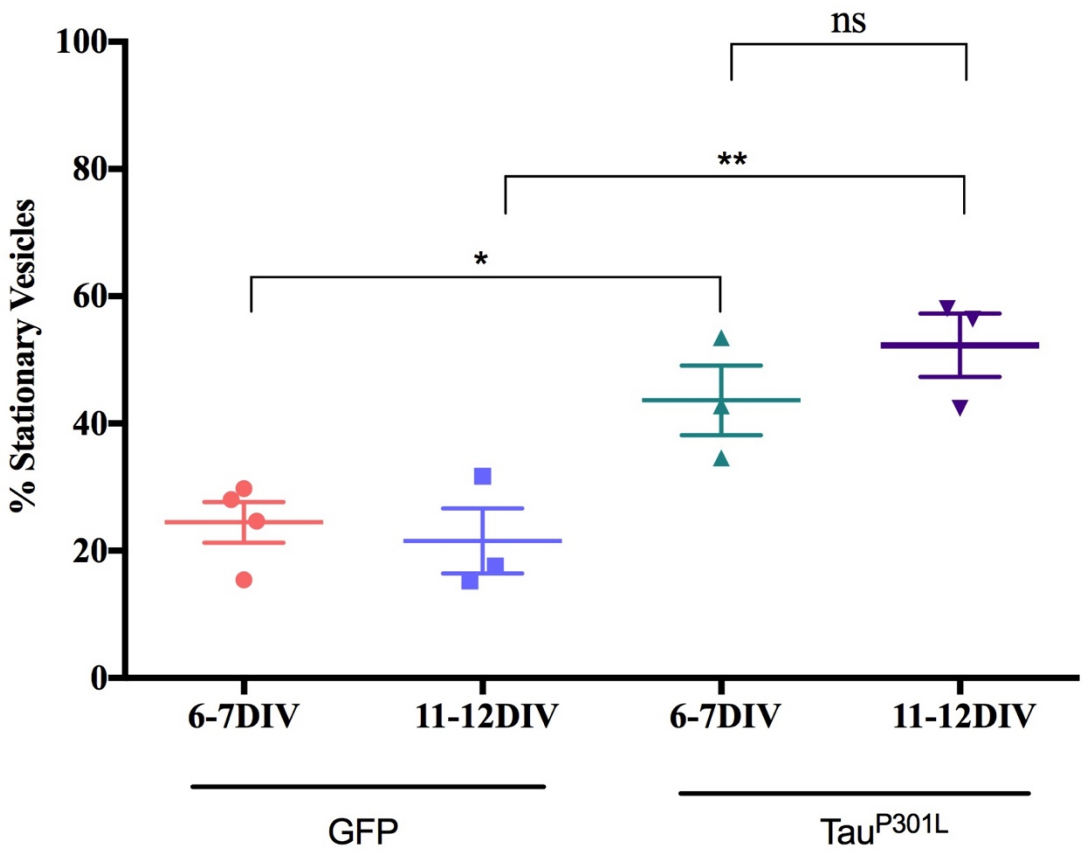

Figure 3-8 Percentage of stationary vesicles is significantly altered in Tau^{P301L}-expressing axons.

Percentage of stationary BDNF vesicles in GFP and Tau^{P301L}-expressing distal axons is plotted where individual points represent independent experiments. A significant increase in the percentage of stationary vesicles is seen from *DIV6-7* in Tau^{P301L}-expressing cells, compared to controls. There is no progressive increase between the two time-points in Tau^{P301L}-expressing cells. Each point represents an independent culture preparation, with 4+ axons analysed in each culture preparation. There is a statistically significant differences between group means as determined by one-way ANOVA, $p<0.001$.

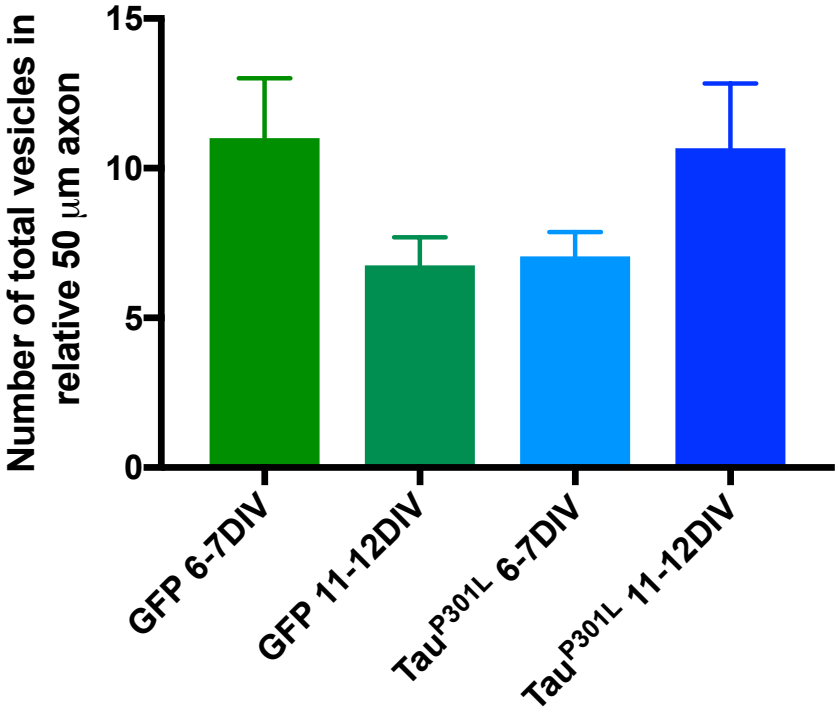

Figure 3-9 Total number of vesicles in GFP and Tau^{P301L}-expressing cells.
The total number of vesicles in distal axonal regions were measured from the same axons used to measure the percentage of stationary vesicles. The number of vesicles were normalised to 50 μm axonal length. There is no significant difference in the number of vesicles in distal axonal region in GFP and Tau^{P301L}-expressing cells at both *DIV6-7* and *DIV11-12*. n= 3 independent culture preparations, with 3+ axons analysed in each culture. Total number of vesicles in each condition, relative to 50 μm axonal length: GFP *DIV6-7*: 32 vesicles ; GFP *DIV11-12*: 35 vesicles; Tau^{P301L} *6-7DIV*: 28 vesicles; Tau^{P301L} *DIV11-12*: 32 vesicles. One-way ANOVA. Error bars: SEM.

3.3.2.3 Tau^{P301L} expression hinders bi-directional BDNF transport

I analysed the instantaneous speed of the moving BDNF vesicles from one frame to the next. This was captured as moving fluorescing puncta along axonal stretches, a commonly used technique to visualise transport of cargo within neuronal processes[134,189–191]. Moving vesicles were defined as those that are able to move in either anterograde or retrograde manner over 50 μm along the axonal stretch. The quantification of moving BDNF vesicle data illustrates the variation in velocity between both conditions and demonstrates the difference between *DIV6-7* and *DIV11-12* in Tau^{P301L} expressing cells (Figure 3-10). Between the two time-points, a progressive change in BDNF vesicle movement is seen, whereby significantly slower moving vesicles are seen in Tau^{P301L}-expressing cells at *DIV11-12*. BDNF vesicles in Tau^{P301L}-expressing cells at *DIV6-7* share a similar profile to the movement of BDNF vesicles in GFP-expressing cells. However, by *DIV11-12*, BDNF vesicle movement is severely disrupted, as majority move at 0.2 μm/s. looking at BDNF vesicle movement in GFP-expressing cells, between both time-points, BDNF vesicle movement is consistent from *DIV6-7* to *DIV11-12*. This is line with published work which shows an average of <0.5 μm/s BDNF vesicle movement in cells which have a disrupted transport mechanism[192]. From this I concluded that the Tau^{P301L} mutation has a direct impact on cargo transport, due to the changes in axonal integrity.

(A)

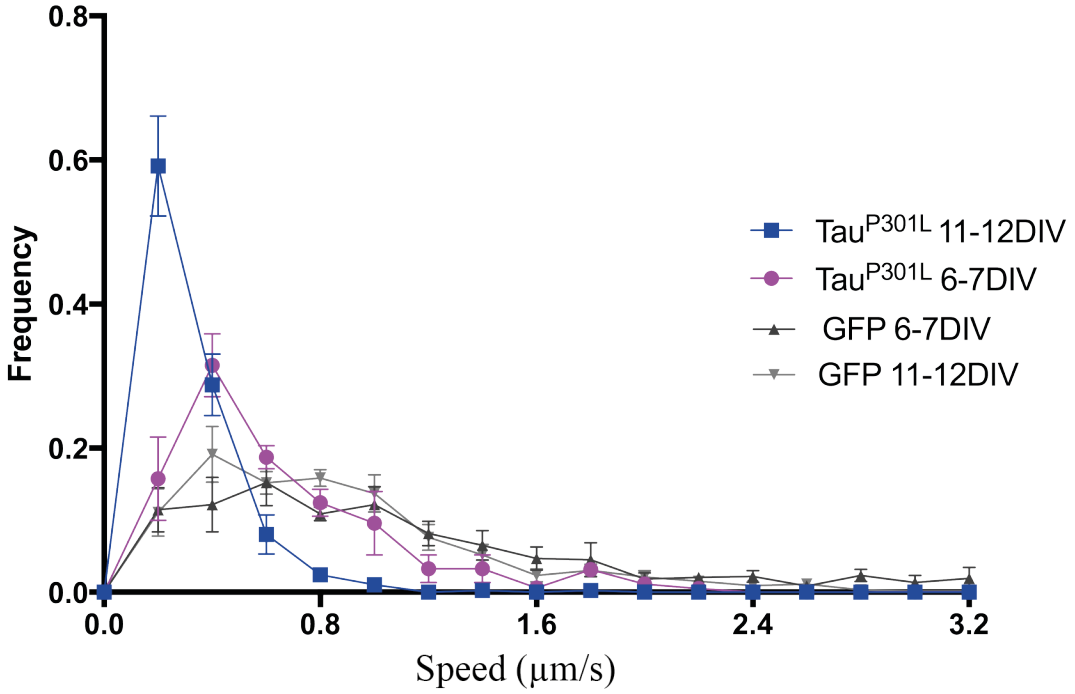

Figure 3-10 Tau^{P301L} expression progressively alters bi-directional transport of BDNF. Velocity of BDNF vesicle transport in Tau^{P301L} and GFP-expressing cells was measured at *DIV6-7* and *DIV11-12*. The frequency was plotted so display the bi-directional movement of BDNF within each condition. Here, progressive disruption in BDNF transport can be seen, where in Tau^{P301L}-expressing cells, there is a high proportion of slower-moving vesicles in an age-dependent manner, compared to the BDNF transport in GFP-expressing cells. From n= 3+ independent culture preparations, 2+ axons were analysed from each preparation. A total of 62 BDNF vesicles were assessed in GFP *DIV6-7* and 72 BDNF vesicles at *DIV11-12*. A total of 60 vesicles were assessed in Tau^{P301L}-expressing axons at *DIV6-7* and 56 BDNF vesicles at *DIV11-12*.

3.3.2.4 Anterograde transport is more susceptible to microtubule changes

Taking into consideration that transport of cargo within the cell is bi-directional, I wanted to dissect out the two processes and analyse the impact of the Tau^{P301L} mutation on anterograde and retrograde transport separately. We already know that the regulation of tau is important for the transport of cargo within the cell[193]. Therefore, I wanted to see whether the expression of mutant tau effected the efficient transport of the distinct motor proteins. From each live cell imaging video of BDNF movement, I noted the location of each cell soma, and thus could determine the direction of transport, with BDNF vesicles moving towards the cell soma as retrograde transport and those towards the axonal ends as anterograde transport.

Using the same method to track the velocity of BDNF movement as described in section 3.3.2.3, both anterograde and retrograde transport was tracked, from separate experiments. The graph for each direction compares the movement of BDNF vesicles between *DIV6-7* and *DIV11-12* of Tau^{P301L}-expressing axons (Figure 3-11). From this data, I can see that anterograde transport is more susceptible earlier (*DIV6-7*) in Tau^{P310L}-expressing axons, whereas, retrograde transport is altered in a progressive manner, from *DIV6-7* to *DIV11-12*, where at the later time-point, transport disruption is more prominent. This suggests, that kinesin-driven transport, the main component of anterograde-dependent trafficking is more susceptible to the changes caused by the Tau^{P301L} mutation than dynein-driven motor proteins. This result is in-line with published worked whereby changes in tau concentration impacts kinesin-driven transport[183]. We know that tau interacts with kinesin motor light-chain and therefore the abnormal kinesin transport is expected in tauopathies[194,195]. It should be noted that an increase in velocity is seen in GFP-expressing cells at *DIV*6-7 in both retrograde and anterograde movement (Figure 3-10 and Figure 3-11). This can be seen as these vesicles could be undergoing fast axonal transport, however fast axonal transport can also be seen at *DIV11-12* (between 0.4 μm/s to 0.8 μm /s)

In light of these differential changes between kinesin and dynein, two important questions arise: (1) whether the delivery of newly synthesised TrkB receptor and BDNF to axonal ends (an anterograde-dependent transport) is implicated and (2) does the relay of signal from the axonal end to cell soma change? This second question would also shed light on whether signal transduction is a transport-dependent mechanism, as hypothesised[12,196].

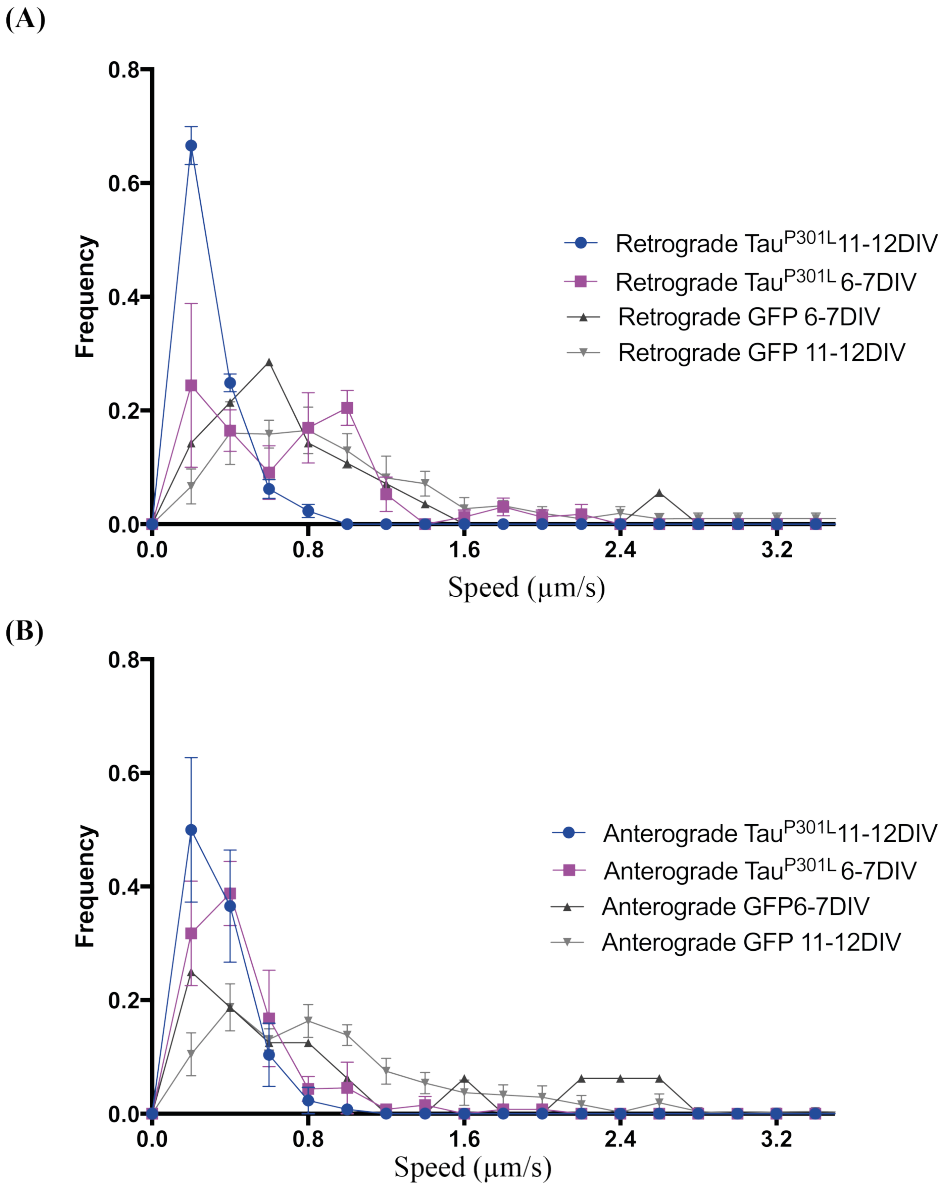

Figure 3-11 Anterograde transport is more susceptible to changes in axonal integrity in Tau^{P301L}-expressing cells.

BDNF vesicle transport was dissected into (A) retrograde and (B) anterograde BDNF vesicles for Tau^{P301L} and GFP-expressing cells at each time point. Clear differences can be seen between the two transport vesicles where disruption in retrograde vesicles is progressive, at *DIV11-12*. Whereas with anterograde vesicles, early disruption is seen by *DIV6-7* in Tau^{P301L}-expressing cell. Transport in GFP-expressing cells remains consistent. Error bars: SEM. n= 3+ independent culture experiments. A total of 40+ BDNF vesicles were assessed from GFP *DIV6-7* and *DIV11-12* axons. A total of 30+ vesicles were assessed from Tau^{P301L}-expressing axons at *DIV6-7* and *DIV11-12*.

3.3.2.5 BDNF vesicles take a longer time to move through an axonal stretch in Tau^{P301L}-expressing cells

To visualise the total length of BDNF vesicle movement in Tau^{P301L}-expressing axons, I generated the cumulative frequency. This allows the me to see if the BDNF vesicles moved , so that the pause time and overall time taken to move through a 50 μm axonal stretch is easily visualised. Moreover, this type of data illustrates the behaviour of the vesicles within each condition. Representational cumulative plots show the in GFP-expressing cells at both *DIV6* and *DIV11*, the BDNF vesicles take a short time to move through a 50 μm axonal stretch, with relatively short pause times. However, in Tau^{P301L}-expressing cells, BDNF vesicles take longer pauses between each movement, and occur at higher frequencies at *DIV11* compared to what is seen in GFP control cells. However, the same profile is not seen at the earlier time-point of *DIV6-7* in Tau^{P301L}-expressing cells. this suggests that the BDNF vesicles that are moving, are doing so at a similar rate to that seen in GFP-expressing cells. Looking at the general movement of BDNF vesicles in Tau^{P301L}-expressing cells, many vesicles do not travel the entire length, or take a substantial amount of time to move through the axonal stretch. From this, it could be suggested that within the Tau^{P301L}-expressing cells, BDNF vesicle transport is distorted and many factors are affected such as the number of stationary vesicles. As there are changes observed in Tau^{P301L} in hippocampal cells compared to GFP-expressing cells, this model can be used to examine long-distance BDNF signalling in a degenerative context.

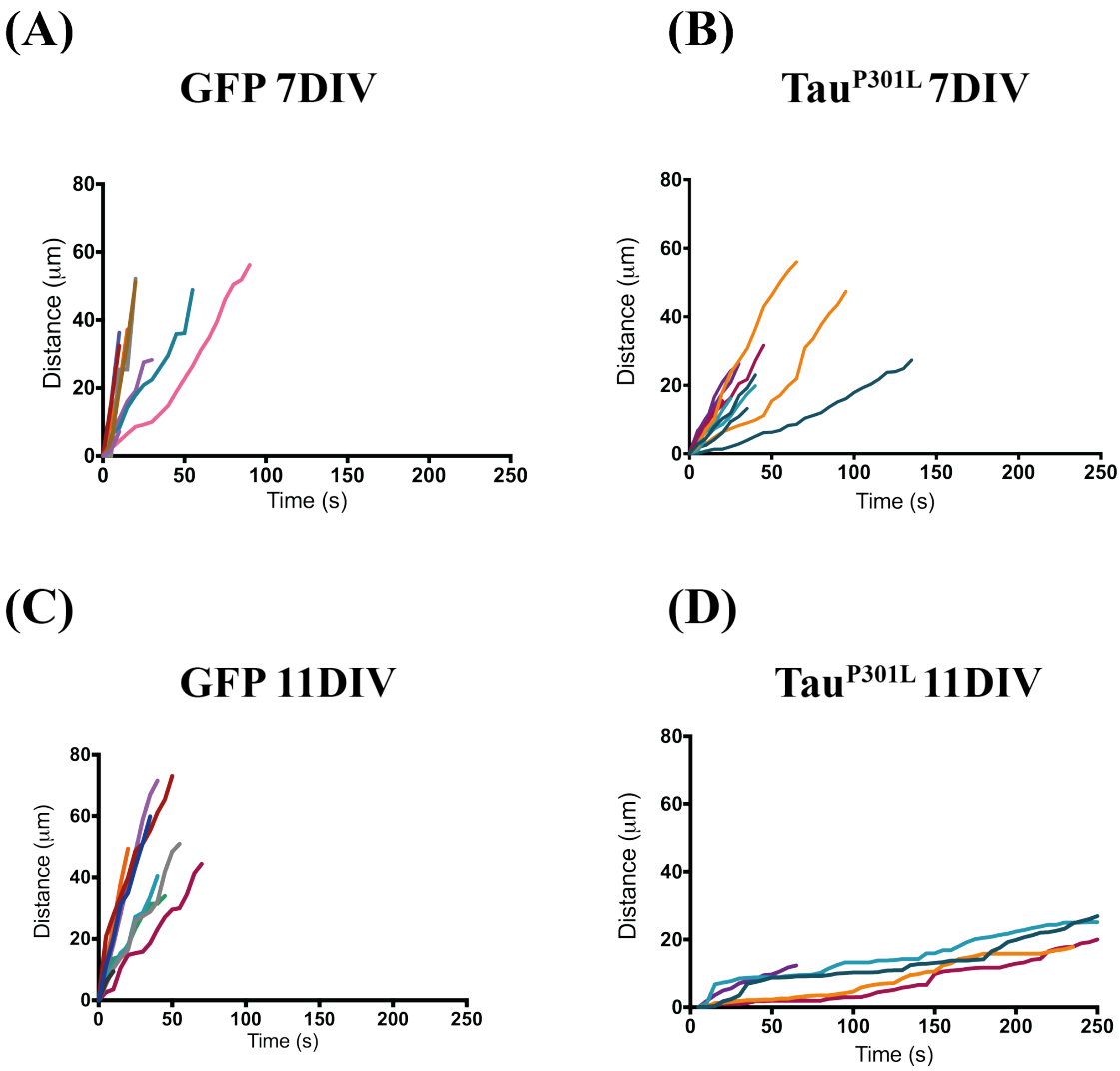

Figure 3-12 Cumulative profiles of BDNF vesicle movement in GFP and Tau^{P301L}-expressing cells.

Representative cumulative profiles of BDNF vesicle movement in (A, C) GFP and (B, D) Tau^{P301L}-expressing cells. These profiles illustrate pause time, where BDNF vesicles take a substantial amount of time to move through the distal axonal stretch. (D) This can be seen in Tau^{P301L}-expressing axon only at *DIV11*,which is distinctly different to the profile seen in (C) GFP-expressing cells at *DIV11*. (B) However, BDNF vesicle movement at *DIV7*, is similar to that seen in (A) GFP-expressing cells at the same time-point. These graphs were generated from the data collected from the BDNF displacement experiments, where data was collected from n=3+ independent culture preparations.

3.4Determining Tau aggregation stage in Tau^{P301L}-expressing neurons

3.4.1 Tau^{P301L} expression in hippocampal neurons leads to intracellular aggregate formation

In order to determine if Tau^{P301L} expression causes tau aggregate formation along axonal processes, similar to what is being observed in mouse models of FTLD-17, I expressed Tau^{P310L} in neurons at *DIV5* and then examined the distribution of tau along distal axons at *DIV6-7* and *DIV11-12*. As control, I expressed GFP in neurons for the same duration. hTau^{WT} was also used as control and these cells were transfected at *DIV1* and imaged by Dr Grace Hallinan. I hypothesised, that both hTau^{WT} and GFP-only would not aggregate within the distal axons of these expressing cells, whereas, Tau^{P301L} would cause tau aggregates within the axonal stretches, mirroring the results of tau aggregation seen in Tg4510 mice and other tauopathy models. I observed that the expression of Tau^{P301L} in hippocampal neurons led to the accumulation of fluorescent tau deposits along the distal axonal stretches (Figure 3-14). These tau deposits appear as intense fluorescent regions distributed at irregular intervals along the axonal stretch. This is assumed to be tau aggregates as it is previously reported that tau sticks together forming aggregated deposits. Moreover, using ImageJ, plot profile of these axonal stretches was generated, and the high intense fluorescent areas corresponded to increased pixel values. Therefore, it is assumed that these regions are tau aggregates, whereby Tau^{P301L} has stuck together forming these high intense fluorescent areas.

To confirm that these are in fact tau aggregates, Tau^{P301L}-expressing axonal stretches were compared to control cells expressing GFP and hTau^{WT}. hTau^{WT} and GFP-only constructs were expressed in hippocampal cells from. The fluorescent distribution in hTau^{WT} and GFP-only expressing cells is distinctly different from that seen in Tau^{P301L}. In both cases, an even, smooth fluorescent distribution was seen, as confirmed by the plot profile (Figure 3-13).

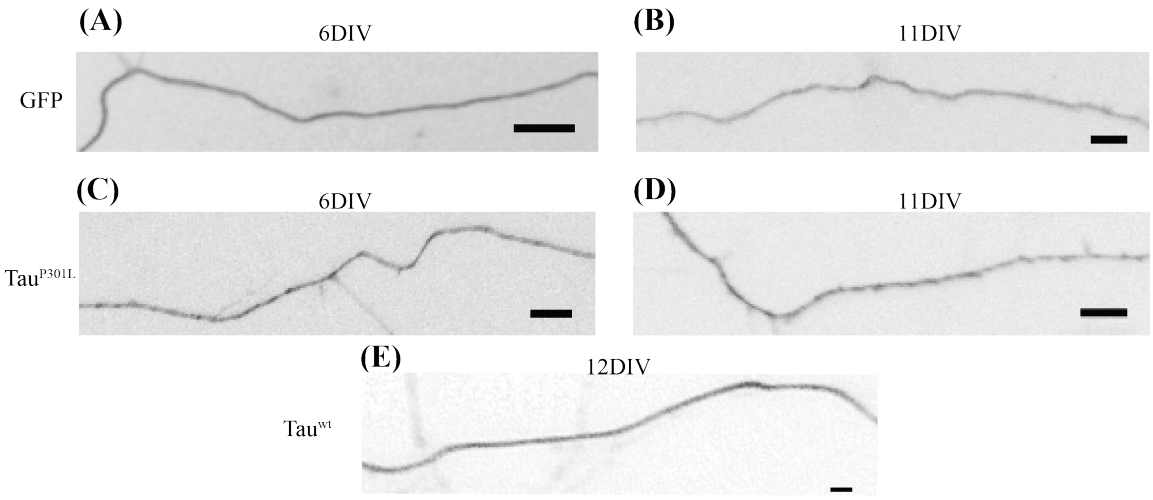

Figure 3-13 Representative distal axonal regions captured from GFP, hTau^{WT} and Tau^{P301L}-expressing cells.

Smooth fluorescence distribution is seen in GFP-expressing cells at (A) *DIV6* and (B) *DIV11* and in hTau^{WT} cells at (E) *DIV12*. Uneven fluorescence distribution in Tau^{P301L}-expressing cells at (C) *DIV6* and (D) *DIV11*. hTau^{WT}-expressing cells were cultured and images were taken by Dr Grace Hallinan. Scale bar: 10 μm.

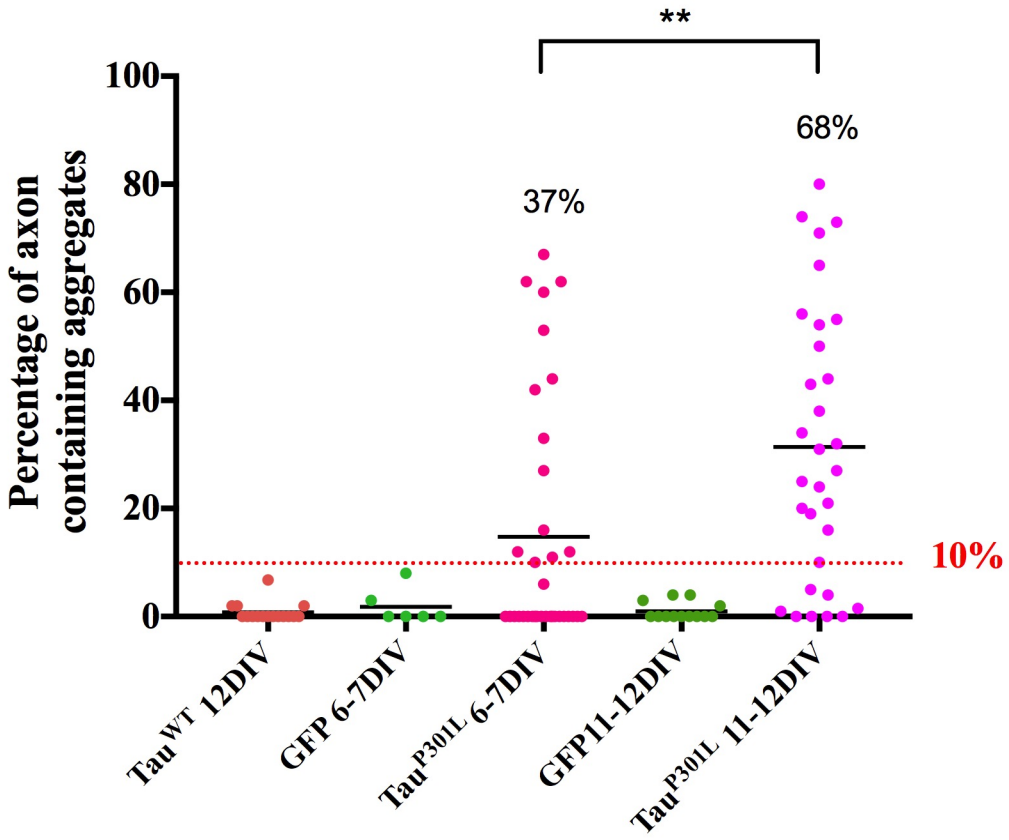

Figure 3-14 Tau^{P301L} expression induces aggregate formation in a progressive manner. Fluorescence values of Tau^{P301L}, hTau^{WT} and GFP expressing distal axons were analysed using the MATLAB script (see Appendix B) to calculate the percentage of axons containing aggregate for each condition. Analysis on hTau^{WT} cells was carried out by Dr Grace Hallinan and used here as a comparison against a non-aggregating phenotype. Any cell that has less than 10% of its axon containing aggregate points is considered aggregate-negative, this is highlighted by the dotted line. The percentage value over both Tau^{P301L}-expressing cells is the proportion of axons that is over the 10% threshold. Black line = mean; each point represents an individual axon, taken from 3 independent experiments. hTau^{WT} *DIV12*, n=6+ cells in each culture preparation. GFP *DIV6-7*, n=2+ cells in each culture preparation. Tau^{P301L} *DIV6-7*, n=8+ cells in each culture preparation. GFP *DIV11-12*, n=4+ cells in each culture preparation. Tau^{P301L} *DIV11-12*, n=7+ cells in each culture preparation. One-way ANOVA, $p<0.0001$; **$p<0.01$.

3.5 Discussion

In order to investigate whether BDNF can signal correctly in cells undergoing neurodegeneration, I transfected primary mouse hippocampal cells with Tau^{P301L}. Before looking into answering the question above, I investigated the consequence of transfecting the mutant Tau^{P301L} in primary mouse neurons. Through live image analysis, I have observed disrupted axonal transport where axonal integrity is compromised. I have also observed the impact of Tau^{P301L} mutation on microtubule dynamics. Having understood the knowing the pathological state my primary cultures at two time points (*DIV6-7* and *DIV11-12*), I can now move forward with investigating TrkB expression and BDNF signalling in my mouse model.

The current study used a GFP only construct as a 'healthy' comparison against the observations seen by EGFP-Tau^{P301L}-expressing cells. It could be argued that expressing $hTau^{WT}$ would be a better model for comparison against a mutant model. However, the Tau^{WT} model was not chosen in this case as it is shown to disrupt the normal function of axonal transport and in transgenic mouse models, it has shown to cause tau hyperphosphorylation. For instance, a transgenic mouse model expressing $hTau^{WT}$ (at a two-fold rate) progressively increased hyperphosphorylated tau pathology[182]. Moreover, the expression of $hTau^{WT}$ in primary culture has shown to disrupt the normal function of motor proteins, with particular susceptibility of kinesin transport proteins[182,183]. It should be noted that the expression of $hTau^{WT}$ in culture has not shown signs of pathology[147]. As this differs to what is seen in $hTau^{WT}$ transgenic models, the rate of over-expression is an important consideration for observing pathology. If $hTau^{WT}$ was used in this study, the rate of over-expression would be difficult to measure. However, using $hTau^{WT}$ would help to determine what level of impact of Tau^{P301L} has on transport and microtubule dynamics. For instance, the rate of transport observed in Tau^{WT} expressing cells can be compared against the rate observed in Tau^{P301L} expressing cells to understand what impact the addition of the missense mutation has on transport and other functions such as microtubule dynamics. Thus, an additional condition would have been advantageous in this respect. Nonetheless, fluorescent probes are commonly used for research purposes and are a widely accepted tool to visualise

specific proteins of interest. As the EGFP-Tau^{P301L} construct utilises a similar nm wavelength to the GFP used as the control, a comparison between the two expressing cells was deemed acceptable.

Throughout this research, the Tau^{P301L} model was used to disrupt axonal transport as a means to test whether BDNF signalling would continue to work in the same manner as seen in healthy neuronal mouse cells (Figure 1-15). The Tau^{P301L} mutation was the chosen mutation as it is widely used by labs at the University of Southampton. Moreover, this is a well-established mutation which is used by other researchers as it is robust in mimicking neurodegeneration[152–154,156,179,180,197]. Expressing Tau^{P301L} in mouse primary culture causes an imbalance in the total amount of tau being produced by rodent primary cells; this is a model of tau over-expression[147]. This mutation has previously shown to mislocalise tau, in the somato-dendritic compartments of primary mouse neurons[147]. In this project, the Tau^{P301L} missense mutation has shown to disrupt BDNF transport progressively by *DIV11-12* and also disrupt the normal function of microtubules.

Other studies which have used the Tau^{P301L} mutation have also shown disrupted axonal transport[198,199]. For instance, using a knock-in of Tau^{P301L} transgenic mice, a 50% reduction in mitochondrial transport was observed, compared to wild-type neurons[198]. What should be noted here, is that this particular study used murine P301L tau, not human (which is used in this study). However, in a rTg4510 transgenic mouse line, where the human Tau^{P301L} mutation is over-expressed (approximately 13 times the level of endogenous murine tau), axonal transport is also disrupted[199]. Regardless of which method is used to express the missense P301L mutation, the above two studies, and this project utilise an overexpression system. The primary culture system used in this study does not truly mimic the CNS physiological environment as it also lacks glial cells. Therefore, the results observed in this study represent how cellular mechanisms alter in the face of over-expression of tau. Nonetheless, the results shown in this project will help in understanding how cellular mechanisms and BDNF signalling changes due to Tau^{P301L} over-expression (rather than showing how cellular mechanism alter in human tauopathy diseases). It should be noted that an increase in the number of cells analysed is required to fully understand the extent of disruption.

The main observations made during this project, are as follows:

- Increased fluorescent variation in Tau^{P301L} expressing cells
- Axonal transport changes observed via BDNF transport (in stationary vesicles and speed of movement, but not in total number of vesicles)
- Microtubule polymerisation changes

Florescent analysis on cells transfected with Tau^{P301L} was carried out to see if there was variation in the amount of fluorescent distribution. In this instance, comparison was carried out against $hTau^{WT}$ cells, as a previous study which used the same construct has shown that the over expression of Tau^{WT} does not lead to sporadic hyperphosphorylation[147]. Using a MATLAB script to assess the fluorescent distribution of Tau^{P301L} versus $hTau^{WT}$, the percentage of cells containing aggregate deposits were identified. From this initial analysis, an increase in the percentage of aggregate containing Tau^{P301L} expressing cell have been identified from *DIV6-7* and increasing to *DIV11-12*. Other studies have also shown similar using Tau^{P301L} mutations have shown aggregate accumulation[200]. Undoubtedly additional analysis is required to visualise the aggregate formation and confirm the location of these aggregates[147,200,201]. It would be interesting to see if tau accumulation occurs more predominantly in somato-dendritic compartments, as shown by other studies. Moreover, if tau is predominantly mislocalised to somato-dendritic compartments, then it would be interesting to compare the effects of distal and proximal axonal transport , and BDNF IEG gene induction at the cell soma.

Having observed changes in BDNF transport, it could be argued that this change occurs due to increased susceptibility of altered kinesin transport in the face of tau imbalance. In this study, kinesin driven transport (anterograde) is altered more so than dynein driven transport (which is also alerted) early on in cells expressing Tau^{P301L} (from *DIV6-7*). Both tau imbalance and loss of kinesin driven transport have been reported in other studies[183,188,194,200,202]. Interestingly, a study infusing low physiological concentrations of monomeric and filamentous tau in isolated squid axons have shown monomeric tau had no

effect on disrupting fast axonal transport[203]. However, filamentous tau at the same concentration selectively inhibited anterograde transport[203]. It would be interesting to determine what type of tau species are expressed in this projects' Tau^{P301L}-expressing cells. It would also advantageous to examine axonal transport early on in Tau^{P301L}-expression to locate the spatial-temporal location of when kinesin driven transport starts to become susceptible to toxic tau species. This would help to determine the when switch from monomeric filamentous/oligomeric tau species within the cell occurs. In this case, BDNF signalling experiments should be carried at two time-points, the first is while Tau^{P310L}-expressing cells harbour monomeric tau species and the second is tau species become toxic, such as the timepoint chosen within this project at *DIV11-12*.

During this project, microtubule dynamics have been examined using a +TIP protein construct, EB3, which visualises microtubule polymerisation. Within Tau^{P310L}-expressing cells at *DIV11-12*, mature microtubule lattice production is altered, in that shorter lattices are produced. Within the axon, microtubules are organised in a uniform manner, as parallel arrays, varying in size[204]. The role of tau in stabilising microtubule growth is well established. However, tau diffusion ensures microtubules are evenly distributed along neuronal processes, via a cross-linking process[205]. In this respect, tau hyperphosphorylation would disrupt the diffusion of tau, and in turn this could have a consequence on microtubule organisation in Tau^{P301L}-expressing cells. Tau is also shown to directly interact with EB3, where it is required for the proper accumulation of EB proteins at medial and distal axonal regions[206]. Thus, the changes in tau in disease expressing cells will also affect microtubule, which in turn, would have an effect on cargo transport (a process dependent on microtubules).

It should be noted that from the current results, there was no significant different in the number of vesicles observed along the distal axonal stretch of Tau^{P301L}-expressing cells at *DIV6-7* and *DIV11-12* compared to healthy GFP-expressing cells. However, the number of stationary vesicles was significantly higher in Tau^{P301L}-expressing distal axons from *DIV6-7*. Furthermore, an increase in slower moving vesicles in Tau^{P301L}-expressing distal axons was also observed. Taken together, this could suggest that although there is an increase in the number of stationary vesicles, there is still some sort of transport of the endosomes at play,

albeit at a very slow rate. There needs to be an increase in the number of cells analysed in order to fully understand the impact of Tua^{P301L} mutation on transport. Never the less, what is currently known from these results is that there is a degree of change in the transport mechanism compared to healthy GFP expressing cells.

4 Assessing TrkB Receptor Regulation in Tauopathy

4.1 Introduction

Activation of downstream BDNF signals is dependent on two classes of receptors that are expressed on the cell: the p75 neurotrophin receptor, and the TrkB receptor (as mentioned in section1.1). Here, I am focusing on the latter as BDNF-binding to TrkB ultimately leads to induction in genes responsible for synaptic strengthening (as discussed in section 1.5). The TrkB receptor is expressed along the surface of dendritic and axonal processes. The regulation of this receptor is tightly controlled by various proteins. Similar to BDNF, TrkB synthesis and expression into the plasma membrane is dependent on neuronal activity. Increased concentrations of cAMP in hippocampal neurons is seen to enhance TrkB phosphorylation and its translocation to spines[207]. Studies have shown neuronal activity to increase the number of TrkB receptors on the cell surface, thus enhancing the responsiveness of neurons to BDNF[208]. Electrical stimulation can also modulate TrkB levels within the cell, whereby it can facilitate the movement of TrkB from intracellular pools to the cell surface. In this regard, calcium influx via NMDA receptors and activation of CamKII have been shown to be important in TrkB receptor insertion[209].

Similar to BDNF, TrkB can also undergo bidirectional transport[53]. Within the biosynthetic pathway, TrkB is synthesised, processed and package to be delivered for release (as discussed in section 1.6). In order for TrkB receptors to be inserted into the plasma membrane, they must be delivered to axonal ends and thus undergo anterograde transport from the somatodendritic compartment to the distal axonal regions[66]. The mechanism by which TrkB is tethered to Kinesin-1, and anterograde motor protein, is dependent on a protein complex (Sytl-1/Rab27/CRMP-2 complex), where the cytoplasmic tail of TrkB binds to Sytl-1, a synaptotagmin-like protein 1[210]. This however, only accounts for up to 50% of TrkB trafficking along axonal processes. Huang and colleagues (2011) have identified JIP3, a c-jun kinase protein that is exclusively expressed in brain to be involved in anterograde transport of TrkB receptors, where JIP3 directly mediates TrkB interaction

with Kinesin-1[211]. Once TrkB is connected to Kinesin-1 it undergoes anterograde transported to its destination. Here an internal pool of receptors within vesicles are ready to be inserted into the plasma membrane upon neuronal activity[211].

It was important to determine whether the levels of TrkB receptor are implicated in distal axons of Tau^{P301L}-expressing cells. In addition to this, it was also critical to assess how the tau mutant cells respond to changes in their environment. For instance, if there is a decrease in the amount of BDNF being released by degenerating cells, as previously reported,[212,213] then are the tau mutant cells able to increase the amount of TrkB receptors on the surface of the cell to compensate for this loss? Conversely, if the concentration of BDNF, or similar peptides created to mimic trophic effects is increased, can the tau mutant cells decrease the amount of TrkB receptor and prevent over stimulation? Thus, it was important to also understand whether Tau^{P301L}-expressing cells can undergo homeostatic scaling, if required to regulate the dynamic expression of TrkB.

4.2 Tau^{P301L}-expressing cells regulate homeostasis of TrkB receptor

4.2.1 Internal pool of TrkB receptors is reduced in tau mutant cells

Having already identified a disrupted transport mechanism in Tau^{P301L}-expressing cells, it was crucial to establish whether this had an impact on the total TrkB levels within the distal axons. I hypothesised that the total amount of TrkB receptors would be decreased in Tau^{P301L}-expressing cells at distal regions, as TrkB receptor transport to axonal ends is depend on efficient transport, which in this case is severely disrupted.

Newly synthesised TrkB receptors are transported to distal regions of axonal processes via Kinesin-1, where an internal pool of receptors accumulates and in an activity-dependent manner, TrkB is inserted to the plasma membrane[210,211]. In order to look at the total number of receptors in the distal axon, I transfected hippocampal cells at *DIV5* with Tau^{P301L} or GFP-only DNA. At *DIV11-12*, I fixed cells and permeabilised the cell membrane in order to stain the total pool of TrkB receptors. I generated a z-stack of the distal axonal process to capture all the TrkB receptors staining within the area, and deconvolved and projected the maximum intensity of each stack onto one plane. Using ImageJ, I measure the average fluorescent intensity of the distal axonal stretch by creating a mask of the Tau^{P301L}- or GFP-only expressing axonal process and overlaid this on top of the TrkB stain to capture the staining within the transfected axonal process only (Figure 2-3). From this, I was able to measure the mean fluorescent intensity of TrkB staining that equates to the proportion of TrkB receptors within the axonal process.

As the antibody I used identifies all TrkB receptors on transfected and untransfected cells, I first checked the specificity of the antibody on PC12 cells which stably express TrkB. These cells were first transfected with GFP as these PC12 cells have previously shown to have over 80% transfection rate. The cells were then incubated with TrkB antibody and imaged. Figure 4-1shows PC12 GFP expressing cells stained for TrkB. The merge image

shows the specific of the antibody, where there is no unspecific binding seen. The DAPI inverted image highlights in high contrast, the debris around the cells, and therefore any dotting seen in the GFP and TrkB channel (as well as in the merge image), is attributed debris within the cell culture, and no to 'dirty' primary or secondary antibodies. Moreover, if any unspecific binding (due to culture debris) is analysed, then this is done so throughout all images, in both GFP and Tau^{P301L} conditions, therefore does not skew the results as from a single culture preparation, cells are divided for GFP and Tau^{P301L} transfection.

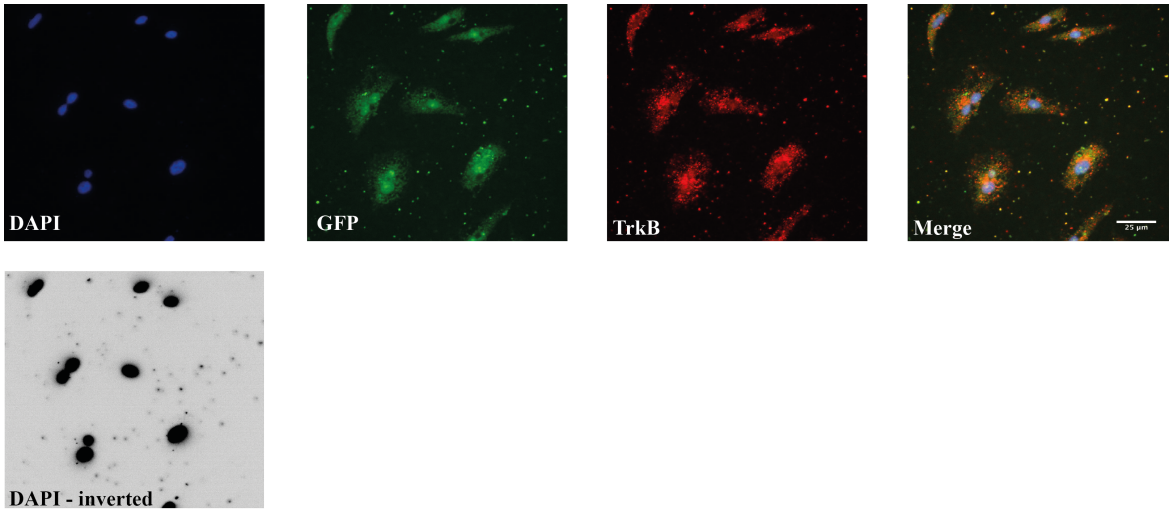

Figure 4-1 TrkB antibody specificity test

Images showcase TrkB antibody specificity on GFP-expressing PC12 cells. These PC12 cells stably express TrkB. The DAPI image highlights PC12 cell nuclei, GFP-expressing cells, TrkB antibody staining, and a merge of all three images. The DAPI inverted image highlights cell culture debris which is not seen in the blue DAPI image (as the inverted image has a high contrast ratio) Scale bar: 25 µm.

The culture method used to assess TrkB receptors was carried out in mass culture, where hippocampal cells were grown in plated on glass coverslips, with supplemented NBM. The hippocampal cells were transfected with GFP or Tau^{P301L}. As predicted, the total amount of TrkB receptors in distal axons relative to GFP control cells was significantly decreased (Figure 4-2 and Figure 4-3). This is in-line with earlier observations of altered anterograde transport. This suggests that the number of vesicles being transported to the distal axons of Tau^{P301L}-expressing cells is substantially reduced due to the effects of the tau mutation on axonal integrity. From this, it can be hypothesised, that similar to TrkB receptors, the internal pool of BDNF vesicles within the distal axons may also reduce in Tau^{P301L}-expressing cells. This could contribute towards potential signalling defects.

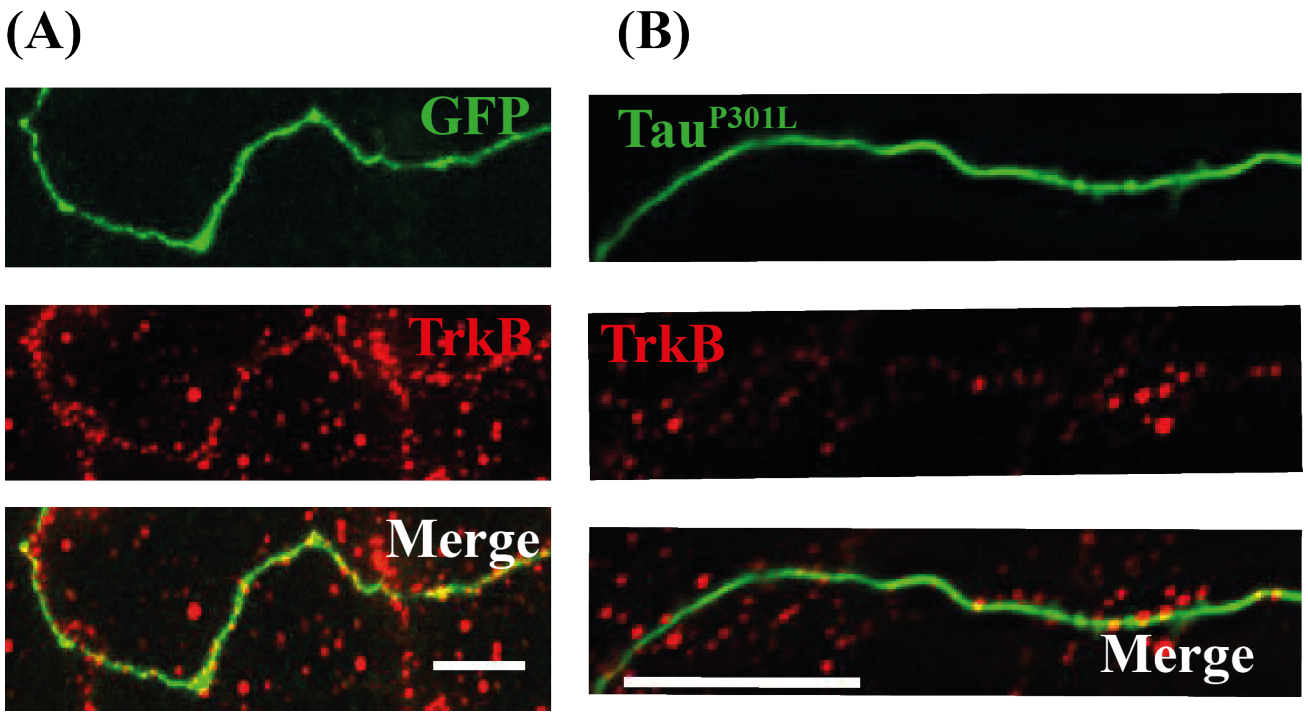

Figure 4-2 Tau^{P301L} expression results in a decreased level of total TrkB receptors at the distal axonal regions.
Representative images of distal axonal regions taken from (A) GFP- or (B) Tau^{P301L}-expressing cells. The transfected distal axon and its corresponding total TrkB stain. Merged image shows the proportion of total TrkB receptors within the distal axons. High proportion of staining can be observed in GFP-expressing cells. The TrkB antibody stains all the available TrkB receptors, on transfected and non-transfected cells. The staining around the transfected cell highlights TrkB receptors from non-transfected cells. Scale bar: 10 μm.

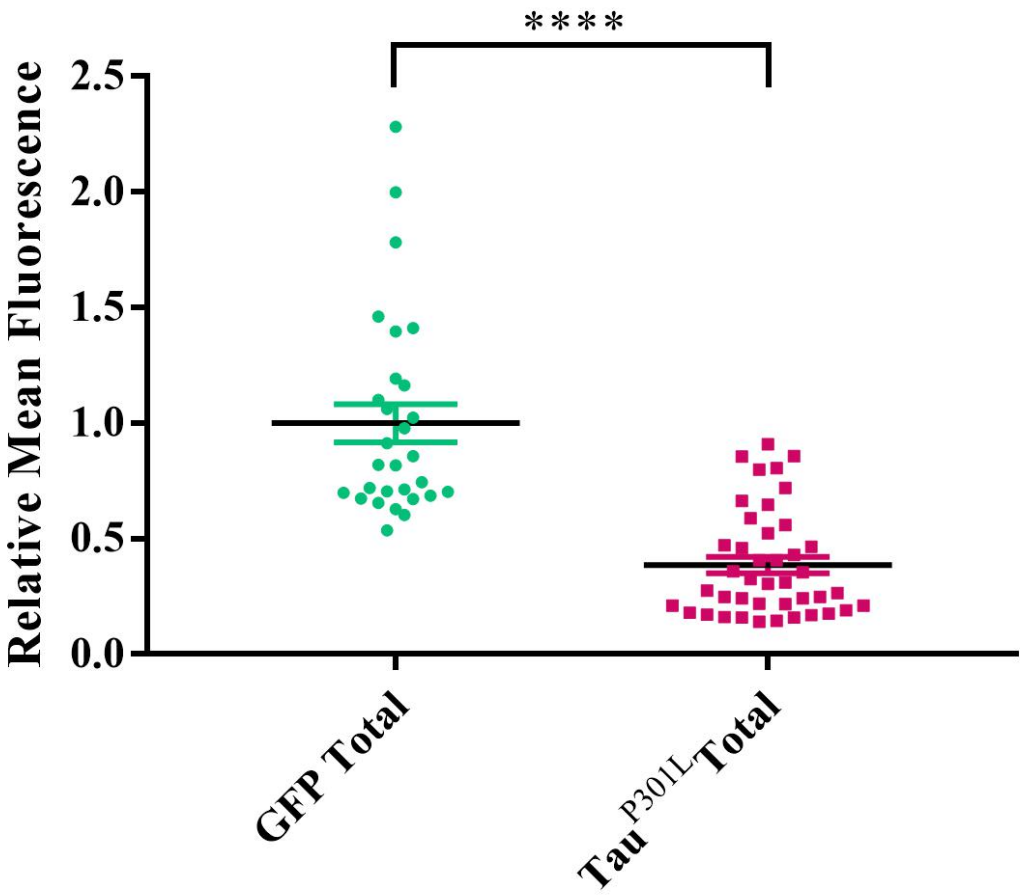

Figure 4-3 Tau^{P301L} expression significantly reduces the internal pool of TrkB receptor in distal axons.

Quantification of mean fluorescent staining of total TrkB receptors in distal axons from Tau^{P301L} and GFP expressing cells. Significant decrease in total TrkB receptors expression in distal axons of Tau^{P301L}-expressing cells is seen when compared to GFP-expressing cells. T-test, $p<0.0001$ from 7> distal axons taken from 4 independent experiments. Error bars = SEM

4.2.2 Surface expression of TrkB receptors is not affected by the Tau^{P301L} mutation

From the observation of decreased total internal pool of TrkB receptors in distal axons of mutant tau cells, I predicted that the number of receptors expressed on the plasma membrane would also, as a result, be reduced. A reason to assess the surface expression of TrkB is because the number of receptors expressed has a consequence on BDNF signalling (as described in 1.5). For instance, if there is a reduction in TrkB expression on the cell surface, this would mean there is less TrkB receptors for BDNF to bind to, and therefore there will be reduced BDNF-TrkB complexes, impacting signal activation.

To measure the number of receptors expressed on the plasma membrane, hippocampal cells were transfected at *DIV5* with Tau^{P301L} or GFP-only DNA and at *DIV11-12*, cells were fixed and stained for TrkB receptors. Using the same antibody as before which detects the extracellular portion of TrkB receptors, the cells were incubated without permeablisation, to keep the cell membrane intact. Images were taken of transfected distal axons, and processed using the same method as described in section 4.2.1.

To my surprise, the number of TrkB receptors relative to control in Tau^{P301L}-expressing distal axons is unchanged (Figure 4-5) This observation can be seen between independent experimental conditions, strengthening the observation of unaltered TrkB receptor expression on the cell in Tau^{P301L}-expressing cells. This suggests that although the total number of receptors (the internal pool + on surface) is significantly decreased, the tau mutant cells are able to detect this alteration, and possibly as a consequently express the same number of receptors to the plasma membrane as GFP control cells (Figure 4-4). In terms of BDNF signalling, this means that if any changes occur in signal propagation, it is not due to receptor availability. Moreover, this means that although pathological changes are taking place in cells expressing mutant tau, it has not yet affected the regulation of receptor expression and the Tau^{P301L}-expressing cells are still able to retain their sensitivity to such changes. It needs to be noted that the pathways responsible for receptor recycling and degradation need to be considered in light of this observation, where perhaps recycling

could be upregulated and degradation could be decreased. This could be a realistic possibility as the autophagy-lysosomal pathway has been implicated in multiple neurodegenerative diseases[214–216].

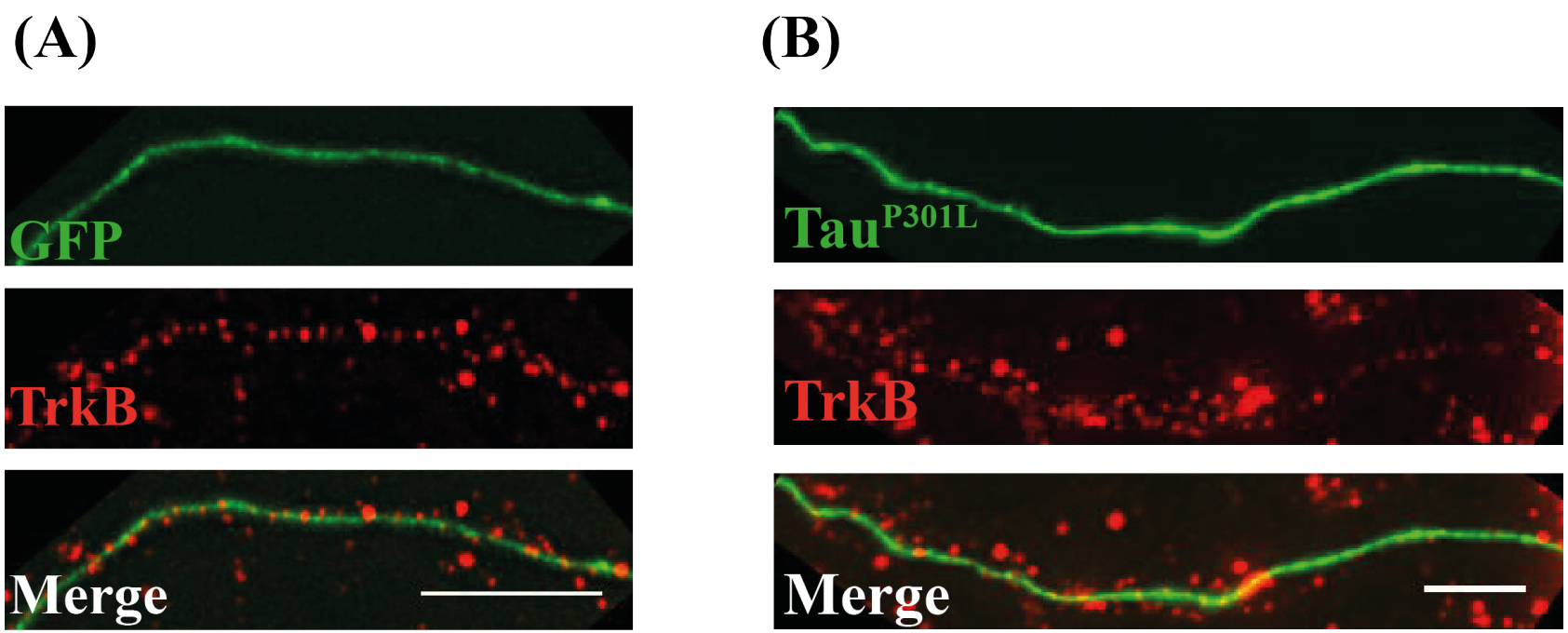

Figure 4-4 Homeostatic regulation of TrkB receptor expression on cell surface is still intact in Tau^{P301L}-expressing cells. Representative images of (A) GFP and (B) Tau^{P301L}-expressing distal axons showing the proportion of TrkB receptors expressed on cell surface is relatively similar. Merged images illustrate very little difference in the amount of TrkB staining between the two distal axonal regions. The TrkB antibody stains all the available TrkB receptors, on transfected and non-transfected cells. The staining around the transfected cell highlights TrkB receptors from non-transfected cells. Scale bar: 10 μm

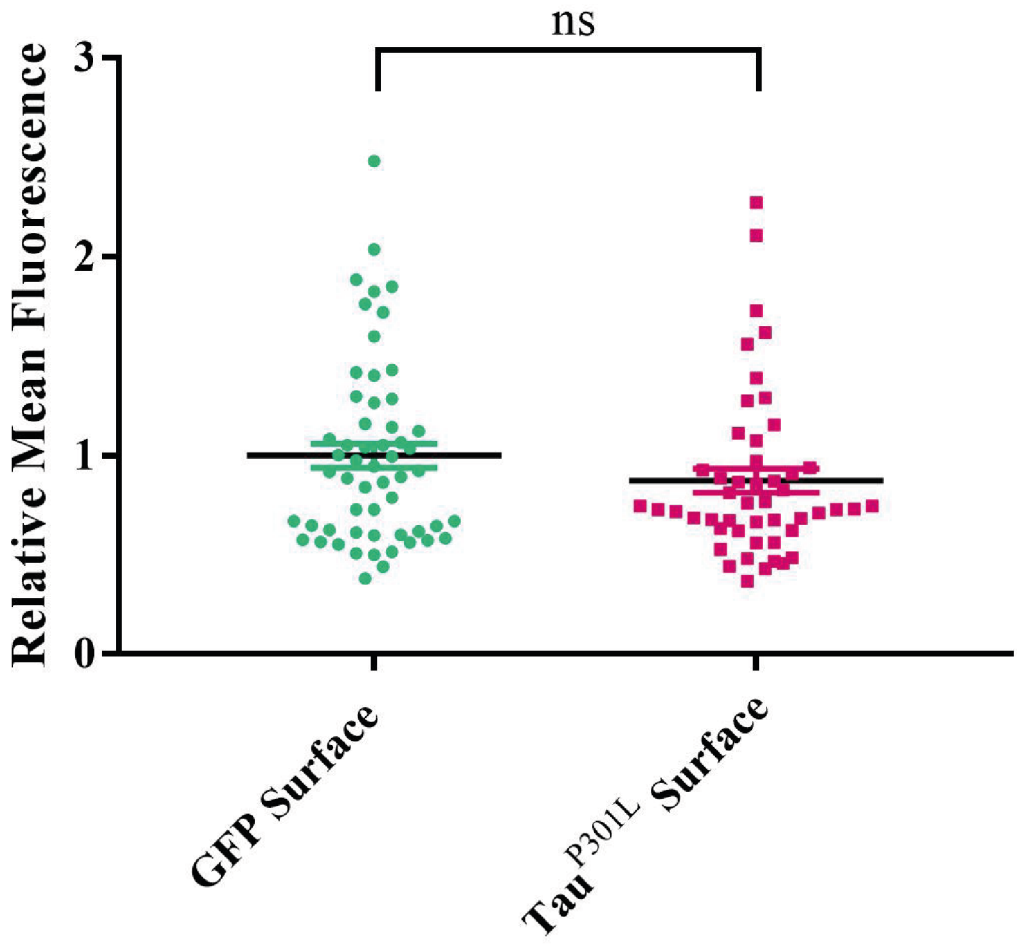

Figure 4-5 Expression of TrkB receptors on cell surface is intact in Tau^{P301L}-expressing cells.

Quantification of surface TrkB receptor expression in distal axons of GFP and Tau^{P301L}-expressing cells shows no significant difference between the conditions. This suggests that Tau^{P301L}-expressing cells can still regulate homeostatic scaling of TrkB receptors in cell surface. Note, in this experiment, the culture medium was only NBM, and did not contain BDNF. T-test, p=0.1573; n= 3 independent culture preparations, with >5 cells per culture; black line indicates mean within each condition.

4.3 TrkB receptor expression is not dynamic during environmental challenges

To test the extent of Tau^{P301L}-expressing cells sensitivity to environmental changes, a range of experiments were carried out. I first wanted to assess whether increased BDNF concentrations changed the amount of TrkB receptors being expressed on the plasma membrane. Under healthy physiological conditions, increased BDNF in the extracellular space would decrease the amount of TrkB receptors on the plasma membrane to avoid over stimulation. Therefore, I wanted to see whether Tau^{P301L}-expressing cells would retain homeostatic plasticity in the same manner.

Hippocampal cells were transfected with Tau^{P301L} or GFP-only at *DIV5*. At *DIV10*, the media of these cells was removed and replaced with media containing 50 ng/ml human BDNF (hBDNF) for 48 hours. After this time, the media was removed and cells were fixed at *DIV12*. Cells were then stained for TrkB receptors in the same manner as described in section 4.2.2. The number of TrkB receptors on the cell were assessed using the same method as detailed in section 4.2.1.

In comparison to GFP-expressing cells treated with BDNF, Tau^{P301L}-expressing cells are able to respond to a similar degree when also treated with hBDNF for 48 hours (receptor expression is non-significant between GFP + BDNF and Tau^{P301L} +BDNF) (Figure 4-7). In response to increased concentrations of BDNF in the surrounding environment of Tau^{P301L}-expressing cells, the cell is able to express the appropriate number of receptors as required, matching how GFP-expressing cells respond to increased BDNF in its environment.

As previously seen in section 4.2, the Tau^{P301L}-expressing cells are able to regulate TrkB receptor expression and insert the required number of receptors on cell surface despite the decreased internal pool. From this, I wanted to assess the Tau^{P301L}-expressing cells ability to increase TrkB receptor insertion. Having observed that Tau^{P301L}-expressing cells are able to insert TrkB receptors on the surface (Figure 4-5), I wanted to evaluate whether this

insertion mechanism is still intact and if the cells sensitivity to its environment can result in an increase in the number of receptors on the cell when the cellular environment has a decrease in hBDNF concentration, as seen in neurodegeneration[209,217].

To manipulate the extracellular environment and decrease concentrations of BDNF, hippocampal cells were transfected with GFP-only or Tau^{P301L} DNA at *DIV5* and at *DIV10*, the media was removed and replaced with media containing 100 ng/ml TrkBFc for 48 hours. After this point, the cells were fixed, stained for TrkB receptors and processed in the same manner as described in section 4.2.2. TrkBFc acts as a scavenger protein, whereby BDNF binds to this protein, but it does not activate the downstream signalling pathways. As a consequence, it depletes the endogenous BDNF levels in the media which would have otherwise bound to the TrkB receptors expressed on the surface. This results in increased TrkB receptor expression on the cell surface to account for this change.

From Figure 4-6, it is clear that the TrkB receptor levels on the surface of distal axons in GFP-expressing cells is higher in the TrkBFc treatment when compared to the hBDNF treatment. This result is in line with what should occur in healthy cells, as predicated. However, when these results are compared to the same treatments carried out in Tau^{P301L}-expressing cell, the same effect is not seen (Figure 4-7). Rather, in the Tau^{P301L}-expressing cells, there is no difference in the number of TrkB receptors being expressed between the two conditions (TrkBFc vs hBDNF). When comparing these results to what is seen in GFP-expressing cells, it is clear that Tau^{P301L}-expressing cells cannot carry out TrkB scaling to the same degree.

These results suggest that Tau^{P301L}-expressing cells are only able to respond to increased BDNF conditions, but not when BDNF is depleted in the environment. Moreover, it raises the question of whether there are mechanistic problems occurring in these cells. If there is an issue in the cells ability to insert receptors as efficiently as needed, then this could explain these results. Therefore, the ability of TrkB receptors insertion into the plasma membrane would need to be evaluated. This would then elucidate whether the cells are in fact sensitive to their environment but simply unable to execute the insertion or internalisation of TrkB receptors.

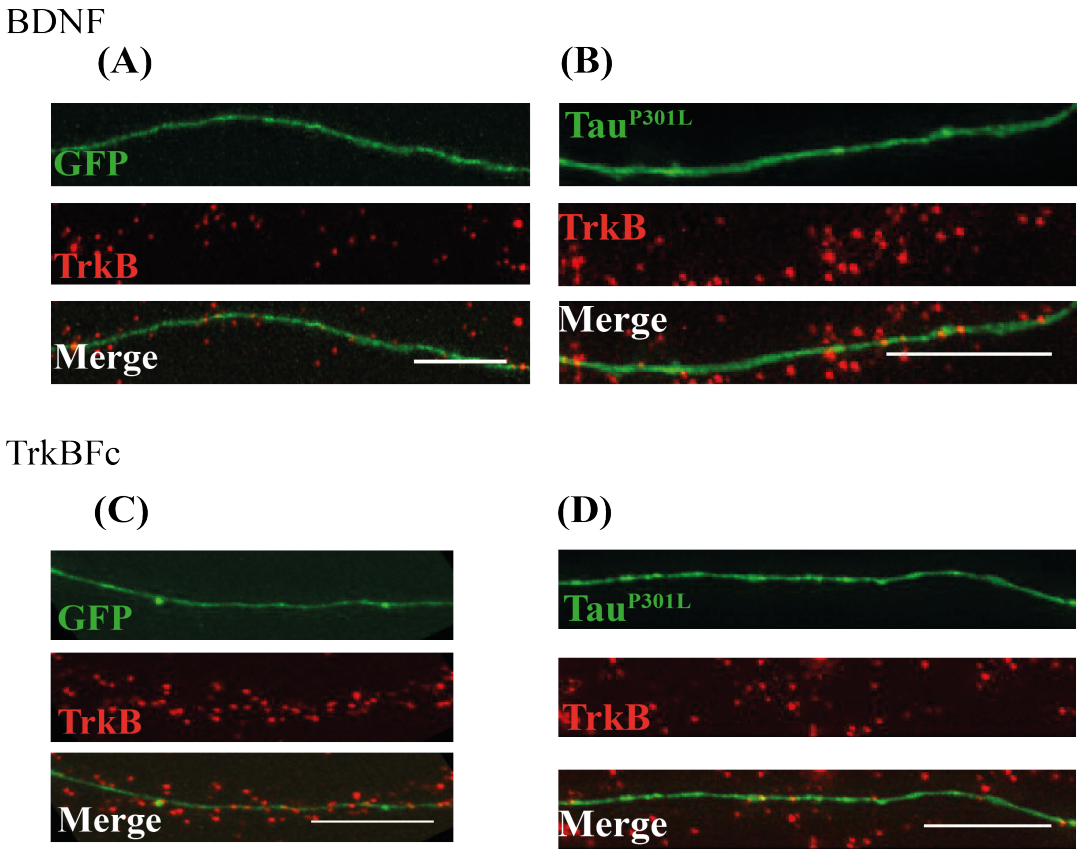

Figure 4-6 Tau^{P301L} expressing cells cannot regulate TrkB receptor expression on cell surface in light of increase or depleted BDNF concentrations. Representative images taken from (A) GFP and (B) Tau^{P301L} expressing distal axon from increased BDNF conditions show similar TrkB receptor staining between the two conditions. (C) GFP-expressing cells display increased TrkB receptor staining in depleted BDNF concentration conditions, however, (D) Tau^{P301L}-expressing cells do not respond to the same extent. . The TrkB antibody stains all the available TrkB receptors, on transfected and non-transfected cells. The staining around the transfected cell highlights TrkB receptors from non-transfected cells. Scale bar: 10 μm

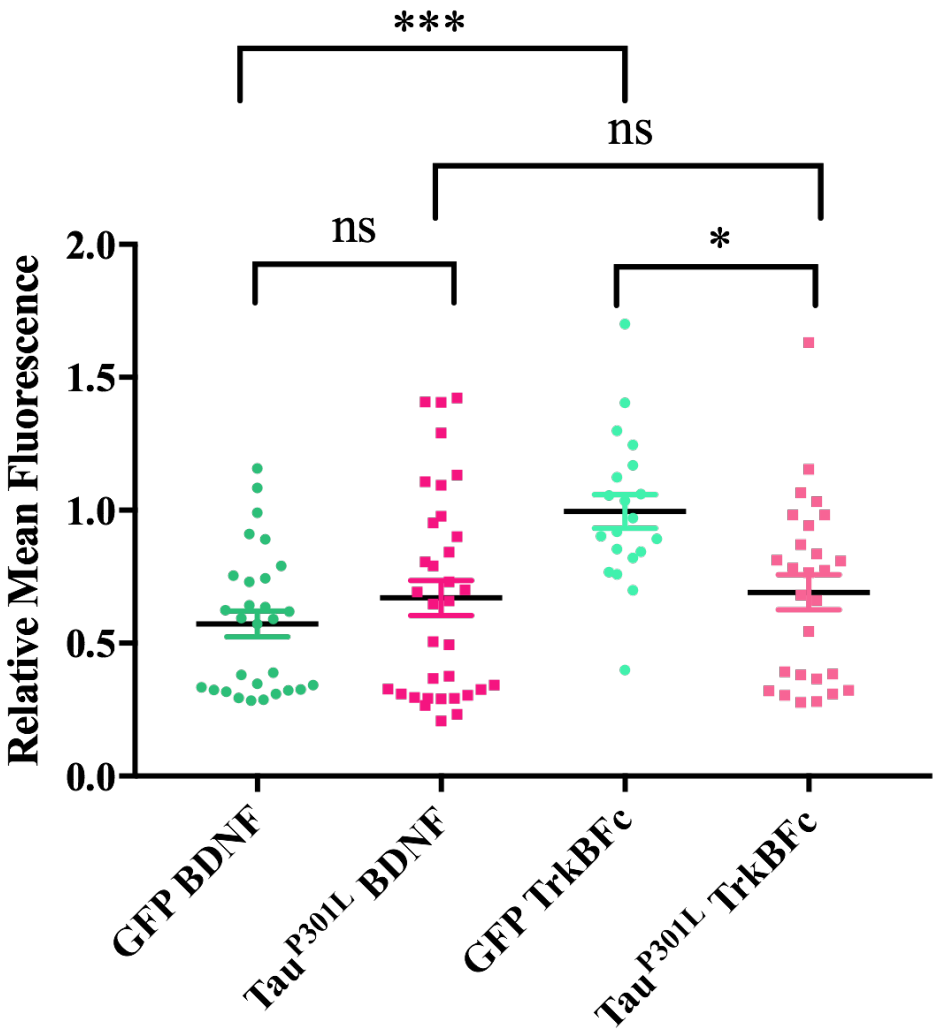

Figure 4-7 Tau^{P301L} expressing cells cannot regulate TrkB receptor expression when BDNF concentration is increased or depleted.

The mean fluorescent intensity of surface TrkB receptors in distal axons of GFP or Tau^{P301L}-expressing cells treated with BDNF or TrkBFc. GFP distal axons treated with TrkBFc for 48hrs shows significant increase in TrkB receptor expression on cell surface compared to GFP distal axons treated with BDNF. The same response is not seen between Tau^{P301L} distal axons. However, Tau^{P301L}-expressing distal axons respond to increased BDNF concentrations to the same degree as GFP-expressing distal axons. One-way ANOVA = $p<0.0001$. *$p<0.05$, ***$p<0.001$, ns = $p>0.05$ from >8 distal axons, taken from 4 independent experiments. Error bars = SEM.

4.4 Discussion

TrkB receptor expression is integral for BDNF-dependent signalling. With previous observation of disrupted axonal transport within Tau^{P301L}-expressing cells, it was crucial to determine if this impacted TrkB receptor levels within the cell as well as the surface expression level, as this could influence BDNF signal initiation. I characterised the expression of TrkB receptors on cell surface and the internal pool TrkB receptors distal axonal regions. From this assay, we can fully appreciate the cells capabilities in regulating its receptor expression in the face of pathological alterations. Despite a decrease in the number of TrkB receptors within the internal pool, the Tau^{P301L}-expressing cells can still express the same number of receptors as GFP control expressing cells in their distal axons.

Within the Tau^{P301L}-expressing neuronal network *in vitro*, I manipulated the cells' environment to understand the extent of the limitations in receptor expression. I created a challenging environment by either increasing BDNF concentrations, whereby the cell needs to respond and scale-back the TrkB receptors on the cells surface, or adding BDNF scavenger protein where the external concentration of BDNF is decreased and as a result the cells must increase TrkB receptor expression. The rationale behind these set of experiments is two-fold. The first is to understand how far we can push the Tau^{P301L}-expressing system. To what degree will TrkB receptor expression be the same as what is seen in control cells in these tau mutant cells. The second is to understand how the Tau^{P301L} cells respond to their environment. If BDNF signalling is a realistic therapy, then researcher will need to manipulate its signalling. Considering the limitations with the blood-brain barrier, modifiers could be synthesised to mimic trophic signals, in which case, TrkB receptor expression will need to be adjusted to account for such trophic peptides. Therefore, it is crucial to assess whether the Tau^{P301L}-expressing cells will respond to its environment, if manipulated by pharmacological agents.

Having challenged the cells environment with hBDNF or TrkFc, I have now concluded that there are limitations within the Tau^{P301L}-expressing system. Originally, when looking at TrkB receptor levels on the cell surface, where the environment is unchallenged, the Tau^{P301L}-expressing cells are able to regulate homeostatic expression and scale the TrkB receptors to the same level as that seen in control GFP-expressing cells. From this, I hypothesised that the cells are still able to regulate receptor expression despite the pathological alterations within the cell. However, from the experiments were the cells environment was manipulated exogenously, I have now concluded that there is a limit to the Tau^{P301L} cells ability to scale TrkB receptor expression. This factor is important when considering BDNF signal targeting for therapeutic purposes. It also needs to be noted, that earlier during disease progression, these limitations may not be an issue. Within the current system, transport deficits have impacted TrkB receptor levels at distal axons. Moreover, axonal integrity is also substantially altered. Considering the impact of pathology on cellular processes, it may be beneficial to investigate if Tau^{P301L}-expressing cells respond differently to environmental challenges early in disease progression.

With these results in mind, it would be important to understand how neuronal cells detect or sense the amount of the receptors which are expressed on its' surface. In order for cells to express a regulated number of receptors on its surface, a signal must be relayed between the cell surface and the internal pool and potentially back to the cell soma. Research on this is limited, however what we do know about TrkB receptor expression is that it is tightly controlled by BDNF and truncated TrkB receptors[105]. BDNF has a direct role in influencing the number of TrkB receptors on the surface, where BDNF bound to TrkB can signals to recruit additional TrkB receptors to the surface[105]. Results from this project show that despite there being low numbers of TrkB receptors in the intracellular pool in tau mutant cells, the expression of the surface is still the same level as control cells. How this type of detection is achieved is yet to be determined. It is important to note that previous studies have shown truncated TrkB receptors to influence full length TrkB expression[105]. Co-expression of truncated TrkB receptors is shown to decreased full length TrkB on the cell surface[105]. In this respect, it would be beneficial to investigate if truncated TrkB receptors are expressed on the surface of Tau^{P301L}-expressing cells. additionally, it would be interesting to carry out the same experiment in older cells to see at what point the expression of TrkB receptors on the surface becomes compromised.

Having measured the limit of homeostatic scaling of TrkB receptor in mutant tau cell using exogenous peptides, the results demonstrate these cells are unable to regulate TrkB receptor expression on cell surface during depletion of BDNF (TrkBFc treatment). However, when during overstimulation (hBDNF treatment) the Tau^{P301L}-expressing cells are surprisingly and remarkably able to detect this and scale down the TrkB receptors on the surface to the same degree as control cells.

To conclude the results observed in this assay in regard to BDNF signalling, TrkB receptor expression on the cell surface will not impede on the ligand-receptor interaction and internalisation, as the number of receptors expressed the plasma membrane are proportional to that seen in control GFP-expressing cells (Figure 4-5). The decrease in TrkB receptors in the internal pool (Figure 4-3) is in line with anterograde transport defected already observed in Tau^{P301L}-expressing cells (Figure 3-11). However, one could argue that the total number of vesicles (BDNF-RFP) measured along distal axonal regions in Tau^{P301L}-expressing cells is no different to the number of vesicles in GFP-expressing cells (Figure 3-9), suggesting endosomes are still being transported along to distal regions, albeit at a slow rate, with increase in the number of stationary vesicles (Figure 3-8). In light of this result, the decrease in the internal pool of TrkB receptors in Tau^{P301L}-expressing distal axons could be due to an increase in degradation rather than a decrease in shuttling the receptor to distal regions. In which case, TrkB receptors are favouring the degradation pathway. If this is the case, then additional experiments need to be carried out understand what role the degradation and recycling pathways are having on TrkB receptor expression. However, it should be noted that BDNF-RFP was overexpressed in Tau^{P301L} and GFP-expressing cells and therefore as the cells are producing BDNF-RFP at a higher rate, it is not unexpected to see the same amount of BDNF-RFP in both conditions at both timepoints. Therefore, it is important to increase the number of cells being analysed to truly understand the degree of change occurring within Tau^{P301L}-expressing cells.

5 Cell signalling

5.1 Introduction

Neurons are highly polarised cells, with axonal processes extending to more than 1 meter long in adult humans[218]. In order for these cells to survive and maintain their function, neurons have to respond to their surrounding environment in both space, in terms of subcompartmental location, and time. Neurotrophic factors have a large influence on neuronal cells both in the CNS and PNS (as described in 1.1and 1.2). For neurons to function in this way and maintain a healthy connected network, BDNF needs to propagate its signal (which could be from distal axonal ends) to the cell soma (as discussed in section 1.2). However, there are multiple layers of complexity involved in neurotrophic signal propagation. Below is a brief summary of basic actions, all of which occur simultaneously in multiple cellular subcompartments[1,61,82,219]:

(1) BDNF will only be synthesized and released in an activity-dependent manner[86].
(2) Once BDNF is released, it can bind to TrkB receptors. However, the availability of these receptors depends on the synthesis and insertion into the plasma membrane which is also activity dependent[66].
(3) Once the BDNF-TrkB complex is internalised, it will either (a) be classed as a signaling endosome and signal back to the cell soma, (b) be degraded or (c) the TrkB receptor would be recycled back to the surface[220].
(4) If the BDNF-TrkB complex signals back to the cell body, then the correct signals need to be active in order for the right output[1].
(5) Finally, all of these actions are highly dependent on the over health of the cell, and more importantly the integrity of axonal transport[61].

Therefore, considering pathological alterations in diseases such as Alzheimer's disease, the likelihood of one or more of these actions failing is inevitable. In fact, a compromised axonal

integrity has been identified in a number of occasions in multiple diseases and hence the premise of this project, as highlighted in Chapter 3[112,136,153,181,189,193,221].

The main research question for this project was to determine whether BDNF can signal over large distances and carry out its physiological functions in cells undergoing pathological changes. In order to investigate this question, a suitable disease-relevant platform where axonal integrity is compromised created (Chapter 3) and the availability of TrkB receptors on the surface of distal axonal ends has been examined (Chapter 4).

In order to determine the signal relay of BDNF from axonal ends to cell soma, the use of microfluidic devices was implemented. Hippocampal cells are seeded immediately after dissociation within the 'cell soma chamber'. After 5 days, the cells are transfected within these microfluidic devices with either a control DNA construct, GFP, or the experimental condition, GFP-Tau^{P301L}. From this set-up, two experiments were carried out to investigate whether BDNF signals are relayed back to the cell body upon the application of BDNF to distal axonal ends. For this, an immunocytochemistry technique was used to investigate Arc induction. The hippocampal cells by *DIV11-12* have their axonal processes projecting into the 'axonal chamber'. At this point, BDNF is applied within this axonal chamber, where it binds to TrkB receptors (only to those expressed on the surface of these projecting axonal ends). Once internalised, the signal is relayed along the axonal processes back to the cell soma, in which case Arc induction should be observed. As a positive control condition, BDNF is also applied to the cell soma chamber. In this condition, the signal reaches the cell soma without the need to travel over large distances. For the negative control, media only is applied to the axonal ends or to the cell soma in which case only basal activity should be observed.

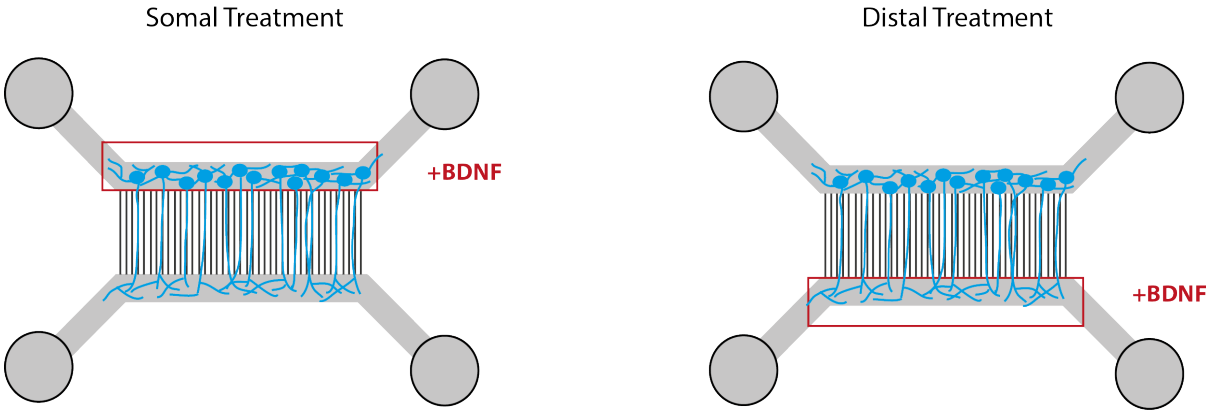

Figure 5-1 Simplified schematic of local and distal treatments within microfluidic devices. For somal treatments, with BDNF or vehicle control is applied to the somal compartment. Here, BDNF binds to TrkB receptors proximal to the cell body, negating the need for signal to travel over large distances. For distal treatments, BDNF or vehicle is applied to the distal compartment where only the projecting axons receive the treatment. Here, BDNF only binds to TrkB receptors on the projecting axonal ends, the signal then travels the entire length of the axon to the cell body to induce IEG induction.

5.2 Microfluidic Device Methods

5.2.1 Device Design

Customised microfluidic devices were designed using Draftsight-I Software based on existing designs[222,223]. The device was designed to contain 2 to 4 culture chambers of 2 cm wide, 500 µm length and 50 µm height. For the diode device, these culture chambers connect via tapered microchannels of 900 µm in length, 15 µm to 3 µm tapering width and 3 µm height (Figure 6.2). These designs were printed on a high-resolution mask (JD Photo-tools, UK). Photolithography is used to pattern the microfluidic design onto a silicone wafer (Microsystems Technology, Germany) containing a photoresist SU-8 layer. When the SU-8 is patterned onto the silicon wafer, it forms a permanent structure and this patterned wafer is used as a master mould to create the PDMS replica devices. Additional moulds of the devices can be made using polyurethane (PU) (section 5.2.3).

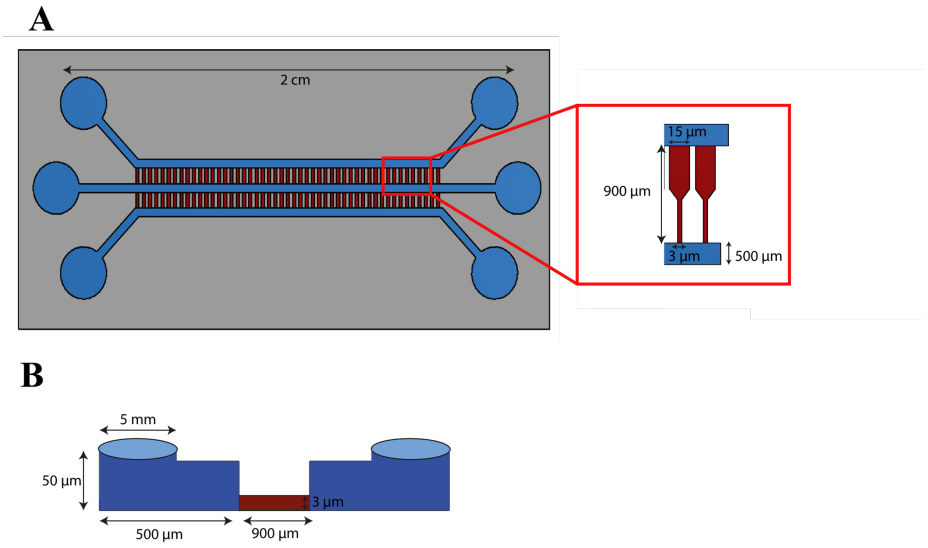

Figure 5-2 Dimensions of the custom diode microfluidic device used in this project. (A) Birds eye-view of the three-channel diode device. Culture chambers in which the hippocampal cells are grown in are 2 cm wide. The tapered diode microchannels are 900 µm

long and taper from 15 μm at the top to 3 μm at the bottom. The culture chamber is 500 μm long (see insert). (B) Side-view of the device illustrates the height of culture chambers (50 μm) and the height of the microchannels of 3 μm. The inlets and outlets are 5mm wide.

5.2.2 Device fabrication using soft lithography

The microfluidic devices are fabricated using Poly-(d)-methylsiloxane (PDMS, Dow Corning) with 9:1 pre-polymer (Silicone Elastomer) to polymer curing agent ratio. The mixtures were vigorously stirred and centrifuged at 600 rotations per minute (rpm) for 7 minutes. The PDMS mixture was poured initially on the master wafer and then into the PU device moulds (see section 5.2.3) and incubated at 60°C for 1 hour (Figure 5-3). The set PDMS devices were removed from wafer and 5 mm holes were punched at the inlet and outlet channel wells using a biopsy punch (Integra Miltex). The punched devices were soaked in 70% EtOH overnight.

5.2.3 Device positive relief pattern reproduction (PU moulds)

To reproduce devices at a faster pace, a PU mould was made from the devices casted from the wafer (section 5.2.2). Whole thick device (with no holes in the inlet and outlet) casted from the wafer was secured with double-sided tape in silicon rectangular mould, where the channels were facing upwards. The silicone moulds with the device were de-gassed for 10 minutes. Using a 1:1 ratio of solution A and solution B EZ-Mix 40 Liquid Rubber (Smooth-On, Inc) a total of 20 ml solution was made and poured into the silicone mould. The silicone mould with the PU solution was de-gassed further for 15 minutes. Once de-gassed, the mould was left to cure for 1 hour. The silicone mould was removed and the PU was cured further at 65°C overnight. The original PDMS device was removed, leaving a positive relief replica that can be reused to make further microfluidic devices with PDMS.

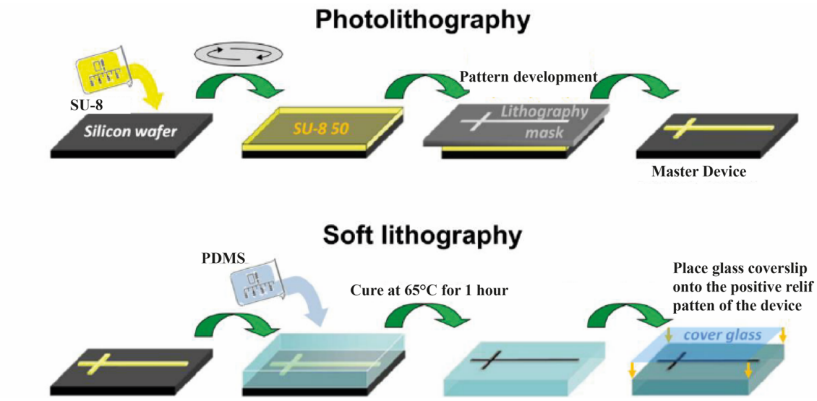

Figure 5-3 Photolithography (top) and soft lithography (bottom) process used for microfluidic device production.

Photolithography: SU-8 photoresist is a spin-coated and baked on a silicone wafer. UV light is exposed over the lithography mask (grey) containing the design of choice. The master device is developed on the mask. Soft lithography: Polydimethylsiloxane (PDMS) solution is poured over the mask and left to cure at 65°C for 1 hour. Cured PDMS is carefully removed from the wafer and 5 mm punches are used to create inlets and outlets (not shown in figure). These devices are stored in 70% ethanol. When ready for use, they are air-dried in laminar flow hoods and the devices are placed onto pre-washed and dried glass coverslips. Devices are ready to be primed and seeded with cells (Adapted from Ma et al., 2013).

5.2.4 Device preparation for cell culture

PDMS microfluidic devices stored in 70% ethanol were air-dried before use and placed on PDL-coated glass coverslips (see section 2.3.1) with the design facing down. To ensure solution flows through the cell chambers and microchannels, the devices were flushed with 20 µl of 100% EtOH followed by 40 µl of 0.1mg/ml PDL per channel incubated overnight at 37°C. After the overnight treatment, PDL was removed and washed twice with neurobasal medium (NBM) supplemented with 2% B27 and 0.5mM GlutaMAX (Gibco). NBM was added to all cell culture chambers and incubated overnight at 37°C. These devices were then ready for cell seeding.

Cells were obtained as described in section 2.3.2 and centrifuged at 1200 rpm for 4 minutes. The cell pellet was resuspended in a dilution with NBM to obtain 70,000 cells per 10 µl solution. The overnight media from the devices was removed and 10 µl of cells (70,000 cells) was added to the one cell culture chamber in each device. Once the cells adhered to the glass, NBM was added on top of the inlet ports. Medium was exchanged every 48 hours by removing a small volume of media from one side of the ports and adding fresh media to the ports on the other side of the device. This was carried out to removed debris and waste, and to encourage the exchange of nutrients.

The above protocol was set-up by Dr Bailey, who carried out many experiments to determine the best concentration for seeding and priming of the device. The throughput of data produce from these microfluidic devices is low due to a number of factors:

1. All devices must completely adhere to the PDL treated glass coverslips. Any air bubbles can result in cells leaking into other compartments. Moreover, fluidic diffusion into other compartments means distal regions cannot be fluidically isolated.
2. Infections can spread quickly throughout the micro-compartments. This can occur for a number of reasons, for instance if the NBM used contains an infection, or if the re-used device has any residual dirt. Moreover, during transfection, if any solutions have pre-existing contamination, this can result in a fast spread of infections. Therefore, it is vital that any experiments with these devices is carried out in a precise and clean manner.
3. PDL treatment of the glass is vital for cells to adhere and grow through the microchannels. If the glass has not been treated with PDL, then cells will ‘wash away’.

If all of the above-mentioned factors are avoided, then cells can be successfully treated with BDNF to observe for local and long-distance signalling (Figure 5-4). However, during this project, a number of above factors did occur, meaning the output of data for long-distance signalling was low. In comparisons to other methods, such as mass culture, successfully culturing hippocampal cells within microfluidic devices is difficult.

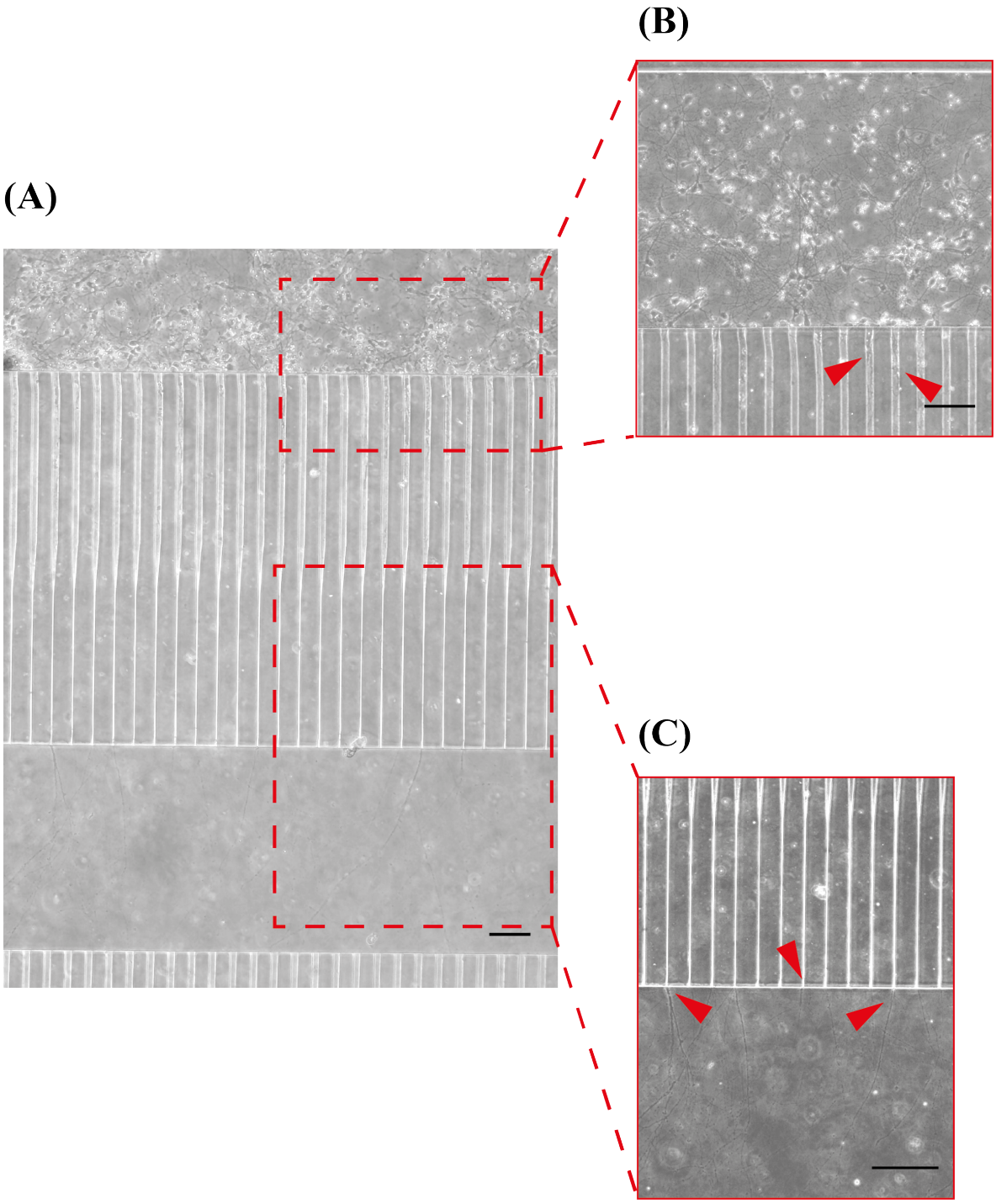

Figure 5-4 Microfluidic device with hippocampal cells, growing into the microchannels. (A) Example image of successfully cultured cells in microfluidic device used for local and long-distance signalling experiments. This image shows (B) the somatodendritic compartment, where the cell soma and dendrites sit, and (C) where the axons grow through the microchannels into the axonal compartment. The red arrows indicate axons growing into the microchannels. Scale bar: 10 μm.

5.2.5 Cell transfection in microfluidic devices

For transfections in microfluidic devices, the same protocol to prepare the 1:1 ratio of Lipofectamine:DNA at *DIV5* was followed as described in section 2.4.1. All the NBM was removed from ports and replaced with 50 µl of Lipofectamine-DNA mix and incubated at 37°C for 40 minutes. After this time, all the solution was removed from the microfluidic devices and replaced with fresh NBM.

Cells in devices were fixed for immunocytochemistry in a similar manner as described in section 2.5, with 10 minutes pause time between each loading solutions into the port to allow enough time for the solution to pass through the microchannels. The final mounting step was not performed as the cells were already mounted onto coverslips. Imaging was carried out with the devices still adhered to the glass coverslips. Devices were topped with 1xTBS to ensure the cells did not dry out. Figure 5-5 is an example of GFP transfected cells in microfluidic devices.

5.2.6 Arc staining analysis

To look at BDNF signalling relay in GFP-Tau^{P301L} expressing cells, BDNF stimulation was carried within the devices, where BDNF was added either to the distal projecting ends, or at the cell bodies (Figure 5-4). Cells were stained for Arc expression, and a z-stack against the nucleus was created. Z-stack images were taken in the TRITC channel for Arc staining and using the deconvolved image; the maximum fluorescence was projected as a 2-D image. To quantify Arc staining, a similar method was used as outlined in section 2.7.1. The nucleus was the chosen area to measure as quantifying dendrites can lead to subjective errors, in terms of where along the dendrites Arc signal is chosen to be measured, and whether primary or secondary dendrites are chosen. Therefore, the nucleus was used as a mask and overlaid

against the Arc stain. The mean fluorescent intensity was measured and data was plotted in GraphPad for each experimental condition.

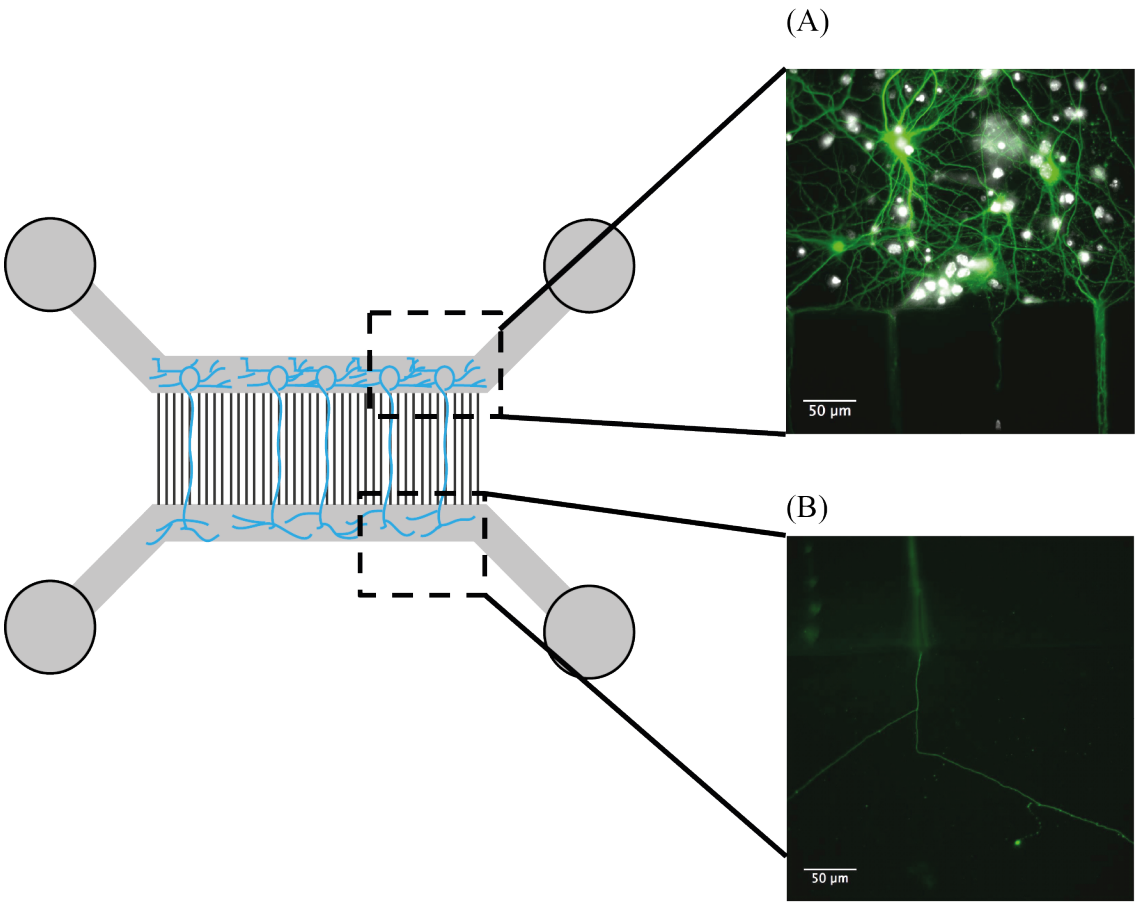

Figure 5-5 Microfluidic device showing GFP transfected cells.
Two fields of view images taken from successfully transfected microfluidic devices. (A) Somatodendritic compartment where cell soma and dendrites sit. Here GFP-expressing cells can be visualised (in green) with cell soma in white. Surrounding the transfected GFP cells are non-transfected cells. (B) GRP expressing axon growing through the microchannel. Here non-transfected axons are also able to growth through the microchannel (but are not visible).

5.3 Local and long-distance signalling is disrupted in Tau^{P301L}-expressing neurons

The rationale behind this experiment was to identify whether in Tau^{P301L}-expresssing cells, if signal relay is disrupted, is it due to the unsuccessful propagation of signal over large distances, a process possibly dependent on axonal transport or whether there is a fault in signal activation/translation. Long-distance signalling was compared to local signalling, where the application of BDNF to cell soma negates the need for neurotrophic signals to travel over large distances. Therefore, BDNF will bind to TrkB receptors located along the plasma membrane of the cell soma and dendritic processes and induce IEGs.

Upon BDNF application, within 30 minutes, Arc, an IEG downstream of BDNF is induced, with induction lasting beyond 2 hours[224,225]. With this in mind, after 2 hours of BDNF application (50 ng/ml either at the soma or distal axons), hippocampal cells were fixed within the microfluidic devices and probed for Arc induction using ICC.

In GFP-expressing cells at *DIV11-12*, BDNF application to cell soma induced Arc induction within 2 hours of treatment compared to GFP-expressing cells treated with culture medium only (control condition) (Figure 5-7 and Figure 5-6). From the quantification (Figure 5-6), there is a larger spread of mean fluorescence intensity of Arc in GFP somal conditions compared to that in GFP control conditions. Nonetheless, upon BDNF application to cell soma, Arc induction is observed ($p<0.001$). Although only 2 cells were analysed for distal GFP-expressing cells Arc induction can be observed. From our lab, Dr Joanna Bailey has shown successful long-distance BDNF signalling in healthy hippocampal cells (Figure 1-15). Using microfluidic devices, Dr Bailey treated axonal processes with BDNF (15 ng/ml) for either 4 hours, for protein analysis or for 6 hours for gene induction. From Western blot protein analysis, phosphorylation of Erk1/2 can be observed at axonal ends and at the cell soma after 4 hours of distal BDNF (15 ng/ml) application. From RNA extraction and PCR amplification, Dr Bailey has shown Arc induction at cell soma following 6 hours of distal

BDNF (15 ng/ml) application in healthy control cells. Arc induction cannot be seen in RNA extracted from axonal ends, as expected. This data, together with GFP-expressing cell data shows that in healthy cells, BDNF signalling both locally and over long-distances is fully functional and intact, where BDNF signal can be detected in at both somal and axonal compartments.

In Tau^{P301L}-expressing cells, Arc levels in control conditions is the same as that seen in GFP control conditions. However, upon BDNF stimulation at cell soma, Tau^{P301L}-expressing cells are unable to induce Arc expression to the same level as that seen in GFP-expressing cells (Figure 5-6 and Figure 5-8; $p<0.0001$). The relative mean of Arc induction in Tau^{P301L}-expressing cell upon BDNF application to cell soma is not significantly different to the expression in Tau^{P301L} control conditions.

Distal application of BDNF to Tau^{P301L}-expressing axonal ends at *DIV11-12* did not induce Arc expression over control conditions, in fact, Arc induction is the same that seen in Tau^{P301L} control condition. However, a significant difference is seen between Tau^{P301L} somal and distal conditions. Nevertheless, the induction in not greater what is observed in control conditions. Preliminary data from BDNF application to distal axons of GFP-expressing cells shows possible Arc induction, similar to what is seen by GFP-expressing cells exposed to BDNF at cell soma. Moreover, the two cells analysed within this condition have the same spread in mean fluorescence intensity as the GFP somal condition. However, due to low cell count and overall number of independent preparations carried out, a true comparison cannot be made. Only two cells were analysed for this condition due to the low throughput of the experiment, and also due to the time-restraints on the project, as these experiment were carried out towards the end of the project. These results shed a light on gene induction downstream of BDNF in disease conditions and gives an indication as to the likelihood of BDNF signal propagation in disease.

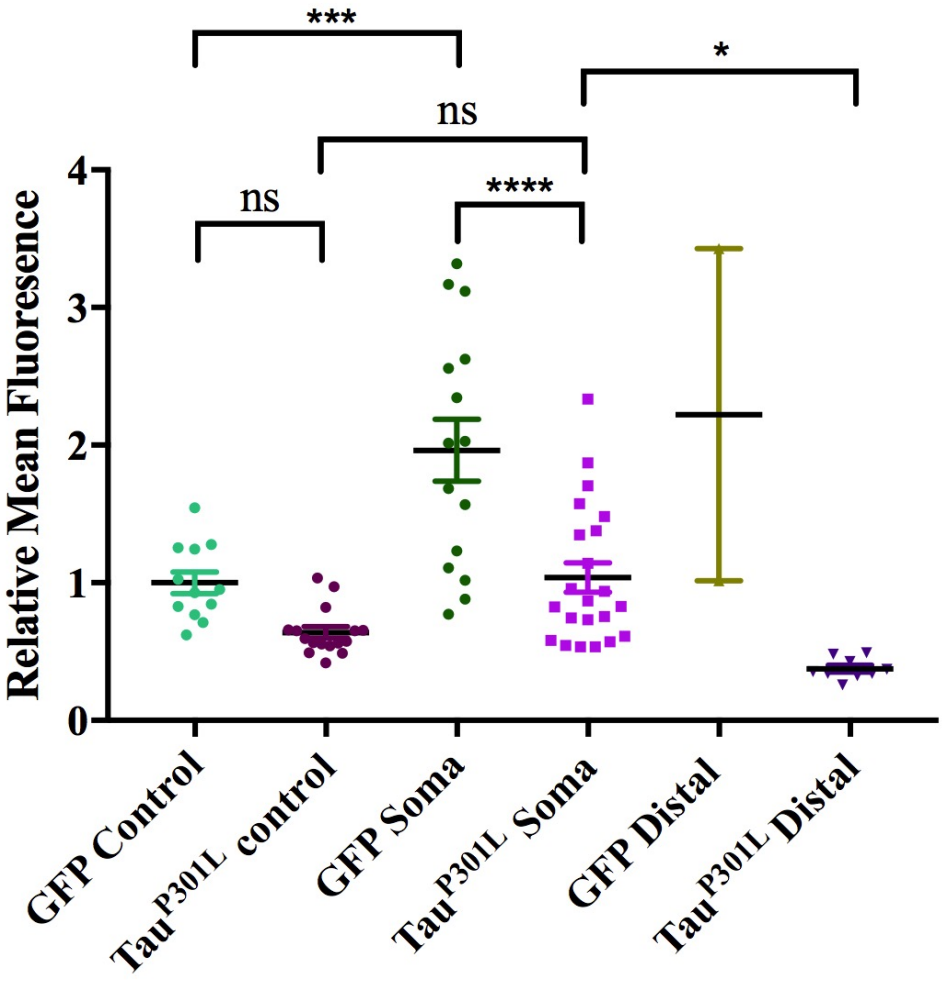

Figure 5-6 Quantification of *Arc* induction in GFP and Tau^{P301L}-expressing cells upon BDNF Stimulation at *DIV11-12*.

Quantification of relative mean fluorescence of Arc induction 2 hours after either control (media treatment) or 25 ng/ml BDNF application in GFP and Tau^{P301L}-expressing cells *DIV11-12*. Upon local BDNF application to GFP cells soma, significant Arc induction is observed compared to control conditions. The same is not seen in Tau^{P301L}-expressing cells. Preliminary data from GFP distal treatment shows GFP-expressing cells can induce Arc expression upon BDNF distal application. This is not seen in Tau^{P301L}-expressing cells treated with distal BDNF. One-way ANOVA, $p<0.0001$. ***$p<0.0001$, **$p<0.001$, $p<0.01$. n= 3 independent culture preparations, GFP distal treatment is from n=2 independent culture preparations; each point represents individual cells. Error bars: SEM.

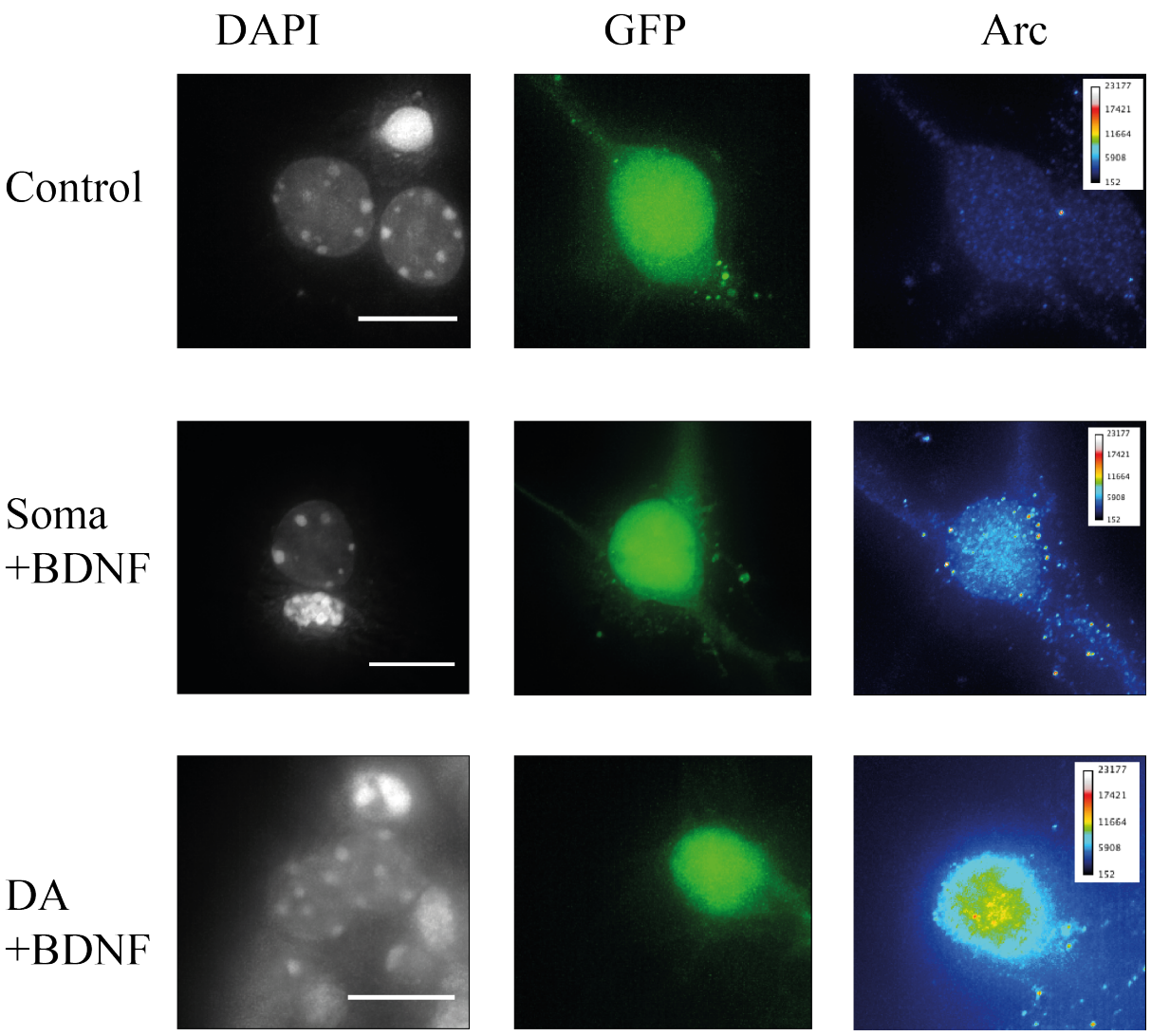

Figure 5-7 GFP-expressing cells can induce *Arc* signals both locally and over long-distance. Representative images taken from GFP-expressing cells treated with either control neurobasal medium (Control) at cell soma or BDNF (25 ng/ml) application, either locally at cell soma (Soma + BDNF), or at axonal ends for long-distance induction (DA + BDNF) at *DIV11-12*. *Arc* induction is seen both upon local and distal application (Scale bar: 10 μm).

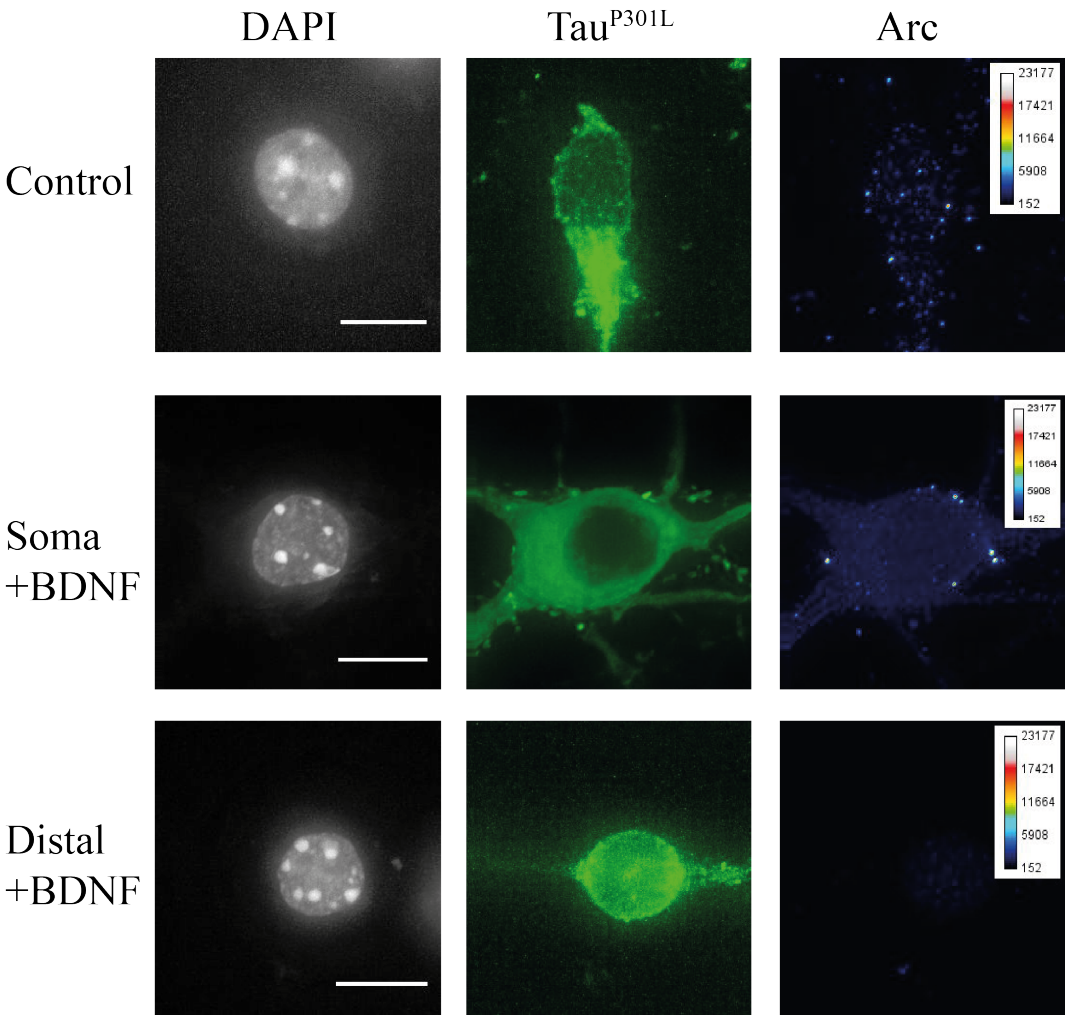

Figure 5-8 Tau^{P301L}-expressing cells disrupts local and long-distance *Arc* induction. Representative images taken from Tau^{P301L}-expressing cells treated with either neurobasal medium (control) or BDNF at soma (Soma +BDNF) or at distal axons (Distal +BDNF) for 2 hours and stained for IEG Arc *DIV11-12*. Arc induction is not seen in cells expressing the Tau^{P301L} mutation. (Scale bars: 10 μm).

5.4 Discussion

Having already established the availability of TrkB receptors on the surface of Tau^{P301L}-expressing cells, BDNF signal propagation was investigated. In order to identify whether BDNF signal propagation is still intact, I first looked at BDNF local signalling. BDNF mRNA is located in distinct subcellular compartments such as soma, dendrites, axons and spines, leading to spatial and temporal effects elicited by this neurotrophic factor[226]. Different mRNA transcripts are localised in these areas to induce specific local effects. For instance, long 3'UTR mRNA are localised in dendrites and short 3'UTR mRNA is restricted to the cell soma[227]. Impairment in long 3'UTR has shown to effect dendritic pruning and selective impairment of LTP in dendrites[227].

If BDNF signalling is dependent on axonal transport, then activating BDNF downstream signalling pathways locally, by applying BDNF directly on top of cell soma (where cell signalling is does not require the transport mechanism), should induce IEGs, such as Arc, within the first hour, as previously reported[228]. However, in Tau^{P301L}-expressing cells, this IEG induction was not seen within 2 hours of BDNF application at *DIV11-12* (however, Arc induction was observed in control healthy GFP-expressing cells at *DIV11-12*). This suggests that there may be a defect in signal interpretation itself. This result was unexpected as initially I hypothesised that local signalling would be intact in Tau^{P301L}-expressing cells, as IEG induction from direct application of BDNF does not depend on axonal transport. However, long-distance signalling was initially hypothesised to be effected due to axonal transport disruption, which is the mechanism required for signal relay[131,229]. This could still be the case in Tau^{P301L}-expressing cells. Never the less, local signalling results led to the new hypothesis that BDNF long-distance signalling in Tau^{P301L}-expressing cells will also be disrupted or delayed due to an error in signal translation. Thus, the results from the long-distance signalling experiments, although preliminary, are not surprising as it is in line with the results from local signalling (which shows IEG Arc is not induced upon BDNF application on cell soma on Tau^{P301L}-expressing cells).

From further investigation, a study support the current findings by showing a significant change in IEG induction upon BDNF stimulation in transgenic disease mouse models[230]. Within this Parkinson's disease mouse model, axonal transport is also affected[230]. Interestingly, TrkB levels are the same between the transgenic and non-transgenic brain tissue[230], similar to what was observed in Chapter 4. In addition, this study also shows increase in Rab5, an early endosomal maker[57]. This particular study concluded that impaired BDNF signalling is due to altered endocytic pathways that impacts signal trafficking[230]. In this respect, it would be beneficial to investigate the level of Rab5 and other markers in Tau^{P301L}-expressing cells.

It is important to note that the current experiment was carried out at a 2-hour time point, however, further timepoints are needed to determine if BDNF signal propagation is prolonged over a larger time frame. From preliminary examination of long-distance signalling in Tau^{P301L}-expressing cells, Arc induction is the same level as that seen in local BDNF stimulation and what you would expect to see in control non-stimulated cells. Data generated by Dr Joanna Bailey has shown successful long-distance signalling in healthy cells using a similar microfluidic set-up which has been used in this project (Figure 1-15). From her results, phosphorylation of Erk1/2 within axonal processes and cell soma is observed. This is similar to what has been reported previously[14]. Arc induction was also apparent in cell soma upon distal BDNF application. However, it should be noted that the experiment carried out by Dr Joanna Bailey were at different timepoints (4 hours and 6 hours) compared to the experiments carried out in this project (2 hours). Never the less, this data shows that long-distance BDNF signalling is intact in healthy cells. In light of this, seeing both Tau^{P301L}-expressing cells are unable to induce Arc at 2 hours following both somal and distal BDNF application raises questions as to the integrity of BDNF signal transmission. From current literature, it is not known why signal induction does not occur upon local simulation. In order to understand why Arc is not induce upon local BDNF stimulation, additional experiments on healthy cells are required, such as the use of Erk1/2 signal inhibitors and cytoskeletal modifiers to mimic axonal transport dysfunction. Using the above-mentioned modifiers at local and distal compartments will allow us to determine what mechanism is behind the unsuccessful local IEG induction.

6 Neurotrophic Modifiers

6.1 Introduction

For many neurodegenerative diseases, efforts have been made to identify potential targets for therapeutic approaches. In most cases, therapies have targeted the removal of toxic species such as amyloid-β (Aβ) aggregates or tau tangles in AD. However, from phase III clinical trials, many of these strategies have failed[231,232]. It is well established that the progression of neurodegenerative diseases is tightly correlated with synaptic loss[233–235]. With this in mind, the removal of pathogenic proteins is only part of the solution. Therapies need to target the neuronal network as whole, strengthening the synaptic connections before the onset of irreversible neuronal death. Scientists are now focusing their attention to understand which mechanism should be targeted to slower the synaptic deficits[236,237]. BDNF has been identified as a potential candidate[148,233,238,239] and thus the purpose of this project was to understand the likelihood of BDNF signalling pathways as a successful therapeutic candidate.

From Chapter 4, TrkB receptor expression in Tau^{P301L}-expressing cells has been examined. From the results reported in this chapter, TrkB expression on the surface of Tau^{P301L}-expressing distal axons is no different to the amount on GFP-expressing distal axons at *DIV11-12* (Figure 4-5), however, the internal pool of receptors in Tau^{P301L}-expressing distal axons is depleted compared to control cells (Figure 4-3). This suggests that the transport of newly synthesised TrkB is disrupted, and it could be hypothesised, that beyond *DIV11-12*, the number of receptors on the surface of Tau^{P301L}-expressing distal axons could be depleted. This would have an impact on BDNF signalling, as there would be less receptors for BDNF to bind to, and potentially dampen BDNF signal induction. In this case, it would be useful to develop an agent/peptide which could enhance BDNF signalling, in cells that have a decreased level of TrkB receptors. In this case, a peptide could compensate for the dampened BDNF signal. In addition to this, from section 3, axonal transport in distal Tau^{P301L}-

expressing axons was also established. This would suggest that transport of newly synthesised BDNF could be decreased due to axonal transport disruption, in which case, a decrease in BDNF release would occur. In this situation, a peptide that mimics BDNF structure, could bind to TrkB, and activate downstream signalling cascades. In both instances, it is useful to test whether such peptides could be designed and developed for therapeutic intervention. However, it should be noted that further experiments are required to establish signal relay disruption in Tau^{P301L}-expressing cells, before attempting to develop peptides which could mimic or heighten BDNF signalling.

To understand the process of drug development and how drugs can be employed to interfere with cell signalling, I collaborated with Professor Ali Tavassoli's group from the Department of Chemistry at the University of Southampton. A PhD researcher within Professor Tavassoli's group, Dr Jamie Ingram, has developed inhibitors that can block the activity of BDNF and NGF[240]. The rationale behind Dr Ingram's research was based on Pfizer's Tanezumab drug, which is used to treat chronic pain in patients with osteoarthritis and chronic lower back pain[166]. Tanezumab is a monoclonal antibody that binds to NGF which in turn prevents NGF from binding to its receptor, TrkA. Studies on Tanezumab have shown to dramatically reduce nociception, however they have also shown significant discontinuations due to adverse effects[166]. Therefore, Dr Ingram sought to further develop a number of neurotrophic inhibitors. The aim of our collaboration was for me was to understand whether the development of peptides that interact with NGF and BDNF can be used to enhance cell signalling.

To identified peptides that interact and bind to NGF or BDNF, Dr Ingram carried out a phage display. The adherence of these peptides was tested for its target specificity, and an ELISA screen was used to assess agonist/antagonist activity. Dr Ingram then synthesised and further assessed these peptides to determine binding data. Finally, the biological activity of the lead peptides was tested against TrkB/PC12 cells in western blot and morphology assays. This latter testing was carried out by myself and Dr Deinhardt.

The phage display was used to identify small peptide loops capable of binding to NGF and BDNF, and thus influence downstream signalling cascades. Phage display is a high throughput technique used to identify peptide sequences that are able to bind to a specific target (in this case, NGF and BDNF). To carry out a phage display screen, the target of interest is bound to a surface and exposed to the library of phage. Phages expressing modified coat proteins capable of adhering to the target are retained, whilst non-binders are removed by washing. This cycle is then repeated several times under more stringent conditions to remove weaker affinity binders. Finally sequencing the phage genome is used to rapidly elucidate hits. Dr Ingram used a commercially available phage library.

To test whether the identified phage was selective for NGF or BDNF an ELISA screen was carried out by Dr Ingram. However, before commencing an ELISA, a buffer test was developed to ensure NGF or BDNF do not unfold or misfold in solution. Protein stability in solution was tested by using thermal shift assays, where NGF and BDNF is dissolved in various buffers that contain SYPRO Orange dye (ThermoFisher Scientific, catalogue number S6650). This fluorescent dye will significantly increase in quantum yield upon binding to hydrophobic regions in denatured proteins. From this experiment, PBS with glycerol was identified as the most suitable buffer for NGF and BDNF compared to distilled water and was therefore used in all future assays.

A total of 30 lead peptides were identified. From the current literature, it is known that only mature neurotrophins can bind to Trk receptors and elicit downstream signalling pathway. Pro-neurotrophins are unable to active Trk receptors[2,38,52,241]. Therefore, it is important to understand whether the synthesised peptides have an inhibitory effect on NGF and BDNF downstream signalling.

A total of 30 peptides were identified and tested for their inhibitory activity via a two-component ELISA. NGF bound to TrkA (domain 5) expressed in *E. coli* was used for the assay. By adding tags to the Trk receptors, an ELISA assay was developed by Dr Ingram. Tags were added to the NGF receptor and orthogonally to the TrkA-domain 5 (TrkA-D5). An antibody conjugated to a colourimetry enzyme was used to detect the tagged TrkA-D5. A

colourimetric reaction was used to quantify the relative amount of antibody retained. If peptides are identified as inhibitory then they would bind in place of the TrkA-D5. This in turn would prevent the binding of TrkA-D5 and as a result, the fluorescent signal would be reduced. If the peptides allow for downstream signal activation, then they would not interfere with TrkA-D5 binding and so an increased fluorescent signal would be identified compared to peptides which block TrkA-D5 binding. The plates with NGF and BDNF were then incubated to allow the peptide to bind before addition of TrkA-D5 or TrkB-D5. 13 lead peptides were identified, 5 of which interact with NGF, 6 of which interact with BDNF and 2 are dual-specific, interacting with both NGF and BDNF (Table 6-1).

To determine whether these peptides were biologically active, I carried out an extensive functionality test using pheochromocytoma cell line PC12 that stably express TrkA and TrkB. From current literature, it is already known that PC12 can be used as a platform to assess MAPK signalling[242,243]. One of the well characterised and classical example is whereby incubation of PC12 cells with NGF leads to cell differentiation where neuronal like process protrude from PC12 cell bodies. This occurs when MAPK activation is sustained. However, if PC12 cells are incubated with epidermal growth factor, the same MAPK pathways is only transiently activated, leading to cell proliferation[242,243]. This assay is widely cited and used as an example to highlight the intricate and dynamic MAPK signalling pathway. This morphological assay was performed to investigate whether the 13 peptides were capable of agonising or antagonising MAPK downstream signalling cascades, or affecting the morphological changes.

Peptide Code	Neurotrophic interaction	Mol Mass (Da)
JI.5.1C	NGF/BDNF (antagonist)	1521.58
JI.5.13C	NGF/BDNF (agonist)	1392.57
JI.5.12C	NGF (antagonist)	1456.6
JI.5.14C	NGF (agonist)	1290.46
JI.5.14C.7	NGF (agonist)	1290.46
JI.5.55C	NGF (agonist)	1540.62
JI.5.58C	NGF (antagonist)	1341.56
JI.5.23C.5	BDNF (antagonist)	1410.65
JI.5.23C.6	BDNF (antagonist)	1410.65
JI.5.37C	BDNF (antagonist)	1260.49
JI.5.43C	BDNF (antagonist)	1245.42
JI.5.44C	BDNF (antagonist)	1314.52
JI.5.52C	BDNF (antagonist)	1318.53

Table 6-1 List of synthesised neurotrophic modifiers by Dr Jamie Ingram.
Column 1: The peptide code used to identify each peptide identified from the library screen. Column 2: Neurotrophic interaction – identifies the neurotrophic factor, NGF and/or BDNF the peptide interacts with which was identified from the library screen. Column 3: Molar mass of each peptide in Dalton (Da). A total of 8 BDNF interacting peptides and 7 NGF interacting peptides were tested for their biological activity.

6.2 Methods

6.2.1 Immortal cell lines

PC12 cell line derived from a pheochromocytoma of a rat adrenal medulla stably expressing TrkB and TrkC were grown in T75 flasks in Dulbecco's Eagle Modified Medium (DMEM, with GlutaMAX, 4.5 g/L glucose and pyruvate) supplemented with 10% Foetal Bovine Serum (FBS) and 5% Horse serum, now referred to as PC12 medium. For DMEM only conditions, cells were only incubated in(DMEM, with GlutaMAX, 4.5 g/L glucose and pyruvate. When cells had grown to 80% confluency, they were passaged and diluted into fresh T75 flasks. To do this, the medium was removed and cells were washed once with 1x PBS. 5ml of fresh PC12 medium was added to the T75 flasks and cells were detached by pipetting the medium directly onto the cells. This was repeated until majority of the PC12 cells were detached from the flask. The resuspended cells were then diluted into fresh PC12 medium in 1:10 ration of cell suspension to medium. Cells were incubated at 37°C and 5% CO_2 until use.

6.2.2 PC12 neurite length analysis

PC12 cells that stably express TrkA and TrkB were grown in growth medium until they reached 80% confluency. PC12 cells were aspirated and plated in 12-well plates at 50% confluency. Once the cells adhered to the plate, the PC12 growth medium was removed and replaced with DMEM only medium for 1 hour.

Two experiment were carried out to test the activity of the peptides. The first was to test if the peptides had an inhibitory effect on PC12 cell differentiation. Therefore, to test for antagonist activity, cells were treated with 10 ng/ml NGF or BDNF. The second experiment was to test for agonist activity. For this, a minimal activation was required, whereby agonist peptides

could allow for cell differentiation. To determine the concentrations required for antagonist and agonist activity, PC12 cells were treated with BDNF or NGF at varying concentrations overnight (0.1 ng/ml, 1 ng/ml, 5 ng/ml and 50 ng/ml mixed in DMEM). 10 ng/ml for both NGF and BDNF was seen to induce significant differentiation. Whereas overnight differentiation experiments showed minimal induction at 1 ng/ml NGF, or 0.1 ng/ml BDNF. Therefore, the lead peptides were used to test if they can induce differentiation above baseline (at 1 ng/ml NGF, or 0.1 ng/ml BDNF).

To test the lead peptides for agonist or antagonist activity, experiment was carried out 4 separate times (n=4) and 2 repeats were carried out within one independent experiment. Two fields of view from each well were captured before and at consecutive 24 hours after the treatments for up to 72 hours. Between 48 hours and 72 hours, no visible difference in neurite lengths were observed and therefore, the first 50 neurites were measured in each field of view at the 48-hour time-point. Neurite length was quantified using ImageJ plugin ‘Neurite Tracing’. The first 50 lengths were measured and values were added in an excel file. This data was quantified using a customised MATLAB script (Figure 6-1). I have defined differentiating PC12 cells are those that fall in bin 3, where neurite lengths are 5 times greater the length of the cell body.

(A)

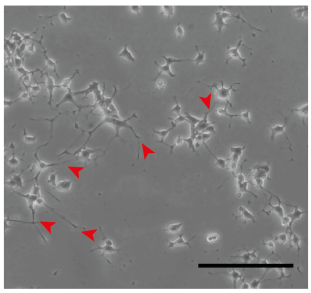

(B)

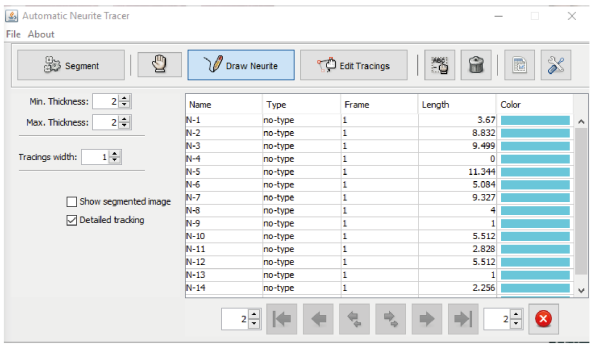

(C)

```
data = dataset('xlsfile',); %add path for spreadsheet
neurites = data. ; %data.column name (peptide)
bin1=neurites<=60;
bin2=neurites>60 &neurites<=100;
bin3=neurites>100;
number= [sum(bin1) sum(bin2) sum(bin3)];
result= number/100
```

Figure 6-1 Method used for PC12 differentiation analysis.

Example of the method employed to assess peptides inhibitory and activation effects on PC12 cells. (A) representative image of PC12 cells in DMEM medium. Red arrows indicate measured neurites. (B) Using ImageJ, individual neurites were measured and the lengths were copied into excel files. (C) Using a customised MATLAB script, objective analysis of PC12 differentiation was carried out, where neurite lengths were binned >5 times cell diameter. Any cells that had neurites over 5 times the cells diameter was classified as differentiating. Scale bar: 10 μm

6.3 Determining threshold concentration for NGF and BDNF

The first step in understanding the mode of action of the lead peptides was to establish the threshold concentrations of NGF and BDNF required to induce differentiation, prior to its incubation with the peptides. As the peptides interact directly with NGF and BDNF, influencing its binding with Trk receptors, it was important to determine the minimum concentration required for sustained MAPK activity, leading to PC12 cell differentiation.

Within the lab, 100 ng/ml of NGF and 50 ng/ml BDNF concentration is used as an over-estimation to induce the downstream pathways. These concentrations are also commonly used by other labs[244]. Therefore, to avoid oversaturation of the Trk receptors and to avoid masking any agonistic/antagonistic activity by the lead peptides, 0.1 ng.ml, 1ng/ml, 5 ng/ml and 50 ng/ml concentrations of NGF and BDNF were tested. Images were taken before and at every 24-hour intervals till 72 hours.

From initial tests, 0.1 ng/ml of NGF treatment over 24 hours on PC12 cells did not induce significant differentiation, whereas treatment with 1 ng/ml of NGF induced significant neurite growth within these PC12 cells (Figure 6-3and Figure 6-4). From this, it was decided that concentration of 1 ng/ml of NGF is the threshold concentration required to induce the MAPK signalling pathway needed to elicit neurite differentiation. Looking at BDNF concentrations, 0.1ng/ml BDNF application on PC12 cells showed a significant increase in neurite growth. However, this was also significantly different to the differentiation noted in treatments with 1 ng/ml BDNF to 50 ng/ml BDNF. Therefore, 0.1 ng/ml of BDNF was used as the lowest concentration required to induce differentiation. As concentrations higher than 5 ng/ml of both NGF and BDNF induce significant PC12 cell differentiation, 10 ng/ml NGF and BDNF concentrations were used to test the effect of antagonist peptides.

Following on from this, I also tested the buffer the peptides are dissolved in to ensure the buffer itself has no effect on PC12 cell neurite growth. A dilution of 1:15 and 1:2.5 was tested as at this dilution, the peptides are able to dissolve in solution. Before buffer treatment, the PC12 cells were serum starved for 1 hour, followed by the incubation with 10 ng/ml BDNF or NGF with peptide buffer for 48 hours. In both conditions, the peptide did not interfere with neurite differentiation (Figure 6-2).

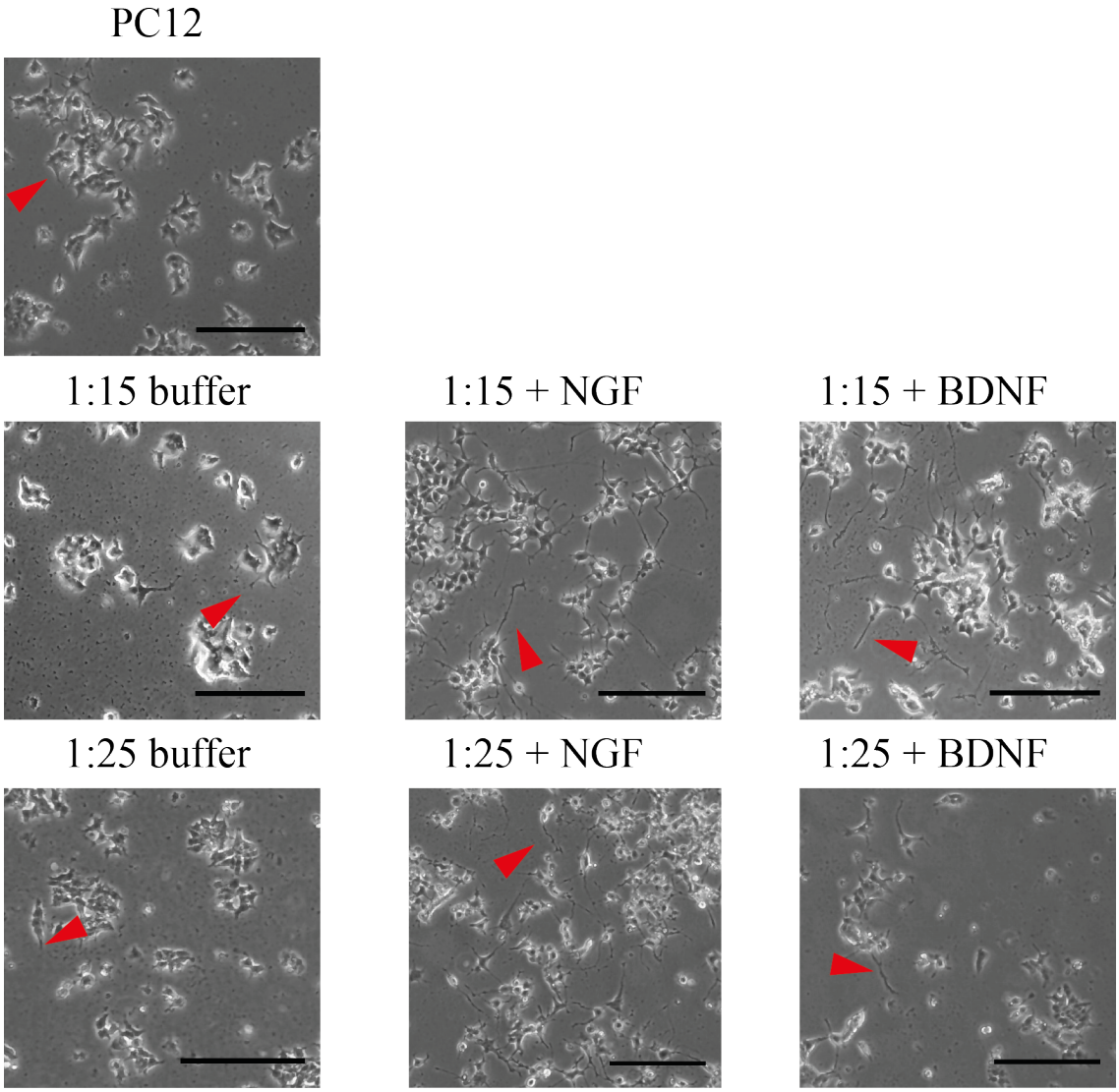

Figure 6-2 Buffer test on PC12 cells using 1:15 and 1:25 concentrations to determine toxicity. The buffer used to dilute the peptides was tested for potential toxicity. A suggested concentration for dilution of 1:25 and a higher concentration of 1:15 was tested for 48 hours, either in alone incubation on PC12 cells or in combination with NGF or BDNF, both at 10 ng/ml. PC12 cell death was not seen in any condition, compared to PC12 medium condition alone. Red arrows indicate PC12 processes. Scale bar: 10 μm.

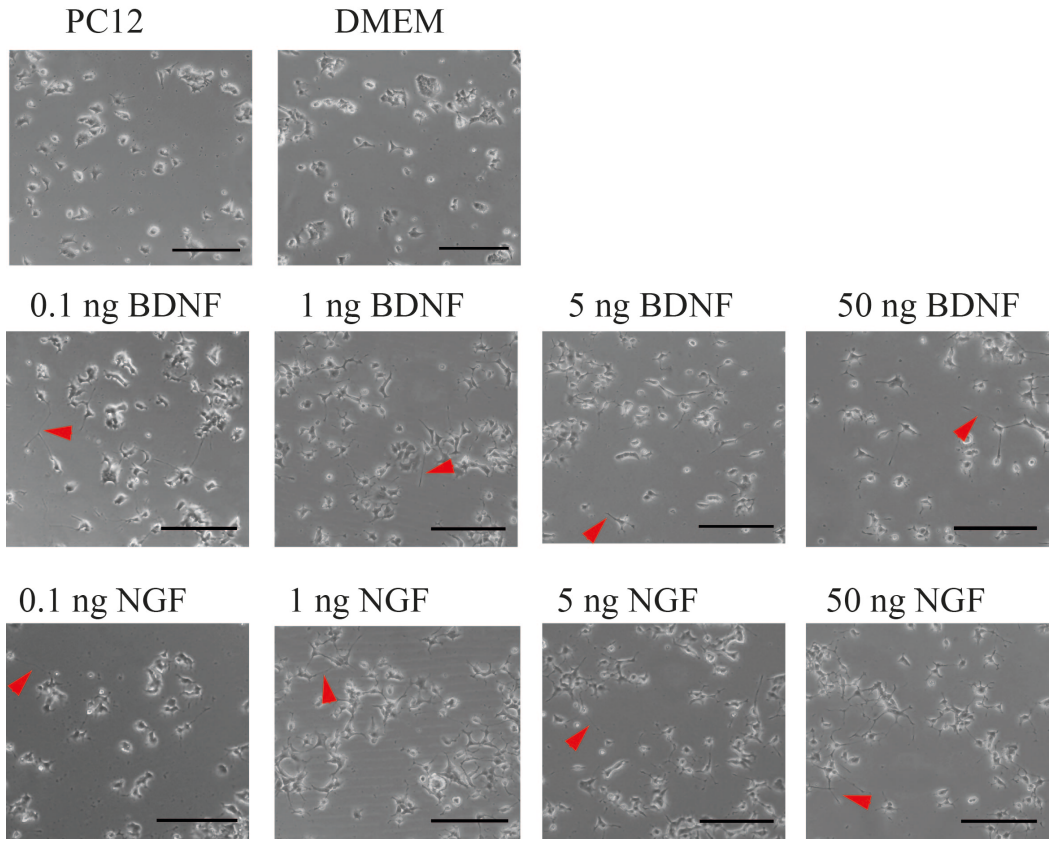

Figure 6-3 Representative images of NGF and BDNF concentration test on PC12 cells.

PC12 cells were incubated with either PC12 medium (DMEM + 10%FBS + 5%HS), DMEM only, varying concentrations of NGF (0.1 ng, 1 ng, 5 ng, 50 ng) and BDNF (0.1 ng, 1 ng, 5 ng, 50 ng) diluted in PC12 medium for 24 hours. Neurite lengths from 50 cells per field of view was measured. In total, four fields of view were captured from two repeat experiments. Red arrows show PC12 neurite differentiation. *$p<0.01$, ***$p<0.0001$, ns=non-significant. Error bars: SEM. Scale bar: 10 μm.

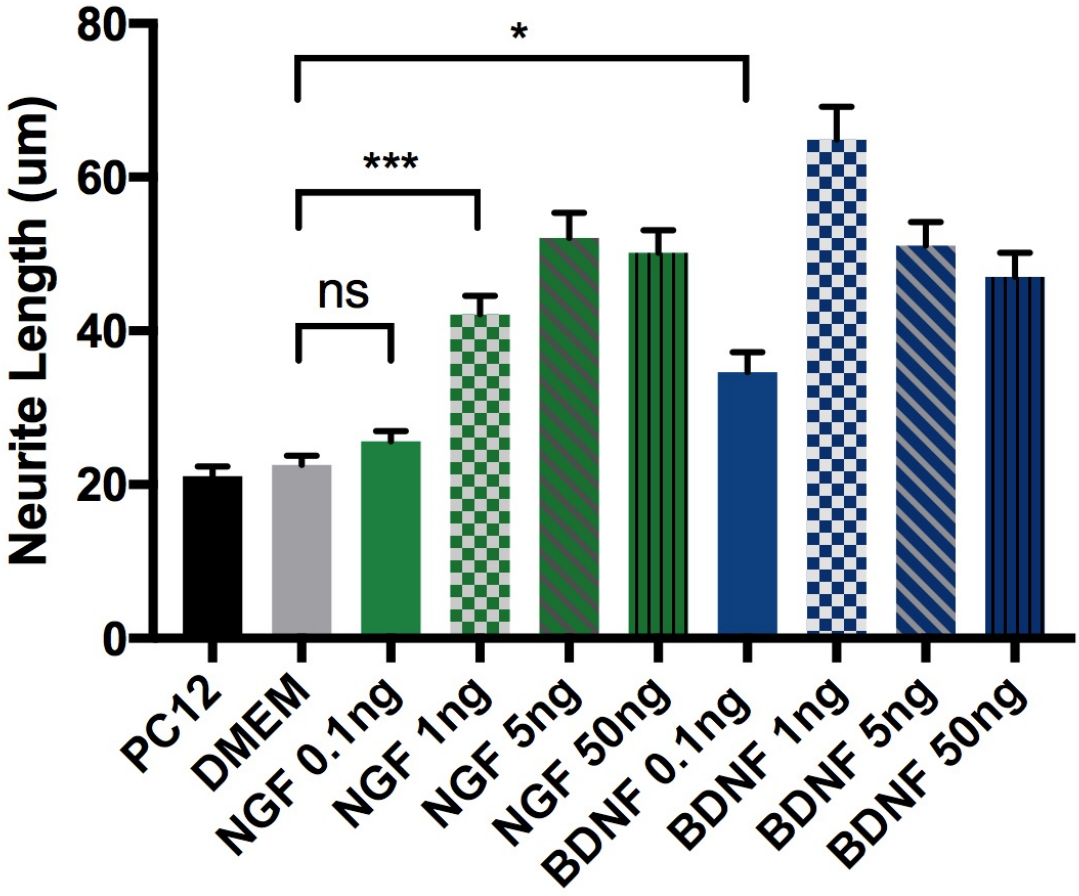

Figure 6-4 Neurotrophic concentration gradient quantification.
Quantification of PC12 neurite lengths measured 24 hours after incubation with PC12 medium contacting varying concentrations of NGF and BDNF. Neurites were measured from 50 cells in four fields of view in one repeat experiment. Two repeats were carried out in total. One-way ANOVA, $p<0.0001$. *$p<0.01$, ***$p<0.0001$, ns=non-significant. Error bars: SEM.

6.4 Neurotrophic modifiers inhibit cell differentiation

BDNF and NGF are both known to induce differentiation in PC12 cells. A functionality test was carried out to see if the peptides can enhance BDNF or NGF-induced neuronal growth or block neurotrophic activity and prevent differentiation. Peptides were mixed with either low concentrations of NGF or BDNF (1 ng or 0.1 ng, respectively) to see if they have the capability of enhancing neurite growth, or with high concentration (10 ng of NGF or BDNF) to see if the peptides block the differentiation induced by NGF or BDNF. As a negative control, PC12 cells were treated with DMEM only and for a positive control, PC12 cells are treated with either the high or low concentrations of neurotrophic factor alone.

13 peptides were tested and examined for their neurotrophic mimicking or blocking properties (Figure 6-5, Figure 6-6). From these peptides, two NGF-interacting and three BDNF-interacting peptides were selected as the most effective and were re-tested (Figure 6-7, Figure 6-8 and Figure 6-9, Figure 6-10). Additional experiments were carried out to increase the number of independent cell culture experiments for robust data outputs. A total of n=5 experiments were carried out, each with two repeats. The combined data for neurite differentiation illustrates peptides 55 and 58 interacts with NGF to enhance its activity (Figure 6-8). Within these conditions, the peptides were incubated with 1 ng of NGF and trends towards the positive control, whereby differentiation is induced at 10 ng of NGF. However, none of the peptides trend towards blocking neurite differentiation. If blocking was seen, the cells would look similar to the 1 ng NGF treatment. Therefore, these peptides only work to enhance NGF-induced cell differentiation.

A selective difference is seen for the BDNF-interacting peptides (Figure 6-10). Peptide 23.5 could have a potential to differentiating morphology, but further analysis is required, whereas the other two peptides (43 and 52) closely match the negative control treatment (incubation of 0.1 ng of BDNF only with PC12 cells). However, when all three peptides (23.5, 43 and 52) are incubated with 10 ng of BDNF, blocking properties are not seen, but rather the peptides

act in a similar manner to the positive control treatment of 10 ng BDNF alone. Therefore, only peptide 23.5 is effective in this assay, demonstrating a possible differentiating phenotype.

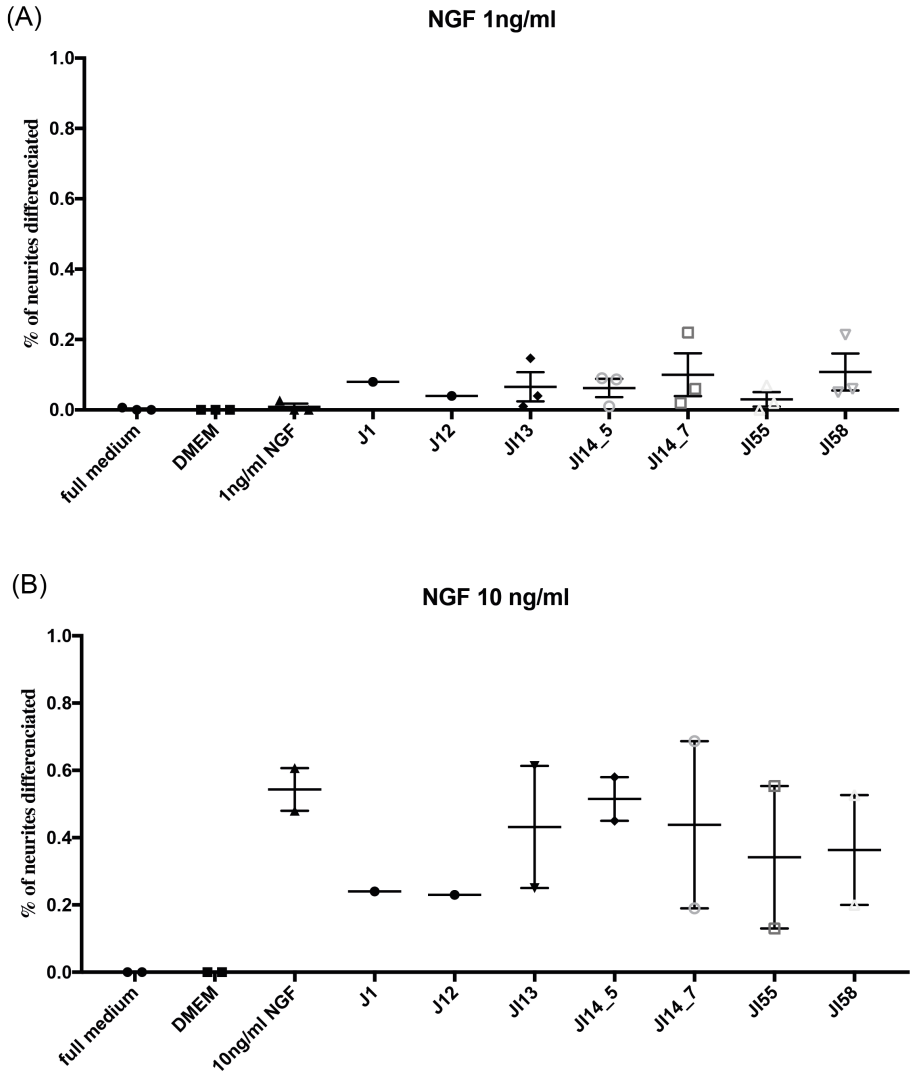

Figure 6-5 PC12 morphology data, testing TrkA interacting peptides with low and high concentrations of NGF.

PC12 cells incubated with full PC12 medium, DMEM (as a negative control) and (A) 1 ng/ml NGF or (B) 10 ng/ml NGF. All NGF interacting peptides (as identified via a screening library by Dr Ingram) were incubated with low (1 ng/ml) or high (10 ng/ml) NGF concentrations. After 48 hours, PC12 cell neurite growth was measured and anything beyond 5 times the diameter of cell body was recorded. From tests with low and high concentrations of NGF, peptides 55 and 58 were chosen for further testing as the mean measurements of neurite lengths when incubated with 10 ng/ml NGF were the lowest compared to other peptides and

treatment with 10 ng/ml NGF alone; suggesting these two peptides may interact with TrkA. Each point represents results from one independent prep, with data combined from two repeats. Error bars: SEM.

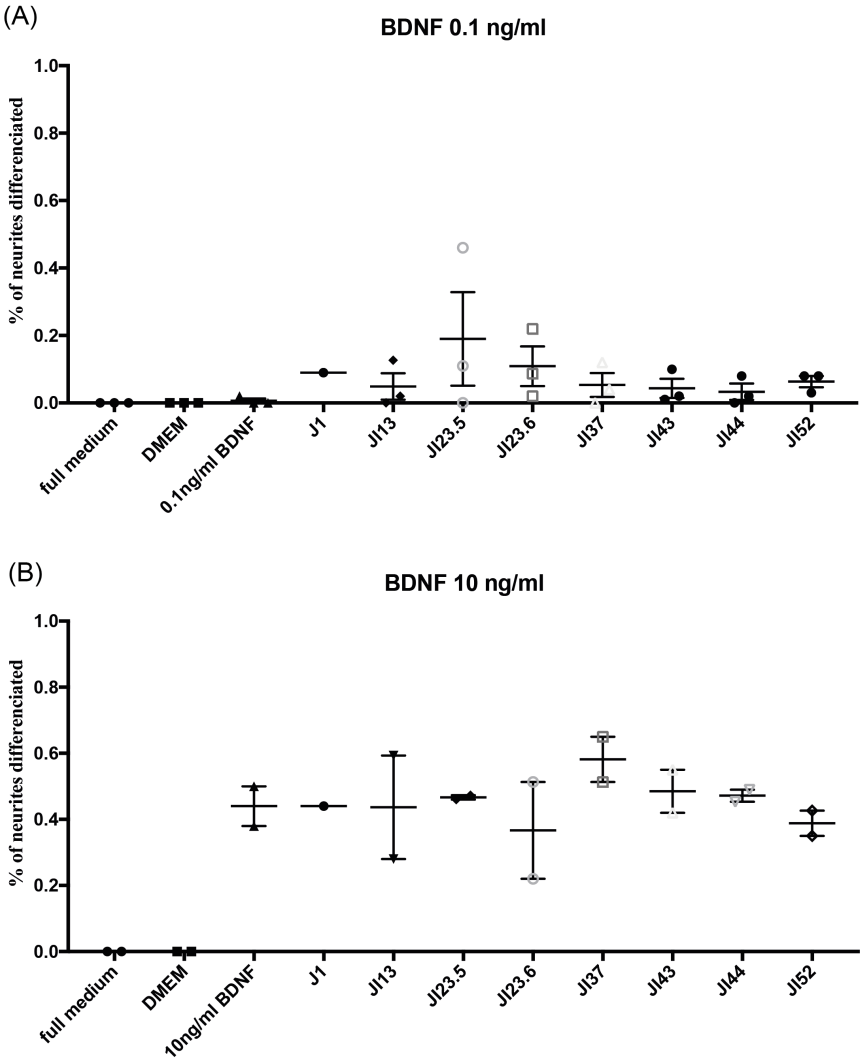

Figure 6-6 PC12 morphology data, testing TrkB interacting peptides with low and high concentrations of BDNF

PC12 cells incubated with full PC12 medium, DMEM (as a negative control) and (A) 0.1 ng/ml BDNF or (B) 10 ng/ml BDNF. All BDNF interacting peptides (as identified via a screening library by Dr Ingram) were incubated with low (0.1 ng/ml) or high (10 ng/ml) BDNF concentrations. After 48 hours, PC12 cell neurite growth was measured and anything beyond 5 times the diameter of the PC12 cell body was recorded. From tests with low and high concentrations of BDNF, peptides 23.5, 43 and 52 were chosen for further testing. The mean measurements of neurite lengths for peptide 23.5 and 52 when incubated with 10 ng/ml BDNF were the lowest compared to other peptides and treatment with 10 ng/ml NGF alone; suggesting this peptide may interact with TrkA. Peptide 23.5 also showed a high mean measurement when incubated with low concentrations of BDNF compared to 1ng BDNF

treatment alone. Peptides 43 was also chosen for further analysis as it could increase neurite growth compared to 0.1 ng/ml BDNF treatment alone. These peptides were also promising form Western Blot data conducted by Dr Deinhardt. Each point represents results from one independent prep, with data combined from two repeats. Error bars: SEM.

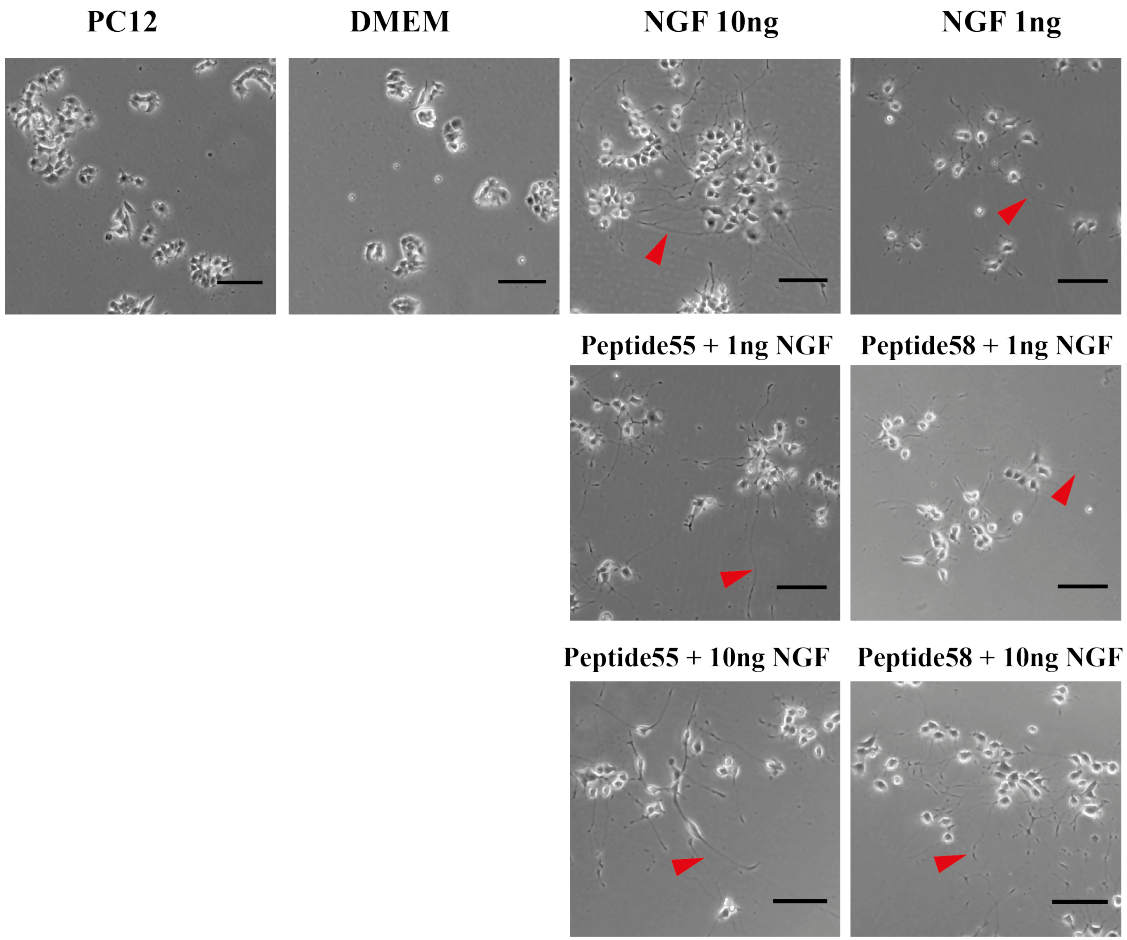

Figure 6-7 Representative images of NGF-interacting peptide treatments on PC12 cells.

Representative images taken 48 hours after treatment of PC12 cells kept in PC12 growth medium, DMEM only medium (negative control), cells incubated with 10 ng (high concentration) or 1 ng (low concentration) of NGF and PC12 cells pre-incubated with either the high or low concentrations of NGF, followed by incubation with peptide 55 and 58. Red arrows show PC12 neurite growth. Scale bar: 100 μm

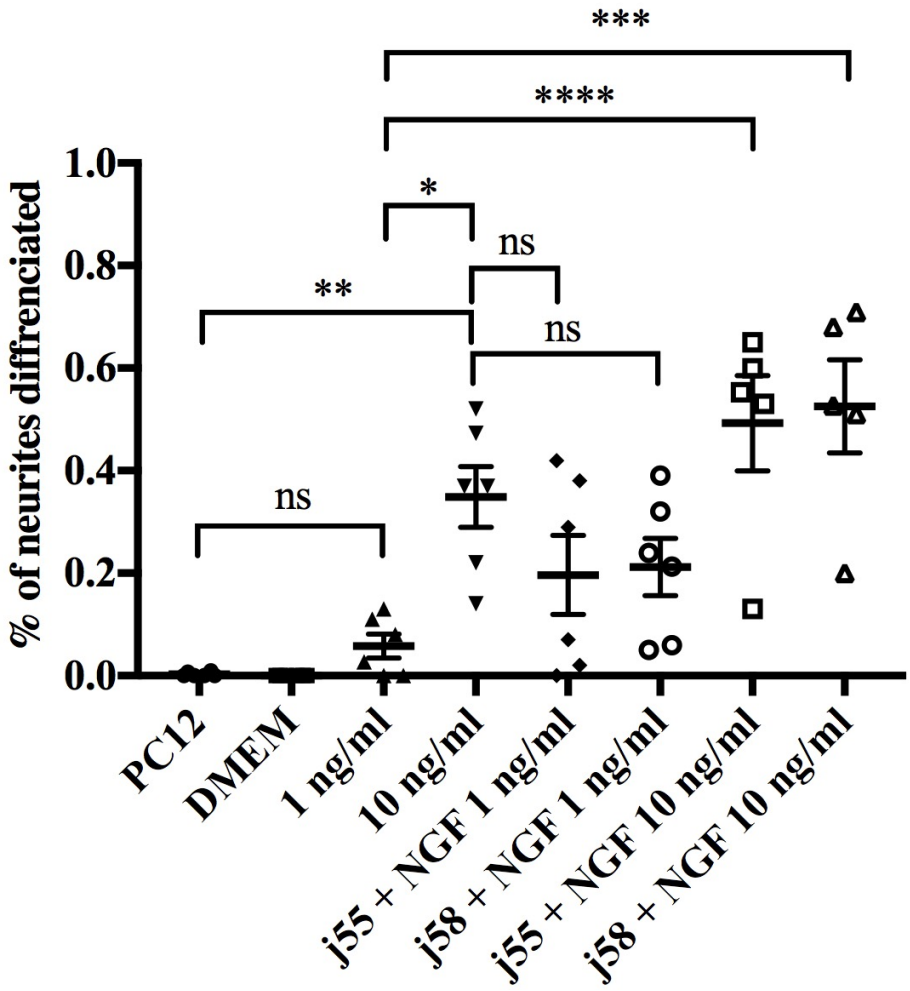

Figure 6-8 NGF-interacting peptides differentiate PC12 cells, similar to NGF.
PC12 cells treated with low concentrations of NGF and TrkA-binding peptides display similar differentiation to the positive control (10 ng NGF alone treatment). However, the neither of the peptides show inhibition of neurite differentiation phenotypes. PC12 cells treated with PC12 medium, DMEM medium, 1ng NGF, 10ng NGF, and peptide 55 and 58 with 1 ng NGF and 10 ng NGF. Images were taken 48 hours after treatment and a total of 100 cells were analysed in each condition from each experiment. One-way ANOVA, $p<0.0001$, n= 5 represents individual experiments. ns=non-significant, ****$p<0.0001$; ***$p<0.001$; **$p<0.01$; *$p<0.05$. Error bars: SEM.

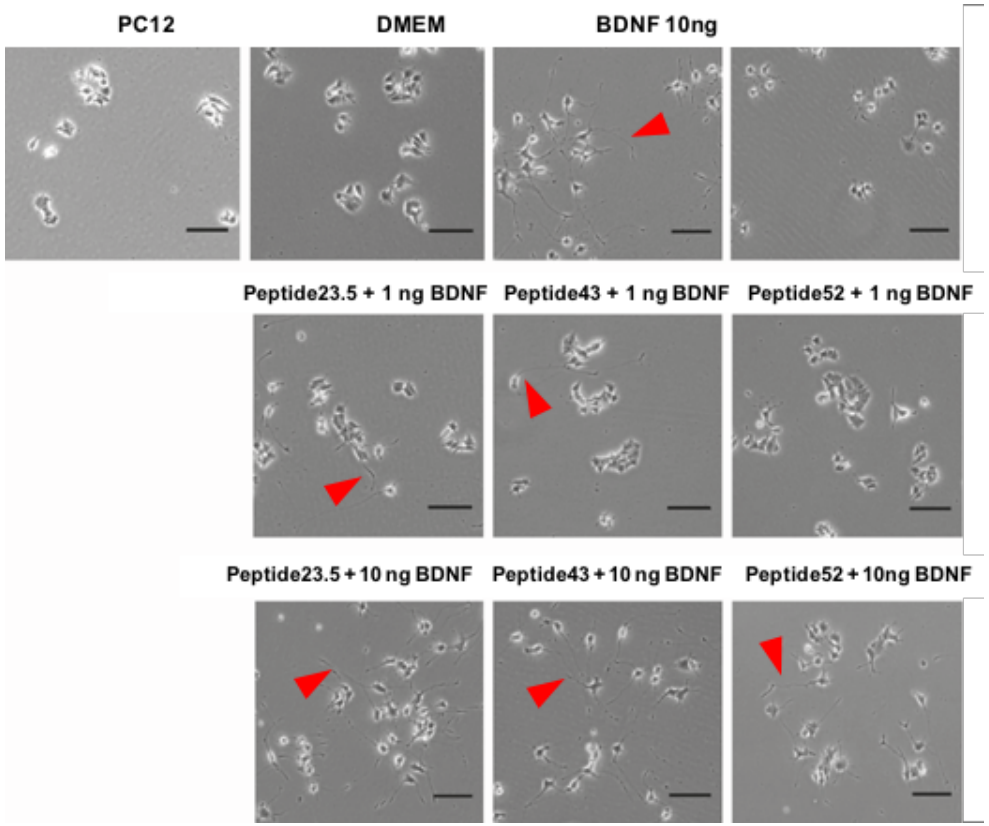

Figure 6-9 Representative images of BDNF-interacting peptide treatment on PC12 cells.

Representative images taken 48 hours after treatment of PC12 cells kept in PC12 growth medium, DMEM only medium (negative control), cells incubated with 10 ng (high concentration) or 1 ng (low concentration) of BDNF and PC12 cells treated with peptide 23.5, 43 and 52 combined with low or high BDNF. Red arrows show PC12 neurite growth. Scale bar: 100 μm

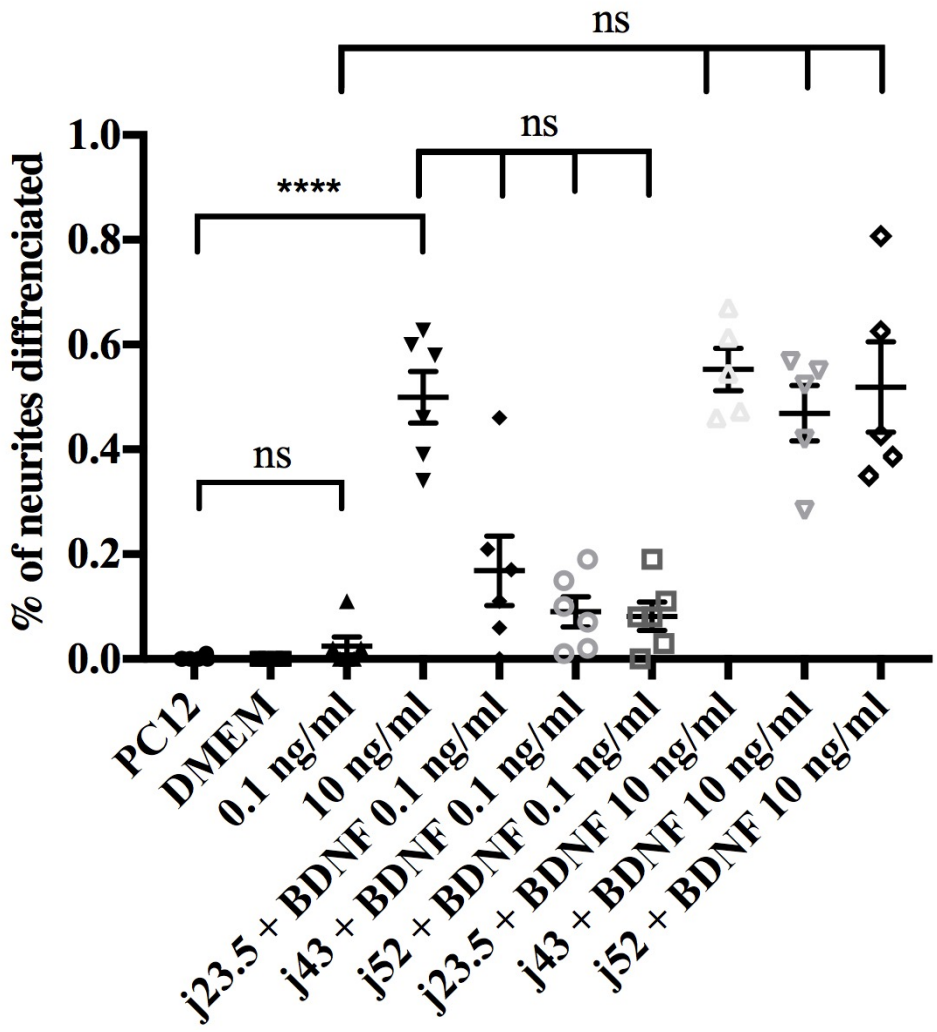

Figure 6-10 Selective effect of BDNF-interacting peptides mediating a differentiation phenotype on PC12 cells.

Treatments containing low concentrations of BDNF have a selective effect in inducing differentiation. Only treatment 23.5A shows an increase in differentiation over the negative control (0.1 ng BDNF), but these cells are not as differentiated as the PC12 cells treated with 10 ng BDNF. PC12 cells treated with peptides containing high concentrations of BDNF do not block trophic activity. PC12 cells treated with PC12 medium, DMEM medium, 0.1ng BDNF, 10 ng BDNF and peptides 23.5, 43 and 52 were treated with 0.1 ng or 10 ng BDNF. Images were taken 48 hours after treatment and a total of 100 cells were analysed in each condition from each experiment. One-way ANOVA, $p<0.0001$, n= 5 represents individual experiments. ns=non-significant, ****$p<0.0001$. Error bars: SEM.

6.5 Discussion

BDNF has been implicated in a number of neurodegenerative diseases, such as Alzheimer's and Huntington's disease[136,239]. Therefore, modulating BDNF's signalling could be used as a therapeutic intervention. In order for this to occur, we need to understand whether BDNF will induce the downstream signals that are downregulated in disease; which is the rationale behind this project. Once this is established, it is also important to know whether BDNF signals can be modulated via external peptides that are small enough to pass the BBB.

At the University of Southampton, Dr Ingram was also interested in modulating BDNF signalling, but for chronic pain. With this shared interest, a collaboration was established, whereby peptides synthesised by Dr Ingram were tested by myself using PC12 cells. Dr Ingram used a phage display to screen large peptide libraries to identify peptides that bind to BDNF or NGF. The peptides were also assessed for their ability to modulate BDNF-TrkB and NGF-TrkA activity. From this screen, several peptides were identified to modulate BDNF-TrkB and NGF-TrkA binding both as agonists and antagonists. To truly test for their activity, PC12 cells were used, and the peptides were incubated with high or low concentrations of BDNF and NGF to assess whether the peptides would identify as agonists or antagonists. All in vitro experiments were carried out by myself in the Deinhardt lab.

The in vitro experiments were carried out to test for the biological efficacy of the lead peptides identified by Dr Ingram. Using PC12 cells, cell differentiation was assessed, whereby, activating to blocking differentiation would mean the peptides are able to influence the MAPK downstream pathway. From the 13 peptides screened, two NGF-interacting peptides, JI.5.55C and JI.5.58 show agonist potential to induce differentiation to the same degree as high NGF concentrations and potentially one BDNF peptide, JI.5.23.5, shows an agonist trend in inducing differentiation when incubated with low concentrations of BDNF. None of the peptides showed a trend for antagonist activity.

This experiment highlights the potential in developing peptides to mimic the effect of BDNF and NGF, at the preliminary stage, these peptides provide the foundation of possible ways to target neurotrophic signalling via MAPK signalling.

In order to understand the true agonists effects of these peptides, further analysis is required. NGF is known to mediate survival of sympathetic and sensory neurons as they innervate their target tissue[245]. Such assay would entail growing NGF-dependent neurons, such as DRG and supplementing the media with the synthesised minimal concentrations of NGF and the NGF-interacting peptides. If the neurons survive, it would mean the peptides are able to boost or at least mimic NGF survival signals. It would also be important to look at genes induced by both NGF and BDNF-binding peptides. This can be done via Western Blotting or IHC staining of IEGs. The fluorescence intensity of Arc can be measured upon peptides treatment pre-incubated with low concentrations of growth factors and compared against 50-100 ng/ml concentration of NGF or BDNF and the low concentration of neurotrophin alone. If results show the peptides can IEGs to the same degree as high concentrations of treatment and signals above the low concentration of neurotrophin, then these peptides could be used as signal boosters of neuronal growth and survival in disease states where concentrations of NGF and BDNF are depleted; such in the case of Alzheimer's disease and other dementias[246–248].

In addition to the above experiments, penetration through the BBB needs to also be considered. Accessing the BBB is a greatest challenge for drug delivery[249]. To briefly highlight, only small hydrophobic compounds, <500 Da, are able to diffuse across the endothelium membrane and the diffusion of polar molecules requires specific transporters[249]. The current synthesised peptides exceed above 500 Da, therefore, access to the BBB via protein shuttles needs to be considered. The variety of protein shuttles are receptors expressed on the brain endothelium and include apolipoproteins, receptor-associated protein and transferrin[249]. Here two things need to be considered: the first is whether the expression of these receptors alter in disease and secondly, considering these 'transporters' are in fact receptors, the synthesised peptides will need to compete with their endogenous ligand counterparts. Thus, even after successfully synthesising peptides that efficiently boost neurotrophic signals, additional research needs to be carried out as to how

these potential peptides can be delivered and penetrate through the layers of cells, to neural tissue and boost the depleted neurotrophic signals.

7 Conclusion

In this research project, I have investigated whether BDNF can signal over long distances to induce IEGs responsible for synaptic strengthening. In doing so, I have also unravelled other cellular processes which are crucial for BDNF signal relay that are altered in Tau^{P301L}-expressing cells. The table below summaries the findings during this research project as well as the unanswered questions. The following sections within this discussion chapter will focus on the various mechanisms needed for successful long-distance BDNF.

Altered Mechanism	**Is this mechanism compromised in Tau^{P301L}-expressing cells?**
Axonal transport	YES
TrkB receptor expression	YES
BDNF local signalling	YES
BDNF long-distance signalling	YES (*more data needed)*
Future directions	
Changes in the synthesis of mature BDNF	Unknown
The balance between proBDNF and mature BDNF	Unknown
p75 receptor expression	Unknown
Altered BDNF mRNA location	Unknown
Changes in the amount of TrkB recycling or degradation	Unknown
Number of signalling endosomes, recycling endosomes and lysosomes	Unknown
Changes in the timing of local BDNF signal induction	Unknown
Can reversing axonal transport deficits help restore any failed mechanisms?	Unknown

Table 7-1 Summary of mechanisms investigated during this research project and future questions.

7.1 BDNF signal relay

The diagram below summaries what was reviewed in the above sections and also attempts to illustrate the number of different processes that impact the likelihood of successful BDNF signal propagation.

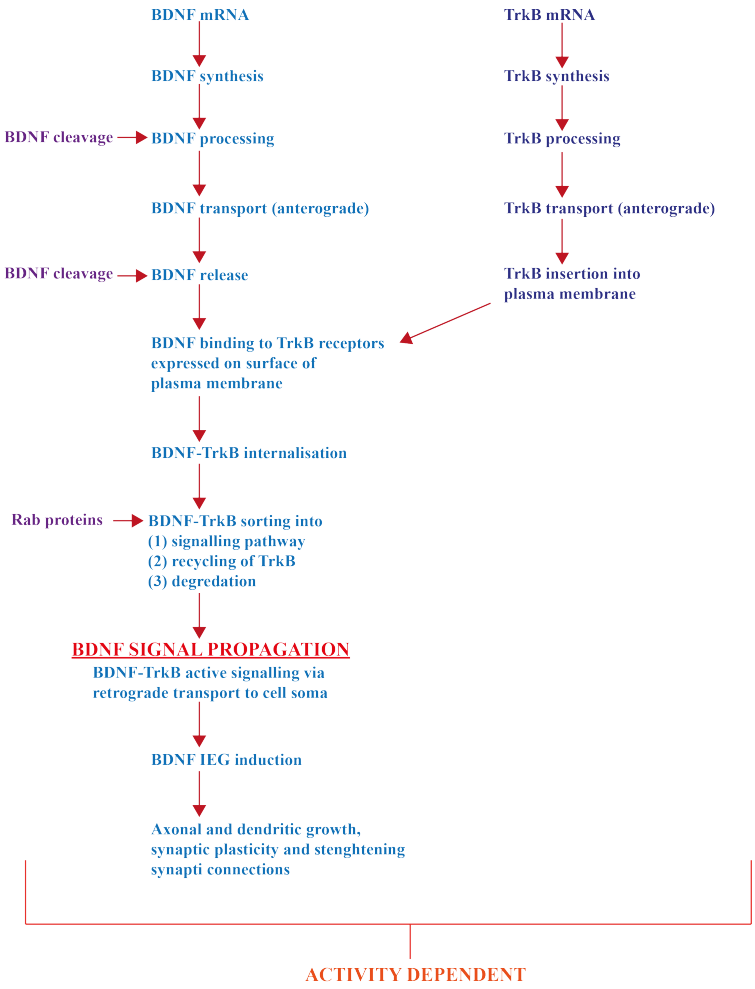

Figure 7-1 Schematic highlighting mechanism behind successful BDNF signal relay. Blue text represents processes behind BDNF regulation, from synthesis to signalling (left-hand side). Dark blue text represented processes behind TrkB regulation from synthesis to expression. Purple text represents the two mechanisms that regulate BDNF processing and BDNF-TrkB signalling. Both the BDNF and TrkB mechanisms are activity dependent.

7.1.1 BDNF signal disruption

From the results shown in this research project, it is clear that there is a signalling disruption in Tau^{P301L}-expressing cells, as upon local stimulation, Arc is not induced (Figure 5-8) . Previous studies have already shown Arc to be induced within 2 hours of BDNF application[89]. Therefore, seeing that local induction is not achieved in Tau^{P301L}-expressing cells suggests that the signalling cascade could be disrupted. However, the reasons behind this result could be one of two, or a combination of both:

1. BDNF local signalling is disrupted in Tau^{P301L}-expressing cells, however, induction is still possible, but just slower than normal, taking more time to induce Arc.
    a. The reason for this could be attributed to transport defects within the somato-dendritic compartment, where microtubules are organised in a bi-directional manner.
2. There is an issue with in signal coding within Tau^{P301L}-expressing cells which means Arc induction takes long or is completely unsuccessful.

The first options could be a possibility, however, TrkB receptors are also expressed along the surface of the cell soma as well as proximal dendrites, therefore, signals do not need to travel large distances to reach the soma, if signal activation occurs at the soma. Further experiments need to be conducted to assess this option. For instance, other timepoints can be investigated to see if Arc is induced at later timepoints, for instance at 4, 6 and 8 hours after BDNF application at cell soma. Another experiment could be using live-cell imaging techniques to assess CAMKII activity, a well-known BDNF downstream signalling mediator[146,250,251]. The Schuman lab have created a destabilised GFP (dGFP) CAMKII probe to visualise local protein synthesis. This probe can be co-transfected in hippocampal cells with either RFP-Tau^{P301L} or RFP alone as control[252]. Using microfluidic devices in the same manner to visualise Arc induction, BDNF could be applied locally, within the cell body channel, or distally at axonal ends within the axonal channel. The use of dGFP bound

to CAMKII means, there is less background noise as dGFP has a shorter half-life, meaning any signal visualised is attributed to CAMKII induction.

Other probes can also be utilised such as fluorescence resonance energy transfer (FRET)-based sensors. Two examples are an Erk sensor[253] and a Grb2 sensor[254]. According to the authors, the Erk activity sensor, EKAR (extracellular signal-regulated kinase activity reporter), is correlated with Erk phosphorylation and is induced in both dendrites and nucleus of hippocampal pyramidal neurons in brain slices works[253]. The second sensors are Grb2, which is a mediator of BDNF signalling. It works by interacting with SH2 domain and initiates Ras signalling leading to MAPK activation[66]. Both of these were tested in our lab as a secondary measure to Arc immunofluorescence signalling, however, upon BDNF application, the FRET sensors were not robust enough to carry out further experiments (data not shown). Since then, the release of the EKAR sensor, other research groups have optimised this sensor to improve the FRET signal by modifying the fluorophores and the linkers between substrate and binding domain[255]. In particular, this group narrowed down the optimal combination of the best FRET pairs, which includes CeruleanFP and mTurquoise as donors and Cp-Venus and Cp-Venus-Venus as acceptors. Therefore, this adapted probe could be used to see if Erk signalling is induced upon BDNF application to cell soma of Tau^{P301L}-expressing cells.

7.1.2 Signal coding – is it corrupt in disease?

From the signalling results presented in this research project, it is apparent change in BDNF signalling, as Arc induction is not observed upon local application of BDNF to cell soma of Tau^{P301L}-expressing cells. This raises the question as to whether these Tau^{P301L}-expressing cells are still capable of decoding signalling and inducing IEGs.

In order to investigate this, the first thing which need to be determined is whether the three classical pathways (MAPK, PLCγ & PI3K) are induced and detectable in Tau^{P301L}-expressing cells. One method of investigating this is already mentioned in the previous section, utilising live probes for Erk and Grb2. Another method would be to utilise

Western blot analysis or RT-PCR. Using microfluidic devices, Dr Joanna Bailey from our lab has successfully extracted RNA and quantified gene induction using RT-PCR. In this experiment, BDNF was applied both at cell soma, or at axonal ends, where Arc induction was is seen within hours of BDNF application, therefore demonstrating both local and long-distance signalling in healthy hippocampal cells. A similar method can be applied where hippocampal murine cells are electroporated to express the Tau^{P301L} mutation. These cells can be seeded in cell culture plates, where BDNF can be applied directly on top of cells for local stimulation, or in microfluidic devices, where BDNF can be applied to distal axons to assess long-distance signalling. Using this method, RNA can be extracted or cell lysates for Western blot analysis can be harvested. This would allow us to decipher firstly, if immediate downstream signals are being activated and relayed locally or over-long distances. Thereafter, IEG induction can be determined in a similar manner. Therefore, one of four scenario is possible:

1. Local signalling: There are issues in activating the signalling cascade.
2. Long-distance signalling: The immediate signals are being activated in distal axons and relayed from the distal axon to the soma, but IEGs are not induced. This would mean BDNF signal relay is **independent** of any axonal transport deficits.
3. Long-distance signalling: The immediate signals (e.g. the MAPK pathway) are being activated at distal regions, at the site of TrkB, BDNF activation, but not relayed back to cell soma for IEGs induction. This would mean BDNF signal relay is **dependent** axonal transport deficits.

7.1.2.1 Signal decoding issues in other diseases

Briefly looking into other diseases where signal encoding is disrupted, Wolcott-Rallison syndrome (WRS) is an extremely rare autosomal recessive disorder where the gene translation via eiF2 is disrupted resulting in impaired or abolished PERK expression. WRS patients therefore some clinical symptoms include infantile diabetes, mental retardation and developmental delays as well as bone dysplasia[256]. Looking into WRS and other diseases where gene expression in altered, very little can be done to overcome this. Therefore, further analysis needs to be carried out in order to fully understand the extent behind BDNF signalling failures in Tau^{P301L}-expressing cells.

Having seen disrupted local signalling within Tau^{P301L}-expressing cells, it is no surprise that long-distance signalling will be unsuccessful. Bearing in mind the small n-number for long-distance signalling in GFP-expressing cells, a comparison cannot be made for long-distance BDNF signalling in Tau^{P301L}-expressing cells, however, what can be seen from the quantification is Arc induction in long-distance signalling and local signalling in Tau^{P301L}-expressing cells is indifferent. This result also highlights the some of the challenges working with microfluidic devices. Although a great platform to investigate long-distance signalling, whereby axonal ends can be fluidically isolated from cell soma, the throughput is very low and each technique needs to be separately optimised, from IHC, Western blot, RNA extraction, live cell imaging and even transfections and electroporation. In this sense, this platform can be challenging. The optimisation of each technique can be extremely time consuming, however, once optimised, the results are extremely valuable. As it stands a microfluidic platform is currently the only method which can be used to investigate long-distance signalling, therefore, further efforts need to be made to overcome experimental challenges when investigating BDNF signalling as well as other experiments which requires compartmentalised, fluidically-isolated region.

Appendix A List of buffer recipes

50X TAE

Ingredient	Amount	Final Concentration
Tris Base	242 g	
Glacial Acetic Acid	57.1 ml	2 M
EDTA	37.5 g	0.05 M
Water	To 1 L	
Adjusted to pH 8.3		

10X TBS

Ingredient	Amount	Final Concentration
Tris Base	24.22 g	100 mM
NaCl	163.6 g	1.4 M
H_2O	Up to 2 L	

PBS

Ingredient	Amount	Final Concentration
NaCl	8g	
KCl	0.2g	
Na_2HPO_4	1.44g	
$KH2PO_4$	0.24g	
H_2O	Up to 1L	

Appendix A

LB broth

Ingredient	Amount	Final Concentration
NaCl	5g	1%
Tryptome	5g	1%
Yeast Extract	2.5g	0.5%
H_2O	Up to 500 ml	

LB agar

Ingredient	Amount	Final Concentration
LB broth	500 ml	
Agar	7.5g	1.5%

Mowiol

Ingredient	Amount	Final Concentration
Mowiol 4-88	2.4 g	
Glycerol	6 mL	
0.2 M Tris-Cl pH 8.5	12 mL	0.1 M
H_2O	6 mL	

Lameeli Buffer

Ingredient	Amount	Final Concentration
Mowiol 4-88	2.4 g	
Glycerol	6 mL	
0.2 M Tris-Cl pH 8.5	12 mL	0.1 M
H_2O	6 mL	

Stock of Transfer Buffer

Ingredient	Amount	Final Concentration
100% Methanol	100 mL	10X
Glycerol	6 mL	
0.2 M Tris-Cl pH 8.5	12 mL	0.1 M
H_2O	6 mL	

Working Recipe for Transfer Buffer

Ingredient	Amount	Final Concentration
100% Methanol	100 mL	10%
Transfer Buffer	100 m L	10%
H_2O	Up to 1 L	

5x Sample Buffer

Ingredient	Amount	Final Concentration
Tris pH 6.8	2.12 g	350 mM
Glycerol	15 mL	30%
10 % SDS	5 mL	
DTT	4.63 g	600 mM
BPB	0.006 g	0.012%

Appendix A

SDS-PAGE Gel

Ingredients	**8%**	**10%**	**15%**	**Stacking**
1.5M Tris pH 8.8	3mL	3mL		
0.5M Tris pH 6.8 with 0.4% SDS				1mL
30% Acrylamide	3.2mL	4mL		0.5mL
ddH_2O	5.8uL	5mL		2.5uL
TEMED *(N,N,N′,N′*-tetramethylethylenediamine)	12uL	24uL		4uL
10% Ammonium persulfate (APS)	120uL	120uL		40uL

Appendix B MATLAB Scripts

```
controlbase=prctile(control,10);
controlzero=control-controlbase;
max=max(controlzero);
include=max<245;
controlzero2=controlzero(:,include);
deviation=std(controlzero2);
mean=mean(deviation);
logicctl=controlzero>5*mean;
sumcontrol=sum(logicctl);
[n,x]=size(control);
percentagecontrol=sumcontrol/n;
finalcontrol=sum(percentagecontrol>0.1)/x*100;

expbase=prctile(exp,10);
expzero=exp-expbase;
logicexp=expzero>5*mean;
sumexp=sum(logicexp);
[m,y]=size(exp);
percentageexp=sumexp/m;
finalexp=sum(percentageexp>0.1)/y*100;
```

Figure 7-2 MATLAB script to calculate the percentage of axon containing aggregates.

List of References

1. Barbacid, M. Neurotrophic factors and their receptors. *Current Opinion in Cell Biology* **7**, 148–155 (1995).

2. Chao, M. V. & Bothwell, M. Neurotrophins. *Neuron* **33**, 9–12 (2002).

3. Dechant, G., Rodríguez-Tébar, A. & Barde, Y.-A. Neurotrophin receptors. *Progress in Neurobiology* **42**, 347–352 (1994).

4. Lindsay, R. M., Wiegand, S. J., Anthony Altar, C. & DiStefano, P. S. Neurotrophic factors: from molecule to man. *Trends Neurosci.* **17**, 182–190 (1994).

5. Patapoutian, A. & Reichardt, L. F. Trk receptors: mediators of neurotrophin action. *Curr. Opin. Neurobiol.* **11**, 272–280 (2001).

6. Blum, R. & Konnerth, A. Neurotrophin-mediated rapid signaling in the central nervous system: mechanisms and functions. *Physiology (Bethesda)*. **20**, 70–78 (2005).

7. Chen, X. *et al.* A chemical-genetic approach to studying neurotrophin signaling. *Neuron* **46**, 13–21 (2005).

8. Chaldakov, G. N., Tonchev, A. B. & Aloe, L. NGF and BDNF: from nerves to adipose tissue, from neurokines to metabokines. *Riv. Psichiatr.* **44**, 79–87 (2009).

9. Deinhardt, K. & Jeanneteau, F. More Than Just an OFF-Switch: The Essential Role of Protein Dephosphorylation in the Modulation of BDNF Signaling Events. in *Protein Phosphorylation in Human Health* (InTech, 2012). doi:10.5772/50420

10. Cohen, S., Levi-Montalcini, R. & Hamburger, V. A Nerve Growth-Stimulating Factor Isolated from Sarcom as 37 and 18. *Proc. Natl. Acad. Sci.* **40**, 1014–1018 (1954).

11. Levi-Montalcini, R. & Hamburger, V. Selective growth stimulating effects of mouse sarcoma on the sensory and sympathetic nervous system of the chick embryo. *J. Exp. Zool.* **116**, 321–61 (1951).

12. Grimes, M. L. *et al.* Endocytosis of activated TrkA: evidence that nerve growth

factor induces formation of signaling endosomes. *J. Neurosci.* **16**, 7950–7964 (1996).

13. Davies, A. M. The neurotrophic hypothesis: where does it stand? *Philos. Trans. R. Soc. Lond. B. Biol. Sci.* **351**, 389–94 (1996).

14. Riccio, A., Pierchala, B. A., Ciarallo, C. L. & Ginty, D. D. An NGF-TrkA-mediated retrograde signal to transcription factor CREB in sympathetic neurons. *Science* **277**, 1097–100 (1997).

15. Huang, E. J. & Reichardt, L. F. Neurotrophins: roles in neuronal development and function. *Annu. Rev. Neurosci.* **24**, 677–736 (2001).

16. Robertson, R. T., Baratta, J., Yu, J. & Guthrie, K. M. A role for neurotrophin-3 in targeting developing cholinergic axon projections to cerebral cortex. *Neuroscience* **143**, 523–539 (2006).

17. Friedman, W. J., Black, I. B. & Kaplan, D. R. Distribution of the neurotrophins brain-derived neurotrophic factor, neurotrophin-3, and neurotrophin-4/5 in the postnatal rat brain: an immunocytochemical study. *Neuroscience* **84**, 101–14 (1998).

18. Vigers, A. J., Baquet, Z. C. & Jones, K. R. Expression of neurotrophin-3 in the mouse forebrain: insights from a targeted LacZ reporter. *J. Comp. Neurol.* **416**, 398–415 (2000).

19. Kuruvilla, R. *et al.* A neurotrophin signaling cascade coordinates sympathetic neuron development through differential control of TrkA trafficking and retrograde signaling. *Cell* **118**, 243–255 (2004).

20. Xie, C. W. *et al.* Deficient long-term memory and long-lasting long-term potentiation in mice with a targeted deletion of neurotrophin-4 gene. *Proc. Natl. Acad. Sci. U. S. A.* **97**, 8116–21 (2000).

21. Runge, E. M., Hoshino, N., Biehl, M. J., Ton, S. & Rochlin, M. W. Neurotrophin-4 is more potent than brain-derived neurotrophic factor in promoting, attracting and suppressing geniculate ganglion neurite outgrowth. *Dev. Neurosci.* **34**, 389–401 (2012).

22. Lessmann, V., Gottmann, K. & Heumann, R. BDNF and NT-4/5 enhance

glutamatergic synaptic transmission in cultured hippocampal neurones. *Neuroreport* **6**, 21–5 (1994).

23. Ip, N. Y. *et al.* Mammalian neurotrophin-4: structure, chromosomal localization, tissue distribution, and receptor specificity. *Proc. Natl. Acad. Sci. U. S. A.* **89**, 3060–3064 (1992).

24. Fan, G. *et al.* Knocking the NT4 gene into the BDNF locus rescues BDNF deficient mice and reveals distinct NT4 and BDNF activities. *Nat. Neurosci.* **3**, 350–7 (2000).

25. Barde, Y. A., Edgar, D. & Thoenen, H. Purification of a new neurotrophic factor from mammalian brain. *EMBO J.* **1**, 549–53 (1982).

26. Kuczewski, N., Porcher, C., Lessmann, V., Medina, I. & Gaiarsa, J.-L. Activity-dependent dendritic release of BDNF and biological consequences. *Mol. Neurobiol.* **39**, 37–49 (2009).

27. Lu, H., Park, H. & Poo, M.-M. Spike-timing-dependent BDNF secretion and synaptic plasticity. *Philos. Trans. R. Soc. Lond. B. Biol. Sci.* **369**, 20130132 (2014).

28. Deinhardt, K. & Chao, M. V. Shaping neurons: Long and short range effects of mature and proBDNF signalling upon neuronal structure. *Neuropharmacology* **76**, 603–609 (2014).

29. Zheng, F., Luo, Y. & Wang, H. Regulation of BDNF-mediated transcription of immediate early gene Arc by intracellular calcium and calmodulin. *J. Neurosci. Res.* **87**, 380–392 (2009).

30. Pencea, V., Bingaman, K. D., Wiegand, S. J. & Luskin, M. B. Infusion of brain-derived neurotrophic factor into the lateral ventricle of the adult rat leads to new neurons in the parenchyma of the striatum, septum, thalamus, and hypothalamus. *J. Neurosci.* **21**, 6706–17 (2001).

31. Danzer, S. C., Crooks, K. R. C., Lo, D. C. & McNamara, J. O. Increased expression of brain-derived neurotrophic factor induces formation of basal dendrites and axonal branching in dentate granule cells in hippocampal explant cultures. *J. Neurosci.* **22**, 9754–63 (2002).

32. Aid, T., Kazantseva, A., Piirsoo, M., Palm, K. & Timmusk, T. Mouse and rat BDNF

gene structure and expression revisited. *J. Neurosci. Res.* **85**, 525–35 (2007).

33. Cheng, P.-L. *et al.* Self-amplifying autocrine actions of BDNF in axon development. *Proc. Natl. Acad. Sci. U. S. A.* **108**, 18430–5 (2011).

34. Egan, M. F. *et al.* The BDNF val66met polymorphism affects activity-dependent secretion of BDNF and human memory and hippocampal function. *Cell* **112**, 257–269 (2003).

35. Anastasia, A. *et al.* Val66Met polymorphism of BDNF alters prodomain structure to induce neuronal growth cone retraction. *Nat. Commun.* **4**, 2490 (2013).

36. Koshimizu, H. *et al.* Multiple functions of precursor BDNF to CNS neurons: negative regulation of neurite growth, spine formation and cell survival. *Mol. Brain* **2**, 27 (2009).

37. Hempstead, B. L. Brain-Derived Neurotrophic Factor: Three Ligands, Many Actions. *Trans. Am. Clin. Climatol. Assoc.* **126**, 9–19 (2015).

38. Teng, K. K., Felice, S., Kim, T. & Hempstead, B. L. Understanding proneurotrophin actions: Recent advances and challenges. *Developmental Neurobiology* **70**, 350–359 (2010).

39. Yang, J. *et al.* ProBDNF Negatively Regulates Neuronal Remodeling, Synaptic Transmission, and Synaptic Plasticity in Hippocampus. *Cell Rep.* **7**, 796–806 (2014).

40. Hosang, G. M., Shiles, C., Tansey, K. E., McGuffin, P. & Uher, R. Interaction between stress and the BDNF Val66Met polymorphism in depression: A systematic review and meta-analysis. *BMC Med.* **12**, 7 (2014).

41. Strube, W. *et al.* BDNF-Val66Met-polymorphism impact on cortical plasticity in schizophrenia patients: A proof-of-concept study. *Int. J. Neuropsychopharmacol.* **18**, 1–11 (2014).

42. Chen, Z.-Y. *et al.* Variant Brain-Derived Neurotrophic Factor (BDNF) (Met66) Alters the Intracellular Trafficking and Activity-Dependent Secretion of Wild-Type BDNF in Neurosecretory Cells and Cortical Neurons. *J. Neurosci.* **24**, 4401–4411 (2004).

43. Deinhardt, K. *et al.* Neuronal Growth Cone Retraction Relies on Proneurotrophin Receptor Signaling Through Rac. *Sci. Signal.* **4**, ra82–ra82 (2011).

44. Thomas, K. & Davies, A. Neurotrophins: A ticket to ride for BDNF. *Current Biology* **15**, R262–R264 (2005).

45. Cunha, C., Brambilla, R. & Thomas, K. L. A simple role for BDNF in learning and memory? *Front. Mol. Neurosci.* **3**, 1 (2010).

46. Wong, Y.-H., Lee, C.-M., Xie, W., Cui, B. & Poo, M. Activity-dependent BDNF release via endocytic pathways is regulated by synaptotagmin-6 and complexin. *Proc. Natl. Acad. Sci. U. S. A.* **112**, E4475-84 (2015).

47. Dean, C. *et al.* Synaptotagmin-IV modulates synaptic function and long-term potentiation by regulating BDNF release. *Nat. Neurosci.* **12**, 767–76 (2009).

48. Lodish, H. *et al.* Overview of the Secretory Pathway. in *Molecular Cell Biology* (W. H. Freeman, 2000). doi:NBK21471

49. Lin, W. J. & Salton, S. The regulated secretory pathway and human disease: insights from gene variants and single nucleotide polymorphisms. *Front. Endocrinol. (Lausanne).* **4**, 96 (2013).

50. Barrett, G. L. & Bartlett, P. F. The p75 nerve growth factor receptor mediates survival or death depending on the stage of sensory neuron development. *Proc. Natl. Acad. Sci. U. S. A.* **91**, 6501–5 (1994).

51. Roux, P. P. & Barker, P. A. Neurotrophin signaling through the p75 neurotrophin receptor. *Prog. Neurobiol.* **67**, 203–33 (2002).

52. Beattie, M. S. *et al.* ProNGF induces p75-mediated death of oligodendrocytes following spinal cord injury. *Neuron* **36**, 375–86 (2002).

53. Reichardt, L. F. Neurotrophin-regulated signalling pathways. *Philos. Trans. R. Soc. Lond. B. Biol. Sci.* **361**, 1545–1564 (2006).

54. Mizui, T., Tanima, Y., Komatsu, H., Kumanogoh, H. & Kojima, M. The Biological Actions and Mechanisms of Brain-Derived Neurotrophic Factor in Healthy and Disordered Brains. *Neurosci. & Med.* **05**, 183–195 (2014).

55. Howe, C. L., Valletta, J. S., Rusnak, A. S. & Mobley, W. C. NGF signaling from clathrin-coated vesicles: evidence that signaling endosomes serve as a platform for the Ras-MAPK pathway. *Neuron* **32**, 801–14 (2001).

56. Zheng, J. *et al.* Clathrin-dependent endocytosis is required for TrkB-dependent Akt-mediated neuronal protection and dendritic growth. *J. Biol. Chem.* **283**, 13280–13288 (2008).

57. Deinhardt, K. *et al.* Rab5 and Rab7 control endocytic sorting along the axonal retrograde transport pathway. *Neuron* **52**, 293–305 (2006).

58. Stenmark, H. & Olkkonen, V. M. The Rab GTPase family. *Genome Biol.* **2**, REVIEWS3007 (2001).

59. Valdez, G. *et al.* Pincher-mediated macroendocytosis underlies retrograde signaling by neurotrophin receptors. *J. Neurosci.* **25**, 5236–5247 (2005).

60. Poon, W. W. *et al.* B-Amyloid impairs axonal BDNF retrograde trafficking. *Neurobiol. Aging* **32**, 821–833 (2011).

61. Huang, E. J. & Reichardt, L. F. Trk receptors: roles in neuronal signal transduction. *Annu. Rev. Biochem.* **72**, 609–642 (2003).

62. Manning, B. & Cantley, L. AKT/PKB Signalling: Navigating Downstream. *Cell* **129**, 1261–1274 (2007).

63. Qian, X., Riccio, A., Zhang, Y. & Ginty, D. D. Identification and characterization of novel substrates of Trk receptors in developing neurons. *Neuron* **21**, 1017–1029 (1998).

64. Murray, P. S. & Holmes, P. V. An overview of brain-derived neurotrophic factor and implications for excitotoxic vulnerability in the hippocampus. *Int. J. Pept.* **2011**, 654085 (2011).

65. Slutsky, A. B. & Etnier, J. L. Caloric restriction, physical activity, and cognitive performance: A review of evidence and a discussion of the potential mediators of BDNF and TrkB. *International Journal of Sport and Exercise Psychology* 1–17 (2016). doi:10.1080/1612197X.2016.1223422

66. Deinhardt, K. & Chao, M. V. *Neurotrophic Factors*. *Handbook of experimental*

pharmacology **220**, (Springer Berlin Heidelberg, 2014).

67. Franke, T. F., Hornik, C. P., Segev, L., Shostak, G. A. & Sugimoto, C. PI3K/Akt and apoptosis: size matters. *Oncogene* **22**, 8983–8998 (2003).

68. Tsurutani, J., West, K. A., Sayyah, J., Gills, J. J. & Dennis, P. A. Inhibition of the phosphatidylinositol 3-kinase/Akt/mammalian target of rapamycin pathway but not the MEK/ERK pathway attenuates laminin-mediated small cell lung cancer cellular survival and resistance to imatinib mesylate or chemotherapy. *Cancer Res.* **65**, 8423–32 (2005).

69. Roux, P. P. & Blenis, J. ERK and p38 MAPK-activated protein kinases: a family of protein kinases with diverse biological functions. *Microbiol. Mol. Biol. Rev.* **68**, 320–44 (2004).

70. Morrison, D. K. MAP kinase pathways. *Cold Spring Harb. Perspect. Biol.* **4**, (2012).

71. McPherson, P. S. *et al.* A presynaptic inositol-5-phosphatase. *Nature* **379**, 353–7 (1996).

72. Segal, R. A. & Greenberg, M. E. Intracellular signaling pathways activated by neurotrophic factors. *Annu. Rev. Neurosci.* **19**, 463–89 (1996).

73. Thomas, G. M. & Huganir, R. L. MAPK cascade signalling and synaptic plasticity. *Nat. Rev. Neurosci.* **5**, 173–83 (2004).

74. Bozon, B. *et al.* MAPK, CREB and zif268 are all required for the consolidation of recognition memory. *Philos. Trans. R. Soc. Lond. B. Biol. Sci.* **358**, 805–14 (2003).

75. Orban, P. C., Chapman, P. F. & Brambilla, R. Is the Ras-MAPK signalling pathway necessary for long-term memory formation? *Trends Neurosci.* **22**, 38–44 (1999).

76. English, J. D. & Sweatt, J. D. A requirement for the mitogen-activated protein kinase cascade in hippocampal long term potentiation. *J. Biol. Chem.* **272**, 19103–6 (1997).

77. Su, C., Underwood, W., Rybalchenko, N. & Singh, M. ERK1/2 and ERK5 have distinct roles in the regulation of brain-derived neurotrophic factor expression. *J. Neurosci. Res.* **89**, 1542–50 (2011).

78. Regan, C. P. *et al.* Erk5 null mice display multiple extraembryonic vascular and embryonic cardiovascular defects. *Proc. Natl. Acad. Sci. U. S. A.* **99**, 9248–53 (2002).

79. Wang, X. & Tournier, C. Regulation of cellular functions by the ERK5 signalling pathway. *Cell. Signal.* **18**, 753–60 (2006).

80. Watson, F. L. *et al.* Neurotrophins use the Erk5 pathway to mediate a retrograde survival response. *Nat. Neurosci.* **4**, 981–988 (2001).

81. Lin, S. Y. *et al.* BDNF acutely increases tyrosine phosphorylation of the NMDA receptor subunit 2B in cortical and hippocampal postsynaptic densities. *Brain Res. Mol. Brain Res.* **55**, 20–7 (1998).

82. Leal, G., Afonso, P. M., Salazar, I. L. & Duarte, C. B. Regulation of hippocampal synaptic plasticity by BDNF. *Brain Res.* (2014). doi:10.1016/j.brainres.2014.10.019

83. Yamada, M. *et al.* Distinct usages of phospholipase C gamma and Shc in intracellular signaling stimulated by neurotrophins. *Brain Res.* **955**, 183–90 (2002).

84. Gu, X. & Spitzer, N. C. Distinct aspects of neuronal differentiation encoded by frequency of spontaneous Ca2+ transients. *Nature* **375**, 784–7 (1995).

85. Guzowski, J. F., Setlow, B., Wagner, E. K. & McGaugh, J. L. Experience-dependent gene expression in the rat hippocampus after spatial learning: a comparison of the immediate-early genes Arc, c-fos, and zif268. *J. Neurosci.* **21**, 5089–98 (2001).

86. Ying, S.-W. *et al.* Brain-derived neurotrophic factor induces long-term potentiation in intact adult hippocampus: requirement for ERK activation coupled to CREB and upregulation of Arc synthesis. *J. Neurosci.* **22**, 1532–1540 (2002).

87. Link, W. *et al.* Somatodendritic expression of an immediate early gene is regulated by synaptic activity. *Proc. Natl. Acad. Sci. U. S. A.* **92**, 5734–8 (1995).

88. Steward, O., Wallace, C. S., Lyford, G. L. & Worley, P. F. Synaptic activation causes the mRNA for the IEG Arc to localize selectively near activated postsynaptic sites on dendrites. *Neuron* **21**, 741–51 (1998).

89. Yin, Y., Edelman, G. M. & Vanderklish, P. W. The brain-derived neurotrophic factor enhances synthesis of Arc in synaptoneurosomes. *Proc. Natl. Acad. Sci. U. S.*

A. **99**, 2368–73 (2002).

90. Lyford, G. L. *et al.* Arc, a growth factor and activity-regulated gene, encodes a novel cytoskeleton-associated protein that is enriched in neuronal dendrites. *Neuron* **14**, 433–45 (1995).

91. Waltereit, R. *et al.* Arg3.1/Arc mRNA induction by Ca2+ and cAMP requires protein kinase A and mitogen-activated protein kinase/extracellular regulated kinase activation. *J. Neurosci.* **21**, 5484–93 (2001).

92. Sano, K., Nanba, H., Tabuchi, A., Tsuchiya, T. & Tsuda, M. BDNF gene can Be activated by Ca2+ signals without involvement of de novo AP-1 synthesis. *Biochem. Biophys. Res. Commun.* **229**, 788–93 (1996).

93. Bading, H., Ginty, D. D. & Greenberg, M. E. Regulation of gene expression in hippocampal neurons by distinct calcium signaling pathways. *Science* **260**, 181–6 (1993).

94. Imamura, L. *et al.* Repression of activity-dependent c-fos and brain-derived neurotrophic factor mRNA expression by pyrethroid insecticides accompanying a decrease in Ca(2+) influx into neurons. *J. Pharmacol. Exp. Ther.* **295**, 1175–82 (2000).

95. Pizzorusso, T., Ratto, G. M., Putignano, E. & Maffei, L. Brain-derived neurotrophic factor causes cAMP response element-binding protein phosphorylation in absence of calcium increases in slices and cultured neurons from rat visual cortex. *J. Neurosci.* **20**, 2809–16 (2000).

96. Anokhin, K. V, Mileusnic, R., Shamakina, I. Y. & Rose, S. P. Effects of early experience on c-fos gene expression in the chick forebrain. *Brain Res.* **544**, 101–7 (1991).

97. Lau, L. F. & Nathans, D. Expression of a set of growth-related immediate early genes in BALB/c 3T3 cells: coordinate regulation with c-fos or c-myc. *Proc. Natl. Acad. Sci. U. S. A.* **84**, 1182–6 (1987).

98. Saffen, D. W. *et al.* Convulsant-induced increase in transcription factor messenger RNAs in rat brain. *Proc. Natl. Acad. Sci. U. S. A.* **85**, 7795–9 (1988).

99. Reis, R. A. M. *et al.* Sympathetic neuronal survival induced by retinal trophic factors. *J. Neurobiol.* **50**, 13–23 (2002).

100. Jones, M. W. *et al.* A requirement for the immediate early gene Zif268 in the expression of late LTP and long-term memories. *Nat. Neurosci.* **4**, 289–96 (2001).

101. Sgambato, V., Pagès, C., Rogard, M., Besson, M. J. & Caboche, J. Extracellular signal-regulated kinase (ERK) controls immediate early gene induction on corticostriatal stimulation. *J. Neurosci.* **18**, 8814–25 (1998).

102. Markham, a., Bains, R., Franklin, P. & Spedding, M. Changes in mitochondrial function are pivotal in neurodegenerative and psychiatric disorders: How important is BDNF? *Br. J. Pharmacol.* **171**, 2206–2229 (2014).

103. Ohira, K. & Hayashi, M. A new aspect of the TrkB signaling pathway in neural plasticity. *Curr. Neuropharmacol.* **7**, 276–285 (2009).

104. Sandhya, V. K. *et al.* A network map of BDNF/TRKB and BDNF/p75NTR signaling system. *J. Cell Commun. Signal.* **7**, 301–307 (2013).

105. Haapasalo, A. *et al.* Regulation of TRKB surface expression by brain-derived neurotrophic factor and truncated TRKB isoforms. *J. Biol. Chem.* **277**, 43160–43167 (2002).

106. Chen, Z.-Y. A Novel Endocytic Recycling Signal Distinguishes Biological Responses of Trk Neurotrophin Receptors. *Mol. Biol. Cell* **16**, 5761–5772 (2005).

107. Hall, J., Thomas, K. L. & Everitt, B. J. Rapid and selective induction of BDNF expression in the hippocampus during contextual learning. *Nat. Neurosci.* **3**, 533–5 (2000).

108. Baxter, G. T. *et al.* Signal transduction mediated by the truncated trkB receptor isoforms, trkB.T1 and trkB.T2. *J. Neurosci.* **17**, 2683–2690 (1997).

109. Prakash, Y. S. & Martin, R. J. Brain-derived neurotrophic factor in the airways. *Pharmacol. Ther.* **143**, 74–86 (2014).

110. Yanpallewar, S. U., Barrick, C. A., Buckley, H., Becker, J. & Tessarollo, L. Deletion of the BDNF truncated receptor TrkB.T1 delays disease onset in a mouse model of amyotrophic lateral sclerosis. *PLoS One* **7**, e39946 (2012).

111. Perlson, E. *et al.* A switch in retrograde signaling from survival to stress in rapid-onset neurodegeneration. *J. Neurosci.* **29**, 9903–9917 (2009).

112. Colin, E. *et al.* Huntingtin phosphorylation acts as a molecular switch for anterograde/retrograde transport in neurons. *EMBO J.* **27**, 2124–2134 (2008).

113. Wagner, U., Utton, M., Gallo, J. M. & Miller, C. C. Cellular phosphorylation of tau by GSK-3 beta influences tau binding to microtubules and microtubule organisation. *J. Cell Sci.* **109 (Pt 6**, 1537–1543 (1996).

114. Goldstein, L. S. & Yang, Z. Microtubule-based transport systems in neurons: the roles of kinesins and dyneins. *Annu. Rev. Neurosci.* **23**, 39–71 (2000).

115. Lu, B., Nagappan, G., Guan, X., Nathan, P. J. & Wren, P. BDNF-based synaptic repair as a disease-modifying strategy for neurodegenerative diseases. *Nat. Rev. Neurosci.* **14**, 401–416 (2013).

116. Wong, J. Neurotrophin signaling and Alzheimer' s Disease neurodegeneration - Focus on BDNF / TrkB signaling. *Trends cell Signal. pathways neuronal fate Decis.* 181–194 (2013).

117. Gunawardena, S., Anderson, E. & White, J. Axonal transport and neurodegenerative disease: vesicle-motor complex formation and their regulation. *Degener. Neurol. Neuromuscul. Dis.* **4**, 29 (2014).

118. Lodish, H. *et al. Overview of Neuron Structure and Function*. *Molecular Cell Biology* (W. H. Freeman, 1999).

119. Kevenaar, J. T. & Hoogenraad, C. C. The axonal cytoskeleton: from organization to function. *Front. Mol. Neurosci.* **8**, 44 (2015).

120. Höfflin, F. *et al.* Heterogeneity of the Axon Initial Segment in Interneurons and Pyramidal Cells of Rodent Visual Cortex. *Front. Cell. Neurosci.* **11**, 332 (2017).

121. Akhmanova, A. & Steinmetz, M. O. Control of microtubule organization and dynamics: Two ends in the limelight. *Nature Reviews Molecular Cell Biology* **16**, 711–726 (2015).

122. von Bartheld, C. S. *et al.* Retrograde transport of neurotrophins from the eye to the brain in chick embryos: roles of the p75NTR and trkB receptors. *J. Neurosci.* **16**,

2995–3008 (1996).

123. Harrington, A. W. & Ginty, D. D. Long-distance retrograde neurotrophic factor signalling in neurons. *Nat. Rev. Neurosci.* **14**, 177–87 (2013).

124. Hendry, I. A., Stöckel, K., Thoenen, H. & Iversen, L. L. The retrograde axonal transport of nerve growth factor. *Brain Res.* **68**, 103–21 (1974).

125. Delcroix, J.-D. *et al.* NGF signaling in sensory neurons: evidence that early endosomes carry NGF retrograde signals. *Neuron* **39**, 69–84 (2003).

126. Jeanneteau, F., Deinhardt, K., Miyoshi, G., Bennett, A. M. & Chao, M. V. The MAP kinase phosphatase MKP-1 regulates BDNF-induced axon branching. *Nat. Neurosci.* **13**, 1373–1379 (2010).

127. Miller, F. D. & Kaplan, D. R. On Trk for Retrograde Signaling. *Neuron* **32**, 767–770 (2001).

128. Lodish, Berk & Zipursky. Kinesin, Dynein, and Intracellular Transport. in *Molecular Cell Biology* (W. H. Freeman, 2000).

129. Ishikawa, T. Structural biology of cytoplasmic and axonemal dyneins. *Journal of Structural Biology* **179**, 229–234 (2012).

130. Hook, P. & Vallee, R. B. The dynein family at a glance. *J. Cell Sci.* **119**, 4369–4371 (2006).

131. Ginty, D. D. & Segal, R. a. Retrograde neurotrophin signaling: Trk-ing along the axon. *Curr. Opin. Neurobiol.* **12**, 268–274 (2002).

132. Ma & Chisholm. Cytoplasmic dynein-associated structures move bidirectionally in vivo. *J. Cell Sci.* **115**, 1453–1460 (2002).

133. Ligon, L. A., Tokito, M., Finklestein, J. M., Grossman, F. E. & Holzbaur, E. L. F. A Direct Interaction between Cytoplasmic Dynein and Kinesin I May Coordinate Motor Activity. *J. Biol. Chem.* **279**, 19201–19208 (2004).

134. Adachi, N., Kohara, K. & Tsumoto, T. Difference in trafficking of brain-derived neurotrophic factor between axons and dendrites of cortical neurons, revealed by live-cell imaging. *BMC Neurosci.* **6**, 42 (2005).

135. Altar, C. A. A. & DiStefano, P. S. Neurotrophin trafficking by anterograde transport. *Trends Neurosci.* **21**, 433–437 (1998).

136. Gauthier, L. R. *et al.* Huntingtin controls neurotrophic support and survival of neurons by enhancing BDNF vesicular transport along microtubules. *Cell* **118**, 127–138 (2004).

137. Gross, S. P. *et al.* Interactions and regulation of molecular motors in Xenopus melanophores. *J. Cell Biol.* **156**, 855–865 (2002).

138. Rogers, S. L., Tint, I. S., Fanapour, P. C. & Gelfand, V. I. Regulated bidirectional motility of melanophore pigment granules along microtubules in vitro. *Proc. Natl. Acad. Sci. U. S. A.* **94**, 3720–3725 (1997).

139. Gross, S. P. Hither and yon: a review of bi-directional microtubule-based transport. *Phys. Biol.* **1**, 1–11 (2004).

140. Müller, M. J. I., Klumpp, S. & Lipowsky, R. Tug-of-war as a cooperative mechanism for bidirectional cargo transport by molecular motors. *Proc. Natl. Acad. Sci. U. S. A.* **105**, 4609–14 (2008).

141. Kural, C. *et al.* Kinesin and dynein move a peroxisome in vivo: a tug-of-war or coordinated movement? *Science (80-.).* **308**, 1469–72 (2005).

142. Hendricks, A. G. *et al.* Motor Coordination via a Tug-of-War Mechanism Drives Bidirectional Vesicle Transport. *Curr. Biol.* **20**, 697–702 (2010).

143. Encalada, S. E., Szpankowski, L., Xia, C. H. & Goldstein, L. S. B. Stable kinesin and dynein assemblies drive the axonal transport of mammalian prion protein vesicles. *Cell* **144**, 551–565 (2011).

144. Welte, M. A. Bidirectional transport along microtubules. *Current Biology* **14**, R525-37 (2004).

145. Jolly, A. L. & Gelfand, V. I. Bidirectional intracellular transport: utility and mechanism. *Biochem. Soc. Trans.* **39**, 1126–1130 (2011).

146. Bramham, C. R. & Messaoudi, E. BDNF function in adult synaptic plasticity: The synaptic consolidation hypothesis. *Prog. Neurobiol.* **76**, 99–125 (2005).

147. Hoover, B. R. *et al.* Tau mislocalization to dendritic spines mediates synaptic dysfunction independently of neurodegeneration. *Neuron* **68**, 1067–81 (2010).

148. Allen, S. J., Watson, J. J., Shoemark, D. K., Barua, N. U. & Patel, N. K. GDNF, NGF and BDNF as therapeutic options for neurodegeneration. *Pharmacol. Ther.* **138**, 155–75 (2013).

149. Peng, S. *et al.* Decreased brain-derived neurotrophic factor depends on amyloid aggregation state in transgenic mouse models of Alzheimer's disease. *J. Neurosci.* **29**, 9321–9329 (2009).

150. Chen, Q. *et al.* The cellular distribution and Ser262 phosphorylation of tau protein are regulated by BDNF in vitro. *PLoS One* **9**, (2014).

151. Wszolek, Z. K. *et al.* Frontotemporal dementia and parkinsonism linked to chromosome 17 (FTDP-17). *Orphanet Journal of Rare Diseases* **1**, 30 (2006).

152. Mirra, S. S. *et al.* Tau pathology in a family with dementia and a P301L mutation in tau. *J. Neuropathol. Exp. Neurol.* **58**, 335–45 (1999).

153. Song, L. *et al.* Analysis of tau post-translational modifications in rTg4510 mice, a model of tau pathology. *Mol. Neurodegener.* **10**, 14 (2015).

154. Deters, N., Ittner, L. M. & Götz, J. Divergent phosphorylation pattern of tau in P301L tau transgenic mice. *Eur. J. Neurosci.* **28**, 137–47 (2008).

155. Wu, J. W. *et al.* Small misfolded Tau species are internalized via bulk endocytosis and anterogradely and retrogradely transported in neurons. *J. Biol. Chem.* **288**, 1856–70 (2013).

156. Ramsden, M. *et al.* Age-dependent neurofibrillary tangle formation, neuron loss, and memory impairment in a mouse model of human tauopathy (P301L). *J. Neurosci.* **25**, 10637–47 (2005).

157. Dalby, N. O. *et al.* Altered function of hippocampal CA1 pyramidal neurons in the rTg4510 mouse model of tauopathy. *J. Alzheimers. Dis.* **40**, 429–42 (2014).

158. Campenot, R. B. & MacInnis, B. L. Retrograde transport of neurotrophins: fact and function. *J. Neurobiol.* **58**, 217–29 (2004).

159. Campenot, R. B. Local control of neurite development by nerve growth factor. *Proc. Natl. Acad. Sci. U. S. A.* **74**, 4516–9 (1977).

160. Taylor, A. M. *et al.* A microfluidic culture platform for CNS axonal injury, regeneration and transport. *Nat. Methods* **2**, 599–605 (2005).

161. Taylor, A. M., Dieterich, D. C., Ito, H. T., Kim, S. A. & Schuman, E. M. Microfluidic local perfusion chambers for the visualization and manipulation of synapses. *Neuron* **66**, 57–68 (2010).

162. Millet, L. J. & Gillette, M. U. New perspectives on neuronal development via microfluidic environments. *Trends Neurosci.* **35**, 752–61 (2012).

163. Cohen, M. S., Bas Orth, C., Kim, H. J., Jeon, N. L. & Jaffrey, S. R. Neurotrophin-mediated dendrite-to-nucleus signaling revealed by microfluidic compartmentalization of dendrites. *Proc. Natl. Acad. Sci. U. S. A.* **108**, 11246–51 (2011).

164. Cosker, K. E. & Segal, R. a. Neuronal signaling through endocytosis. *Cold Spring Harb. Perspect. Biol.* **6**, 1–16 (2014).

165. Poon, W. W. *et al.* β-Amyloid (Aβ) oligomers impair brain-derived neurotrophic factor retrograde trafficking by down-regulating ubiquitin C-terminal hydrolase, UCH-L1. *J. Biol. Chem.* **288**, 16937–48 (2013).

166. Kan, S. L. *et al.* Tanezumab for Patients with Osteoarthritis of the Knee: A Meta-Analysis. *PLoS One* **11**, e0157105 (2016).

167. Filler, A. G. *et al.* Tri-partite complex for axonal transport drug delivery achieves pharmacological effect. *BMC Neurosci.* **11**, 8 (2010).

168. Taylor, R. J. *et al.* Dynamic analysis of MAPK signaling using a high-throughput microfluidic single-cell imaging platform. *Proc. Natl. Acad. Sci. U. S. A.* **106**, 3758–63 (2009).

169. Frimat, J.-P. *et al.* A microfluidic array with cellular valving for single cell co-culture. *Lab Chip* **11**, 231–7 (2011).

170. Bonito-Oliva, A. *et al.* Cognitive impairment and dentate gyrus synaptic dysfunction in experimental Parkinsonism. *Biol. Psychiatry* **75**, 701–710 (2014).

171. Di, J. *et al.* Abnormal tau induces cognitive impairment through two different mechanisms: Synaptic dysfunction and neuronal loss. *Sci. Rep.* **6**, 20833 (2016).

172. Scheff, S. W., Price, D. A., Schmitt, F. A. & Mufson, E. J. Hippocampal synaptic loss in early Alzheimer's disease and mild cognitive impairment. *Neurobiol. Aging* **27**, 1372–1384 (2006).

173. Rutherford, L. C., Nelson, S. B. & Turrigiano, G. G. BDNF has opposite effects on the quantal amplitude of pyramidal neuron and interneuron excitatory synapses. *Neuron* **21**, 521–30 (1998).

174. Santos, A. R., Comprido, D. & Duarte, C. B. Regulation of local translation at the synapse by BDNF. *Prog. Neurobiol.* **92**, 505–16 (2010).

175. Li, L., Carter, J., Gao, X., Whitehead, J. & Tourtellotte, W. G. The neuroplasticity-associated arc gene is a direct transcriptional target of early growth response (Egr) transcription factors. *Mol. Cell. Biol.* **25**, 10286–10300 (2005).

176. Mokin, M. & Keifer, J. Expression of the immediate-early gene–encoded protein Egr-1 (zif268) during in vitro classical conditioning. *Learn. Mem.* **12**, 144–149 (2005).

177. LeBoeuf, A. C. *et al.* FTDP-17 mutations in Tau alter the regulation of microtubule dynamics: an 'alternative core' model for normal and pathological Tau action. *J. Biol. Chem.* **283**, 36406–15 (2008).

178. Lu, B., Nagappan, G., Guan, X., Nathan, P. J. & Wren, P. BDNF-based synaptic repair as a disease-modifying strategy for neurodegenerative diseases. *Nat Rev Neurosci* **14**, 401–416 (2013).

179. Gilley, J. *et al.* Age-dependent axonal transport and locomotor changes and tau hypophosphorylation in a "P301L" tau knockin mouse. *Neurobiol. Aging* **33**, 621.e1-621.e15 (2012).

180. Bunker, J. M., Kamath, K., Wilson, L., Jordan, M. A. & Feinstein, S. C. FTDP-17 Mutations Compromise the Ability of Tau to Regulate Microtubule Dynamics in Cells. *J. Biol. Chem.* **281**, 11856–11863 (2006).

181. Kopeikina, K. J. *et al.* Synaptic alterations in the rTg4510 mouse model of

tauopathy. *J. Comp. Neurol.* **521**, 1334 (2013).

182. Adams, S. J. *et al.* Overexpression of wild-type murine tau results in progressive tauopathy and neurodegeneration. *Am. J. Pathol.* **175**, 1598–1609 (2009).

183. Dixit, R., Ross, J. L., Goldman, Y. E. & Holzbaur, E. L. F. Differential regulation of dynein and kinesin motor proteins by tau. *Science* **319**, 1086–9 (2008).

184. Liazoghli, D., Perreault, S., Micheva, K. D., Desjardins, M. & Leclerc, N. Fragmentation of the Golgi apparatus induced by the overexpression of wild-type and mutant human tau forms in neurons. *Am. J. Pathol.* **166**, 1499–1514 (2005).

185. Dotti, C. G., Sullivan, C. A. & Banker, G. A. The establishment of polarity by hippocampal neurons in culture. *J. Neurosci.* **8**, 1454–1468 (1988).

186. Tahirovic, S. & Bradke, F. Neuronal Polarity. *Cold Spring Harb. Perspect. Biol.* **1**, a001644–a001644 (2009).

187. Seetapun, D., Castle, B. T., McIntyre, A. J., Tran, P. T. & Odde, D. J. Estimating the Microtubule GTP Cap Size In Vivo. *Curr. Biol.* **22**, 1681–1687 (2012).

188. Chaudhary, A. R., Berger, F., Berger, C. L. & Hendricks, A. G. Tau directs intracellular trafficking by regulating the forces exerted by kinesin and dynein teams. *Traffic* **19**, 111–121 (2017).

189. Umeda, T. *et al.* Intracellular amyloid β oligomers impair organelle transport and induce dendritic spine loss in primary neurons. *Acta Neuropathol. Commun.* **3**, 51 (2015).

190. Volpicelli-Daley, L. A. *et al.* Formation of -synuclein Lewy neurite-like aggregates in axons impedes the transport of distinct endosomes. *Mol. Biol. Cell* **25**, 4010–4023 (2014).

191. Kojima, M. *et al.* Biological characterization and optical imaging of brain-derived neurotrophic factor-green fluorescent protein suggest an activity-dependent local release of brain-derived neurotrophic factor in neurites of cultured hippocampal neurons. *J. Neurosci. Res.* **64**, 1–10 (2001).

192. Zhao, X. *et al.* TRiC subunits enhance BDNF axonal transport and rescue striatal atrophy in Huntington's disease. *Proc. Natl. Acad. Sci.* **113**, E5655–E5664 (2016).

193. Vershinin, M., Carter, B. C., Razafsky, D. S., King, S. J. & Gross, S. P. Multiple-motor based transport and its regulation by Tau. *Proc. Natl. Acad. Sci.* **104**, 87–92 (2007).

194. Yu, D. *et al.* Tau proteins harboring neurodegeneration-linked mutations impair kinesin translocation in vitro. *J. Alzheimer's Dis.* **39**, 301–314 (2014).

195. Cuchillo-Ibanez, I. *et al.* Phosphorylation of tau regulates its axonal transport by controlling its binding to kinesin. *FASEB J.* **22**, 3186–3195 (2008).

196. Grafstein, B. & Forman, D. S. Intracellular transport in neurons. *Physiol. Rev.* **60**, 1167–1283 (1980).

197. Alberici, A. *et al.* Frontotemporal dementia: impact of P301L tau mutation on a healthy carrier. *J. Neurol. Neurosurg. Psychiatry* **75**, 1607–10 (2004).

198. Rodríguez-Martín, T. *et al.* Reduced number of axonal mitochondria and tau hypophosphorylation in mouse P301L tau knockin neurons. *Neurobiol. Dis.* **85**, 1–10 (2016).

199. Majid, T. *et al.* In vivo axonal transport deficits in a mouse model of fronto-temporal dementia. *NeuroImage Clin.* **4**, 711–717 (2014).

200. Falzone, T. L., Gunawardena, S., McCleary, D., Reis, G. F. & Goldstein, L. S. B. Kinesin-1 transport reductions enhance human tau hyperphosphorylation, aggregation and neurodegeneration in animal models of tauopathies. *Hum. Mol. Genet.* **19**, 4399–4408 (2010).

201. Cosacak, M. I. *et al.* Human TAUP301L overexpression results in TAU hyperphosphorylation without neurofibrillary tangles in adult zebrafish brain. *Sci. Rep.* **7**, 12959 (2017).

202. Ebneth, A. *et al.* Overexpression of tau protein inhibits kinesin-dependent trafficking of vesicles, mitochondria, and endoplasmic reticulum: implications for Alzheimer's disease. *J. Cell Biol.* **143**, 777–94 (1998).

203. LaPointe, N. E. *et al.* The amino terminus of tau inhibits kinesin-dependent axonal transport: Implications for filament toxicity. *J. Neurosci. Res.* **87**, 440–451 (2009).

204. Elie, A. *et al.* Tau co-organizes dynamic microtubule and actin networks. *Sci. Rep.*

5, 9964 (2015).

205. Méphon-Gaspard, A. *et al.* Role of tau in the spatial organization of axonal microtubules: keeping parallel microtubules evenly distributed despite macromolecular crowding. *Cell. Mol. Life Sci.* **73**, 3745–3760 (2016).

206. Sayas, C. L. *et al.* Tau regulates the localization and function of End-binding proteins 1 and 3 in developing neuronal cells. *J. Neurochem.* **133**, 653–667 (2015).

207. Ji, Y., Pang, P. T., Feng, L. & Lu, B. Cyclic AMP controls BDNF-induced TrkB phosphorylation and dendritic spine formation in mature hippocampal neurons. *Nat. Neurosci.* **8**, 164–72 (2005).

208. Meyer-Franke, A. *et al.* Depolarization and cAMP elevation rapidly recruit TrkB to the plasma membrane of CNS neurons. *Neuron* **21**, 681–93 (1998).

209. Du, J. *et al.* Regulation of TrkB receptor tyrosine kinase and its internalization by neuronal activity and Ca2+ influx. *J. Cell Biol.* **163**, 385–395 (2003).

210. Arimura, N. *et al.* Anterograde Transport of TrkB in Axons Is Mediated by Direct Interaction with Slp1 and Rab27. *Dev. Cell* **16**, 675–686 (2009).

211. Huang, S.-H. *et al.* JIP3 Mediates TrkB Axonal Anterograde Transport and Enhances BDNF Signaling by Directly Bridging TrkB with Kinesin-1. *J. Neurosci.* **31**, 10602–10614 (2011).

212. Bathina, S. & Das, U. N. Brain-derived neurotrophic factor and its clinical Implications. *Arch. Med. Sci.* **11**, 1164–1178 (2015).

213. Zuccato, C. *et al.* Loss of huntingtin-mediated BDNF gene transcription in Huntington's disease. *Science (80-.).* **293**, 493–498 (2001).

214. Salminen, A. *et al.* Impaired autophagy and APP processing in Alzheimer's disease: The potential role of Beclin 1 interactome. *Prog. Neurobiol.* **106–107**, 33–54 (2013).

215. Ebrahimi-Fakhari, D., Wahlster, L. & McLean, P. J. Protein degradation pathways in Parkinson's disease: Curse or blessing. *Acta Neuropathol.* **124**, 153–172 (2012).

216. Pickford, F. *et al.* The autophagy-related protein beclin 1 shows reduced expression

in early Alzheimer disease and regulates amyloid β accumulation in mice. *J. Clin. Invest.* **118**, 2190–9 (2008).

217. Sebastião, A. M., Assaife-Lopes, N., Diógenes, M. J., Vaz, S. H. & Ribeiro, J. a. Modulation of brain-derived neurotrophic factor (BDNF) actions in the nervous system by adenosine A(2A) receptors and the role of lipid rafts. *Biochim. Biophys. Acta* **1808**, 1340–1349 (2011).

218. Zahavi, E. E., Maimon, R. & Perlson, E. Spatial-specific functions in retrograde neuronal signalling. *Traffic* **18**, 415–424 (2017).

219. Henderson, C. E. Role of neurotrophic factors in neuronal development. *Curr. Opin. Neurobiol.* **6**, 64–70 (1996).

220. Sandow, S. L. *et al.* Signalling organelle for retrograde axonal transport of internalized neurotrophins from the nerve terminal. *Immunol. Cell Biol.* **78**, 430–435 (2000).

221. Quintanilla, R. a., Dolan, P. J., Jin, Y. N. & Johnson, G. V. W. Truncated tau and AB cooperatively impair mitochondria in primary neurons. *Neurobiol. Aging* **33**, 1–17 (2012).

222. Peyrin, J.-M. *et al.* Axon diodes for the reconstruction of oriented neuronal networks in microfluidic chambers. *Lab Chip* **11**, 3663–73 (2011).

223. Taylor, P. *et al.* Analysis of mitochondrial DNA in microfluidic systems. *J. Chromatogr. B. Analyt. Technol. Biomed. Life Sci.* **822**, 78–84 (2005).

224. Wibrand, K. *et al.* MicroRNA Regulation of the Synaptic Plasticity-Related Gene Arc. *PLoS One* **7**, e41688 (2012).

225. Ji, Y. *et al.* Acute and gradual increases in BDNF concentration elicit distinct signaling and functions in neurons. *Nat. Neurosci.* **13**, 302–9 (2010).

226. Tongiorgi, E., Domenici, L. & Simonato, M. What Is the Biological Significance of BDNF mRNA Targeting in the Dendrites?: Clues From Epilepsy and Cortical Development. *Mol. Neurobiol.* **33**, 017–032 (2006).

227. An, J. J. *et al.* Distinct role of long 3' UTR BDNF mRNA in spine morphology and synaptic plasticity in hippocampal neurons. *Cell* **134**, 175–87 (2008).

228. Yasuda, M. *et al.* Robust stimulation of TrkB induces delayed increases in BDNF and Arc mRNA expressions in cultured rat cortical neurons via distinct mechanisms. *J. Neurochem.* **103**, 626–636 (2007).

229. Sharma, N. *et al.* Long-Distance Control of Synapse Assembly by Target-Derived NGF. *Neuron* **67**, 422–434 (2010).

230. Fang, F. *et al.* Synuclein impairs trafficking and signaling of BDNF in a mouse model of Parkinson's disease. *Sci. Rep.* **7**, 3868 (2017).

231. Gilman, S. *et al.* Clinical effects of A immunization (AN1792) in patients with AD in an interrupted trial. *Neurology* **64**, 1553–1562 (2005).

232. Herrmann, N., Chau, S. A., Kircanski, I. & Lanctôt, K. L. Current and Emerging Drug Treatment Options for Alzheimer's Disease. *Drugs* **71**, 2031–2065 (2011).

233. Milnerwood, A. J. & Raymond, L. A. Early synaptic pathophysiology in neurodegeneration: insights from Huntington's disease. *Trends Neurosci.* **33**, 513–523 (2010).

234. Bellucci, A. *et al.* Review: Parkinson's disease: from synaptic loss to connectome dysfunction. *Neuropathol. Appl. Neurobiol.* **42**, 77–94 (2016).

235. Pooler, A. M., Noble, W. & Hanger, D. P. A role for tau at the synapse in Alzheimer's disease pathogenesis. *Neuropharmacology* **76**, 1–8 (2014).

236. Henstridge, C. M., Pickett, E. & Spires-Jones, T. L. Synaptic pathology: A shared mechanism in neurological disease. *Ageing Res. Rev.* **28**, 72–84 (2016).

237. Freeman, O. J. & Mallucci, G. R. The UPR and synaptic dysfunction in neurodegeneration. *Brain Res.* **1648**, 530–537 (2016).

238. Lim, K.-C., Lim, S. T. & Federoff, H. J. Neurotrophin secretory pathways and synaptic plasticity. *Neurobiol. Aging* **24**, 1135–45 (2003).

239. Zuccato, C. & Cattaneo, E. Brain-derived neurotrophic factor in neurodegenerative diseases. *Nat. Rev. Neurol.* **5**, 311–322 (2009).

240. Ingram, J. The identification of inhibitors of nerve growth factor and brain-derived neurotrophic factor. (University of Southampton, 2017).

241. Lu, B. Pro-Region of Neurotrophins. *Neuron* **39**, 735–738 (2003).

242. Morooka, T. & Nishida, E. Requirement of p38 mitogen-activated protein kinase for neuronal differentiation in PC12 cells. *J. Biol. Chem.* **273**, 24285–8 (1998).

243. Traverse, S., Gomez, N., Paterson, H., Marshall, C. & Cohen, P. Sustained activation of the mitogen-activated protein (MAP) kinase cascade may be required for differentiation of PC12 cells. Comparison of the effects of nerve growth factor and epidermal growth factor. *Biochem. J.* **288 (Pt 2**, 351–5 (1992).

244. Melo, C. V. *et al.* BDNF Regulates the Expression and Distribution of Vesicular Glutamate Transporters in Cultured Hippocampal Neurons. *PLoS One* **8**, e53793 (2013).

245. Misko, T. P., Radeke, M. J. & Shooter, E. M. Nerve growth factor in neuronal development and maintenance. *J. Exp. Biol.* **132**, 177–90 (1987).

246. Budni, J., Bellettini-Santos, T., Mina, F., Lima Garcez, M. & Ioppi Zugno, A. The involvement of BDNF, NGF and GDNF in aging and Alzheimer's disease. *Aging Dis.* **6**, 331 (2015).

247. Lee, J. G. *et al.* Decreased Serum Brain-Derived Neurotrophic Factor Levels in Elderly Korean with Dementia. *Psychiatry Investig.* **6**, 299 (2009).

248. Phillips, H. S. *et al.* BDNF mRNA is decreased in the hippocampus of individuals with Alzheimer's disease. *Neuron* **7**, 695–702 (1991).

249. Oller-Salvia, B., Sánchez-Navarro, M., Giralt, E. & Teixidó, M. Blood–brain barrier shuttle peptides: an emerging paradigm for brain delivery. *Chem. Soc. Rev.* **45**, 4690–4707 (2016).

250. Sun, P., Enslen, H., Myung, P. S. & Maurer, R. A. Differential activation of CREB by Ca2+/calmodulin-dependent protein kinases type II and type IV involves phosphorylation of a site that negatively regulates activity. *Genes Dev.* **8**, 2527–2539 (1994).

251. Zheng, F., Luo, Y. & Wang, H. Regulation of BDNF-mediated transcription of immediate early gene Arc by intracellular calcium and calmodulin. *J. Neurosci. Res.* **87**, 380–92 (2009).

252. Aakalu, G., Smith, W. B., Nguyen, N., Jiang, C. & Schuman, E. M. Dynamic visualization of local protein synthesis in hippocampal neurons. *Neuron* **30**, 489–502 (2001).

253. Harvey, C. D. *et al.* A genetically encoded fluorescent sensor of ERK activity. *Proc. Natl. Acad. Sci.* **105**, 19264–19269 (2008).

254. Sorkin, A., McClure, M., Huang, F. & Carter, R. Interaction of EGF receptor and Grb2 in living cells visualized by fluorescence resonance energy transfer (FRET) microscopy. *Curr. Biol.* **10**, 1395–1398 (2000).

255. Vandame, P. *et al.* Optimization of ERK activity biosensors for both ratiometric and lifetime FRET measurements. *Sensors (Switzerland)* **14**, 1140–1154 (2014).

256. Scheper, G. C., Van Der Knaap, M. S. & Proud, C. G. Translation matters: Protein synthesis defects in inherited disease. *Nature Reviews Genetics* **8**, 711–723 (2007).